BIODIESEL PRODUCTION OVER CARBON SULFONATED CATALYSTS

NAWIK ZORAINA DOS RAMOS GAMBOA VAZ SARAIVA

Thesis to obtain the Master of Science Degree in

Energy Engineering and Management

Supervisors: Prof. Ana Paula Vieira Soares Pereira Dias

Prof. Bruna Alexandra Canuto Rijo

Examination Committee

Chairperson: Prof. Edgar Caetano Fernandes

Supervisor: Prof. Ana Paula Vieira Soares Pereira Dias

Member of the Committee: Prof. Catarina Pereira Nobre

May 2023

I declare that this document is an original work of my own authorship and that it fulfils all the requirements of the Code of Conduct and Good Practices of the *Universidade de Lisboa*.

To God be the glory for great things He has done!

To my grandparents Pedro and Cristina Gamboa, for all their love.

Acknowledgements

First of all, I thank my Lord and Saviour Jesus Christ for the gift of life and for continuously taking care and never giving up on me. I also thank Him for leading my way throughout the whole thesis process, giving me the strength and wisdom to conduct and present this piece of work.

I thank my sweet and lovely grandparents, Pedro and Cristina Gamboa, for all their love, dedication, effort, teachings, constant support, and patience to me, all of which shaped my personality, built my character and refined my principles to create the woman and professional that I am today. My grandparents' example of faith, strength, and faithfulness to God are a daily inspiration and continuous motivation for me.

I thank my beautiful mother, for raising me with so much love and affection and allowing me to also grow into the woman I am today. My mother's profession and passion for the energy industry has inspired me and led me to pursue a career in the same field. I can tell that she has led me to take the best decision for my career. Her humility, positiveness, and continuous confidence that I will succeed, no matter what, even from afar, has given me the courage to finish this work.

I thank my adorable unties and uncles, Benilde, Celso, Ivone, Kandia, and Kundi, and my cousins Keone, Keven, Larissa, and Johanna, for always caring for me and embracing me with so much care, happiness, and love. All the moments I was able to share with them were remarkable and are safe and recorded in my mind forever. I also thank my ecstatic cousin Gabriela Figueira for pushing so much for me during the thesis writing process and providing me with care and support during the lowest times of my life.

I thank my friends, or should I say brothers, whom I have a special place in my heart, Sulcivania Uonzo and Ibrahim Avelino for all their love, prayers, constant motivation, and for lifting me up in all moments of my life. A special thank and gratitude for my one and only sister Dalila de Jesus, a soul sister that God has put in my life to help me become a better person each and everyday. I thank for all their help and companionship in this path of life.

I also thank my gracious friend Edson de Jesus, also heaven sent, a man of value that has gifted me with exceptional love and care since the day we met. I can surely say that without him, this thesis process would have been much harder. I truly appreciate the fact that he willingly helps me to carry the multiple burdens of life.

I thank my other friends in Christ, from Unidos em Cristo and Conhecendo as Escrituras for the constant prayers, exhortations, and inspiration. They have also contributed to shape me as a better

human being and server of people and of the Lord.

I thank my intelligent, funny, and adorable colleagues Francisco, Fernando, Erica, Igor, Joana, Tiago, and Pedro, with whom I had the opportunity to share the chemistry laboratory at IST and share numerous remarkable experiences. Their presence in the laboratory turned the environment into a very pleasant and happy place to be. They will all be kept in my heart forever with dearly love.

I thank my new *alma mater*, the Instituto Superior Tecnico at University of Lisbon (UL), for all the opportunities provided and the high quality pursued. Definitely, the good and relevant change to the world can only occur through knowledge, dedication, love, honesty and education. All my professors are in my heart and I will honour them in my career.

I thank my health and dialysis team at Hospital Santa Cruz, including my sweet nurse Sara Lobo for providing me with all means necessary for me to continue to live the best life despite the health issues that have emerged. My team has been such a motivation to me and have cheered me up not to ever give up on my dreams.

Lastly, but definitely not the least, I specially thank one of the sweetest person's I haver ever met in me life, my beautiful advisor, professor Dr. Ana Paula Vieira Soares Pereira Dias. Such an inspiring and carrying woman that I am more than grateful to have built a relationship and share this thesis research with. I am more than sure that I could not get, or want, any other advisor. I thank God everyday for such wonderful opportunity, for all her teachings, time donated and experience shared. Not only that, but for being so caring towards me on a personal level. This thesis is only at this stage due to her.

Abstract

Biodiesel with improved sustainability can be produced by alcoholysis of low-grade fats, with high free fatty acid content, using heterogeneous acid catalysts. Carbon materials with sulphonic surface groups are reported to be active in such esterification reactions. Sugars and sugar alcohols are natural compounds and, therefore, renewable raw materials which can be used as raw materials for char production. Their acid-catalyzed hydro-carbonization results in the formation of carbon materials with acidic functional groups on the surface, which makes them suitable to be used as heterogeneous catalysts in esterification reactions. This work is dedicated to propose an economic and efficient methodology for acidic heterogeneous catalyst synthesis focused in biodiesel production via esterification. The major idea is to produce catalysts based on reduction of expensive reagents and valorizing glycerine, a biodiesel by-product. Hydrochars materials were prepared by low-temperature slow carbonization of glycerol, xylitol sucrose, and glucose in the presence of different amounts of H_2SO_4 (mass ratios from 1 to 4). The carbonaceous materials were extensively characterized and tested in the methanolysis reaction of oleic acid. In terms of characterization, ATR-FTIR, Raman, TGA, XRD and SEM-EDS analysis were carried with all the catalysts. Data analysed shows that all the carbon materials were amorphous with features of polyaromatic sheets with hydroxyl (-OH), carboxylic acid (-COOH), and sulphonic ($-SO_3H$) functional groups. It occurred under the conditions evaluated at 5% wt. of catalyst, methanol/oleic acid = 12 molar ratio, methanol reflux temperature. The sucrose-derived catalyst prepared with the highest H_2SO_4 content showed the best performance, followed by glycerol, allowing full conversion of oleic acid after 90 min.

Keywords

Biodiesel; carbon sulfonated catalyst; acid heterogeneous catalysis; methyl oleate; esterification; glycerine valorisation

Resumo

O biodiesel, um combustível sustentável, pode ser produzido pela alcoólise de gorduras de baixo teor, com alto teor de ácidos graxos livres, usando catalisadores ácidos heterogêneos. Materiais de carbono com grupos de superfície sulfônicos são relatados como sendo ativos em reações de esterificação. Açúcares e álcoois de açúcar são compostos naturais e, portanto, matérias-primas renováveis que podem ser utilizadas como matéria-prima para a produção de catalisadores. A carbonização parcial e sulfonação por ácido resulta na formação de materiais de carbono com grupos funcionais ácidos na superfície, o que os torna adequados a serem usados como catalisadores heterogêneos em reações de esterificação. Este trabalho é dedicado a propor uma metodologia econômica e eficiente para a síntese de catalisadores ácidos heterogêneos com foco na produção de biodiesel via esterificação. A ideia é produzir catalisadores com base na redução de reagentes caros e na valorização da glicerina, um subproduto do biodiesel. Os catalisadores foram preparados por carbonização lenta a baixa temperatura de glicerol, xilitol, sacarose e glicose na presença de diferentes quantidades de H_2SO_4 (com rácios de 1 a 4). Os materiais carbonáceos foram extensivamente caracterizados e testados na reação de metanólise do ácido oleico. Em termos de caracterização, análises de ATR-FTIR, Raman, TGA, XRD e SEM-EDS foram realizadas com todos os catalisadores. Os dados analisados mostram que todos os catalisadores eram amorfos com características de folhas poliaromáticas com grupos funcionais hidroxila (-OH), ácido carboxílico (-COOH) e sulfônico ($-SO_3H$). As condições avaliadas foram de 5% em peso de catalisador, metanol/ácido oleico = racio molar de 12, temperatura de refluxo do metanol. O catalisador derivado da sacarose preparado com o maior teor de H_2SO_4 apresentou o melhor desempenho, seguido pelo glicerol, permitindo a conversão total do ácido oleico após 90 min.

Palavras-chave

Biodiesel; catalisador de carbonização-sulfonação; catalisadores ácidos heterogéneos; metil oleato; esterificação; valorização de glicerina

Table of Contents

List of Figures

List of Tables

List of Abbreviations

AF	Animal Fat
ASTM	American Society for Testing and Materials
CEN	European Committee for Standardization
DAG	Diacylglycerol
DIN	German Institute for Standardization
EDS	Energy Dispersibe Spectroscopy
EIA	Energy Information Administration
FA	Fatty acid
FAME	Fatty Acid Methyl Ester
FAO	FAO - Food and Agriculture Organization
FFA	Free fatty acid
FT	Fisher - Tropsch
GC	Gas chromatography
GHG	Green house gas
ISO	International Standardization Organization
MAG	Monoacylglycerol
MS	Mass Spectrometry
MSW	Municipal Solid Wastes
MTOE	Million Tonnes of Oil Equivalent
PTSA	Para-toluene-sulfonic acid
RM	Raw Material
RSC	Royal Society of Chemistry
SEM	Scanning Electron Microscopy
TAG	Triacylglycerol
TAG	Triglycerides
TPES	Total Primary Energy Supply
TWh	Terawatt hour
UFO	Used Frying Oil
VO	Vegetable oil
WCO	Waste Cooking Oil
XRD	X-Ray Diffraction

Chapter 1

Introduction

1.1 Overview

In April 2020, oil prices plunged to their lowest level in history, with futures closing at a negative $37 per barrel (Gurdus, 2020). Even though this dramatic and unprecedented drop in oil prices has a well know cause, COVID-19, it is a fact that the oil industry has been suffering a wave of economic instability for a long time. Therefore, it is not as reliable to supply the world's demand as it was in the past (Wen et al., 2018). Not only that, but the link between fossil fuels and the greenhouse gas (GHG) effect has also posed a significant concern for the use of fossil fuels.

The transition from fossil fuels is encouraged using alternative fuels. One of these biofuels is biodiesel, a fuel constituted by a mixture of fatty acid esters obtained from vegetable oils. Besides its biodegradability, biodiesel has some other advantages as miscibility in petroleum-derived diesel, lower toxicity, and greenhouse gas emissions than petroleum-derived diesel, high flash point and cetane number, and needless modification for use in internal combustion motors (Fonseca et al., 2022).

Industrially, biodiesel production is performed using alkali catalysts including NaOH, KOH, and CH_3ONa via a homogeneous process. This provides high yields (>98%) in shorter reaction time (30–60 min), requiring lower amounts of catalysts when compared with other catalytic processes. On the other hand, Helwani et al. (2009) stated that the disadvantages of the process are involving the necessity of free fatty acid (FFA) contents lower than 0.5% and water contents lower than 0.05%, which is somewhat unachievable for sustainable feedstocks like waste cooking oils (WCO) and animal fats (AF), difficulty of catalysts recovery and separation from the reaction products, and generation of waste water. The biodiesel can also be obtained through homogeneous acid catalysis – H_2SO_4 and HCl, with the advantage of non-influence of FFA even at high concentrations. However, Narasimharao et al. (2007) argued that this process has its own drawbacks since it is necessary to use high alcohol-to-oil ratios (>30:1), long reaction times, 4000 times slower than base catalysed besides requiring additional washing steps and leading to corrosion of the reactors.

Researchers, including Fonseca et al. (2022) studies the synthesizing of carbon-based heterogeneous acid catalysts, using as precursors sugar and biomass (Toda et al., 2005). These catalysts are known as sulfonated carbons and its surface chemistry is characterized by three acid groups with different strengths: carboxylic acid (–COOH), phenolic acid, (–OH), and sulfonic acid (–SO_3H). The sulfonic group is the main responsible by increase the transesterification and esterification reaction rates, while the others improve the surface properties of the catalyst; not only that but the sulfonated carbons can deliver activities comparable to those reported for sulfuric acid.

Astoundingly, crude glycerine, a biodiesel by-product, is a prominent precursor in the synthesis of carbon-based heterogeneous acid catalysts (Narasimharao, Lee, & Wilson, 2007). If, in fact, glycerine can be converted into acidic heterogeneous catalyst, this would not only contribute to its valorisation, but also to a circular economy in the energy sector.

1.2 Motivation and Objective

All the described scenario brings endorsement to the motivations and objective of this present work in the academia and with the scientific community. The main inspirations of this research, nurtured and matured for many months of research, and continuously pursued during its development, were the goal to combine sustainability and product valorisation to improve the traditional biodiesel production route. All that involved with the desire to also contribute to the advancement of science and technology, and impact global communities in a forward way.

This paper investigates the synthesis sulfonated carbons with crude glycerol among similar precursors and their application as catalysts for biodiesel production. The main covered topics, including the current market of the biodiesel industry, the characteristics of the different biodiesel production pathways, types of catalysts, and the partial carbonization and sulfonation processes. Experimental analysis was conducted based on literature published in the last few years.

1.2.1 Objective

The main objective of this study is to contribute to the transition of biodiesel production homogeneous catalysts to sustainable heterogeneous ones. Specifically, this research aims to endorse a feasible, recent and practical heterogeneous catalyst production methodology for biodiesel generation derived from four types of short chain carbo hydrates, glycerine (a biodiesel by-product), sucrose, glucose, and xylitol. Evidence the effectiveness of biodiesel production and catalyst behaviour with oleic acid as the main raw material via esterification using the synthetized catalysts. Through that, the importance of biodiesel and waste valorisation to the current situation of world's sustainable transition will be emphasized.

.

Chapter 2

Literature Review

2.1 Biofuels

2.1.1 Overview

The EU Commission defines biofuel as a liquid or gaseous fuel that can be used for transportation and with an origin from biomass (EU, 2003). The Food and Agriculture Organization (FAO), on the other hand, defines biofuel as a product originating from renewable sources including plants, vegetable oils, and/or treated wastes from domestic or industrial origin (2015). Ultimately, EIA (2019a) defines biofuels as being any kind of liquid fuel or blending products derived from biomass that can be used firstly as a fuel in the transportation sector.

Biofuels are classified into two main categories: the conventional or first-generation biofuels and the advanced biofuels, subdivided into second, third and fourth generations. This discretization is done based on the type of technology implemented and the degree of development of each fuel. Figure 1 depicts a brief overview of the pathways of biofuel production. Biodiesel can be obtained through the esterification or transesterification of oil crops like rapeseed, palm oil, and/or residual oils including animal fat (AF) and waste cooking oils (WCO).

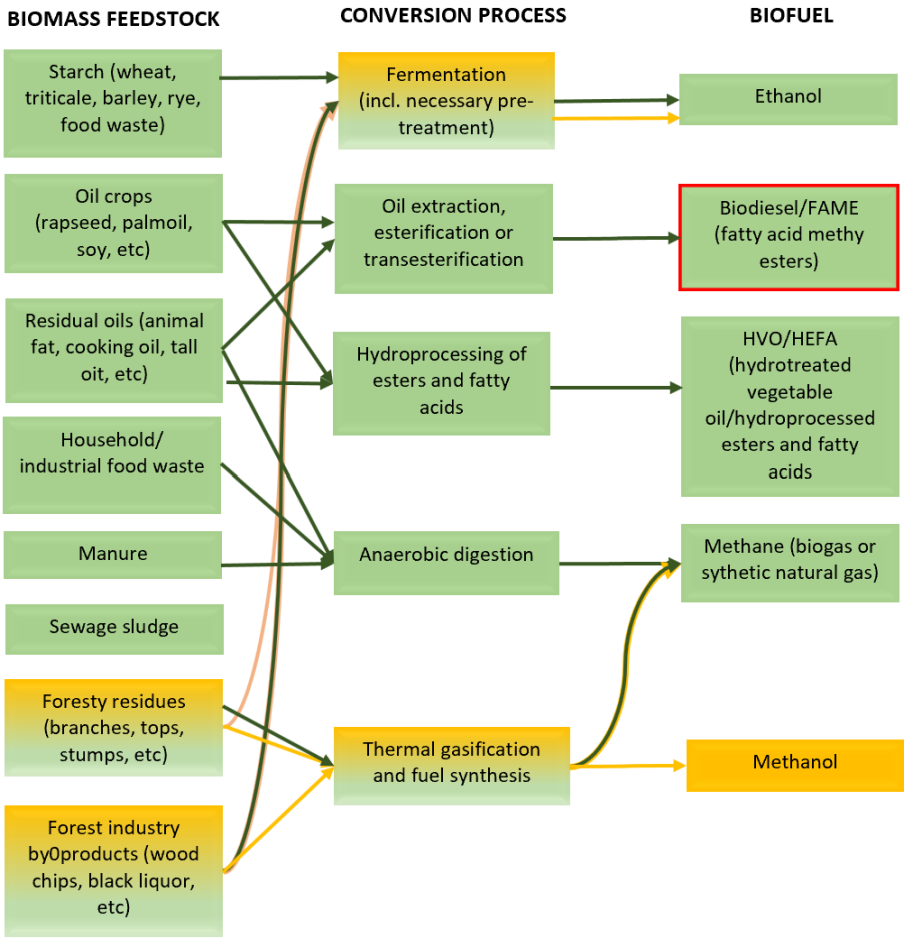

Figure 1 - Biofuel production pathways. Adapted from: Martin et al., 2017.

2.2 Biodiesel

2.2.1 History of Biodiesel

Since the early ages, vegetable oils (VO) have been used not only as food, but also as a fuel to light up pottery lamps and torches. Gas chromatography (GC) coupled to mass spectrometry (MS) conducted on a lipid fraction of residues in ancient oil lamps found at the archaeological site of Sagalassos, south-west Turkey, indicated the presence of plant sterols and long chain alcohols suggesting that a VO was used in these lamps (Kimpe et al., 2001). This practice has been carried on for generations and nowadays VO are still being used as primary biofuel in some regions (Jiménez, 2009). In fact, it was not until 1846 that Friedrich Rochieder devised and described glycerol production via transesterification of castor oil (Dermibas, 2010), followed by the Irish chemist Patrick J. Duffy in 1853 who have then developed the process for biodiesel and soap production (Duffy, 1853), culminating with the Belgium patent[1] of biodiesel, specifically an ethyl ester of palm oil, granted by Georges Chavanne in 1937 (Kutney, 2016). In 1938, a passenger bus fuelled with palm oil ethyl ester plied the route between Brussels and Louvain (Knothe, 2005).

The diesel engine was created in the 1890s by Rudolf Diesel. This engine could run on a variety of fuels, including pure VO. Notwithstanding the novelty of the engine, few people were interested in that given the fact that fossil fuels were inexpensive and easy to access during that time (Pahl, 2005). This scenario has changed slightly with the 1970s petroleum oil embargo, which caused many countries including Austria, South Africa, The United States, and many others to look to VO as a possible fuel, going even further to rediscover that pure VO could be used to run diesel engines; however, eventually the poor quality of that fuel caused by the high viscosity of VO caused damage to the engines. Scientists then conducted experiments to convert VO into biodiesel. As a matter of fact, the word “biodiesel” was probably first introduced in 1984 (Van Gerpen et al., 2005).

Soon after, in 1985, the first biodiesel manufacturing plant specifically designed to produce fuel was started at an agricultural college in Austria (Knothe, 2005). Since 1992, biodiesel has been commercially manufactured across Europe, with Germany being the largest producer. In the United States, biodiesel was first manufactured commercially in 1991 in Kansas City, Missouri. Four years later, the University of Idaho provided biodiesel to Yellowstone National Park, which used the fuel in a truck that has been driven several hundred thousand miles without damage to the engine. Subsequently, other national parks began using biodiesel in their vehicles (Pahl, 2005).

2.2.2 Growth of the Biodiesel Industry

In more recent years, researchers all across the world have been increasingly interested in promoting the use of biofuels, especially in transportation, as a substitute for gasoline and diesel, because they can possibly help nations decrease their reliance on imported fossil fuels and also because they frequently produce less air pollution and net carbon emissions than fossil fuels. As of 2021, the total world energy supply was equivalent to 606 EJ, where Asia accounts for 49.4% of that

amount, the Americas account for 23.1%, Europe accounts for 17.6%, and the other 9.9% corresponds to the rest of the world (IEA, 2021).

Figure 2 presents the introduction of biodiesel to the world energy matrix in around 1984, which combined with other biofuels contributed to 0.07% of total primary energy consumption. Fast forwarding to 2016, when the Paris Climate Accords became officially effective, biofuels consumption accounted for 0.62% (947 TWh or 3.4 EJ) of total energy consumption. As seen in figure 2, there is a decrease in energy consumption for the 2020 due the Covid-19 pandemic and its implications. Nonetheless, the year of 2021 presents a total energy consumption of 163,709 TWh (606 EJ), in which 1,140 TWh (4.3 EJ) accounts for biofuels, 0.70% of total share. From that, one can infer that, though minuscule, there is an increase of 20.38%, 193 TWh, of biofuel consumption across the globe. Even with a slow but sure increase in biofuel consumption in the late years, it is imperative to accelerate the rise of biofuel consumption in the near future due to ongoing political instability and supply shortage that the world is currently facing.

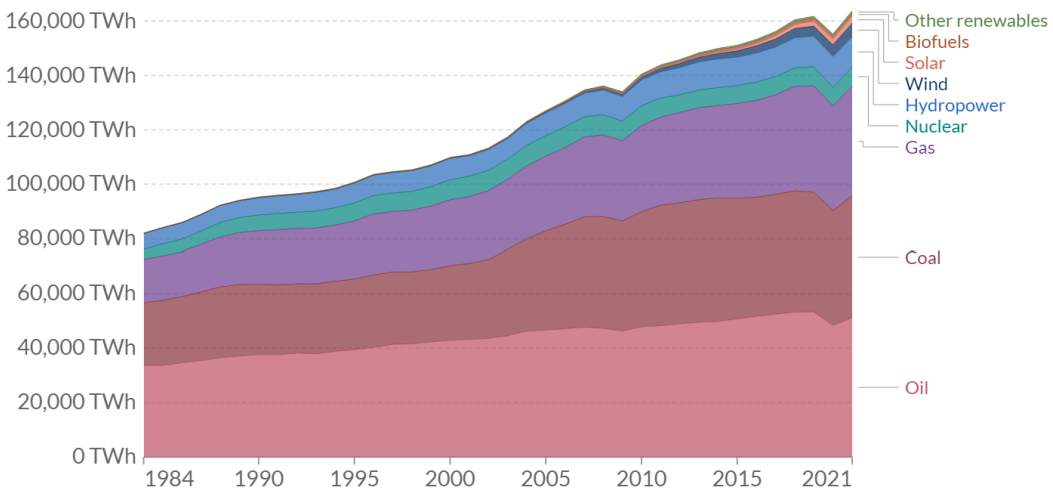

Figure 2 - Total energy consumption by source 1984-2021. (EIA 2021)

As liquid biofuels dependent mostly on natural conditions such as arable areas and weather, some countries have better capacities to harness and to develop a biofuels sector. For instance, among the leaders in liquid biofuels production in the world, there are the United States, Brazil, Indonesia, Germany, and China, according to reports from the United States Energy Information Administration (IEA) (2022). Even though EU is on third place in the biofuel production ranking, most of that biofuel production comes from countries including Germany and France. In fact, EU consumes more than its production; however, without much discrepancies (IEA, 2022).

For a further comprehension of the role fulfilled by the biofuels in todays world's economy, it is suitable to particularize the data to identify the different types of biofuel technologies. Figure 3 illustrates the participation of different types of biofuels.

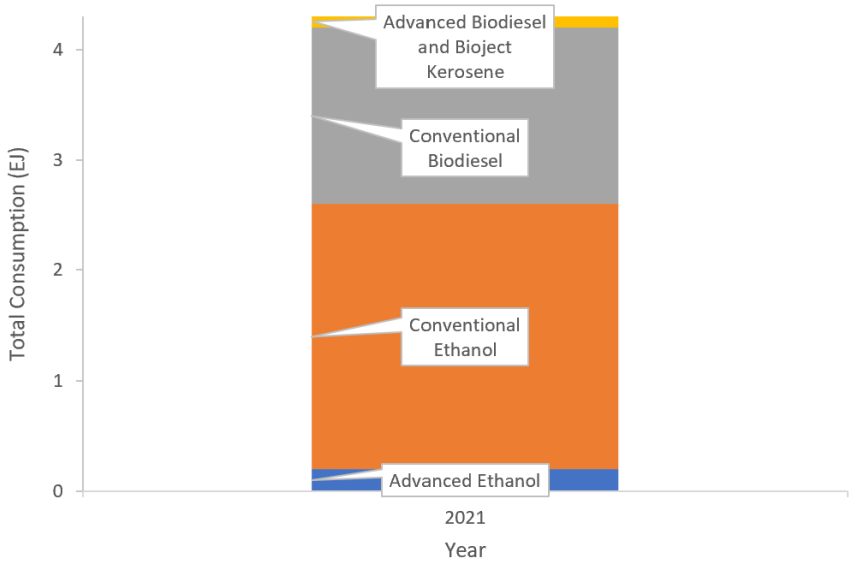

Figure 3 - biofuel production by feedstock and technology for 2021. Adapted from: IEA (2022)

From a total of 4.3 EJ (1,140 TWh) in 2021, 55.9% of that amount, 2.4 EJ, accounts for conventional ethanol, 37.2%, 1.6 EJ, for conventional biodiesel, 4.6%, 0.2, for advanced ethanol, and 2.3%, 0.2 EJ, for advanced biodiesel and bioject kerosene (EIA, 2022).

2.2.3 Biodiesel Quality Standards

For any field of knowledge, including the biodiesel sector, the availability of a reference parameter with the goal of standardizing characterizations and favouring comparison is crucial since it helps to establish a pattern of comparison between samples. For this, there are several technical standards developed by organizations like the International Standardization Organization (ISO) and the American Society for Testing and Materials (ASTM), now simply known as ASTM International. These standards are frequently used as a major reference by many international organizations, including the European Committee for Standardization (from French, CEN) and the German Institute for Standardization (from German, DIN), as cited by Prankl et al. (2004).

The two most important biodiesel standards currently in use around the world are "EN 14214 - Liquid petroleum fluids - Fatty acid methyl esters (FAME) for use in diesel engines and heating applications - Requirements and test methods" in Europe and "ASTM D6751 - Standard Specification for Biodiesel Fuel Blend Stock (B100) for Middle Distillate Fuels" in the USA, both of which were published in 2002. According to Joo & Kumar (2019), the German standard DIN 51606 formed the basis for the European standard, which was created as a result of Directive 2003/ 30/ EC, EU (2003).

As listed in Table A1 (see Appendix A), each of the technical standards – EN 14214 and ASTM D6751 - specifies the prerequisites and restrictions for biodiesel. Table A2 (see Appendix A), on the other hand, presents the standard properties for fuel diesel, pure biodiesel and the blending of biodiesel with other diesel fuels at different proportions.

It is very possible that certain variances in its qualities are noted because biodiesel is manufactured using various methods and the RM can be gathered in different locations across the world, which can also impact the quality of the biodiesel. Also, many challenges and technical effects are anticipated when utilizing biodiesel in engines like lack of efficiency due to the reactional process, poor raw material quality, and contamination as Ma & Hanna (1999) have extensively studied.

For instance, Altazari's et al. (2022), studies have shown that the deterioration of natural rubber gaskets, corrosion of aluminium, flash point effects due to high alcohol content, and formation of carbon deposits due to incomplete combustion of substances like FFAs, glycerine, monoacylglycerol (MAG), diacylglycerol (DAG), and triacylglycerol (TAG) are the most frequent issues with low quality biodiesel. Due to the combustion chamber temperatures not being sufficient to burn them and instead favouring their aggregation in larger molecules, these chemicals can also cause the creation of deposits produced from polymerization; these leftovers may, thereafter, result in engine deposits and filter clogging.

To mitigate the situation, it is imperative that biodiesel raw materials go through a pre-treatment and that the biodiesel may go through a purification process to ensure that each sample has the same aforementioned standards. Pre-treatment and purification processes will be discussed in the next sections.

2.3 Biodiesel Production

Different technologies have become available to produce biodiesel from basic raw materials, including vegetable oils and animal fats. The hydrotreatment (HDT) technology was discussed by Aatola et al. (2008) and Stumborg, Wong & Hogan (1996) as a promising alternative to transesterification or esterification to produce high quality bio-based products molecularly similar to fossil gasoline and diesel. Also, Several other scientists, including Pradana et al. (2018) and Aranda & Machado (2016) have focused their research on a process called hydro esterification, a combination of an esterification reaction and a hydrolysis reaction. According to them, it is ideal for usage with raw materials of low quality, such as AF and WCOs.

In spite of the benefits of the mentioned technologies, the most popular are still the simpler techniques that have been identified by multiple researchers, including Demirbas et al. (2016), Ruhul et al. (2015), and Ma & Hanna (1999); these include the direct usage and/or blending, micro-emulsion, thermal cracking or pyrolysis, esterification and transesterification. For the purposes of this study, both esterification and transesterification will be further evaluated.

2.3.1 Reactants

There is very great variety of materials that can be used for biodiesel production via different technology pathways depending on the type of raw material used. Examples of raw materials include the vegetable derived from oleaginous plants such as soybean, rapeseed, palm tree, sunflower, and jatropha. Residues from different sectors can also be transformed into biodiesel like Waste Cooking Oil (WCO) or Used Frying Oil (UFO), animal fat (AF), which includes tallows from chicken and cattle, pork lard, and fish viscera. They all share a similar chemical characteristic, they all contain fatty acids.

2.3.1.1 Fatty Acids

Fats and oils are hydrophobic substances, animal or vegetal, which are composed of a Chemistry's functional group named carboxylic acid attached to single or several carbons connected to form a chain. In vegetable oils and animal fats, FAs are in the form of triglycerides (TAG), classified as esters or, more accurately, tri esters. The TAGs are made of one mol of glycerol and three fatty acids. TAGs formation is represented in figure 4, where R_1, R_2, and R_3 indicate different radicals composed of carbon atoms and the water released from the reaction is also depicted.

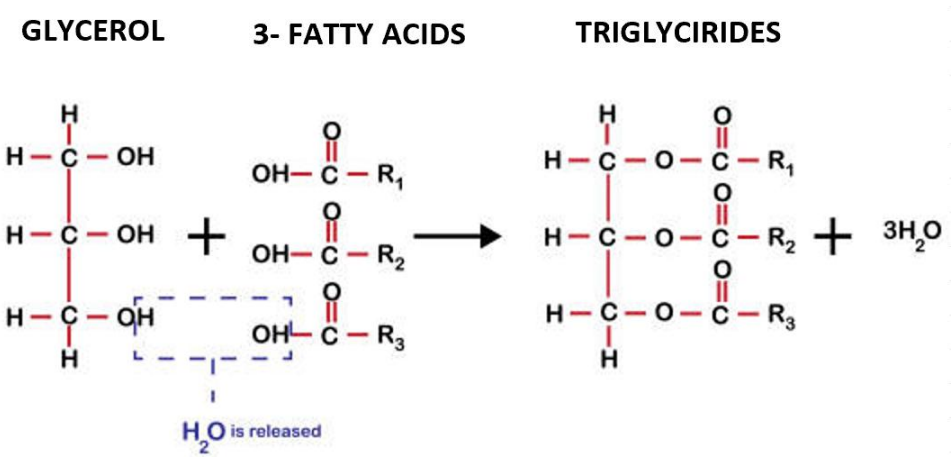

Figure 4 - TAG reaction and general molecular structure. Adapted from: Dermibas, 2008.

Fatty acids, in general, have distinguished physical and chemical properties that enable them to be suitable to biodiesel production and substitute diesel. Figure 5 presents examples of fatty acids and their molecular structures with highlight to the polarity sections of each type of fatty acid.

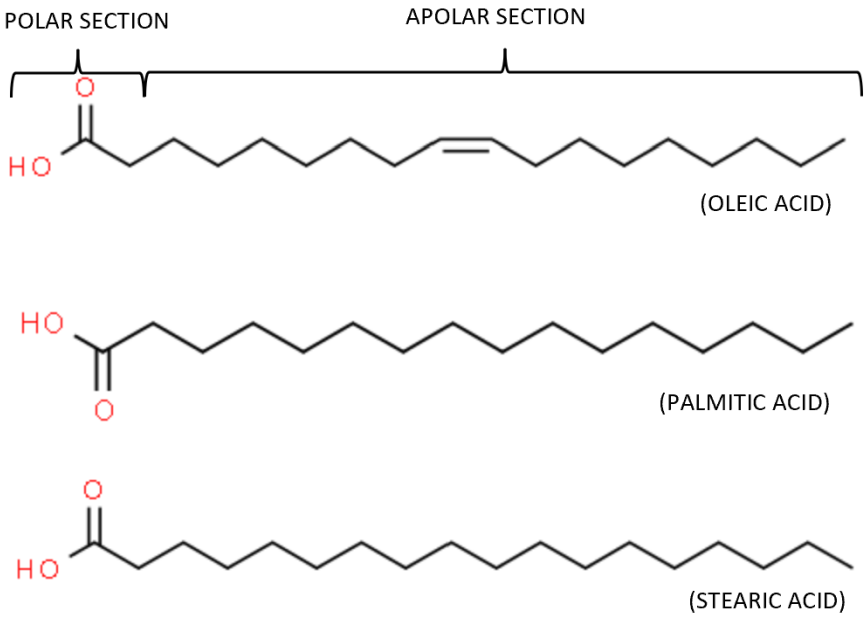

Figure 5 - Molecular structure and polarity sections of fatty acids: oleic acid, palmitic acid, and stearic acid. Adapted from: ChemSpider platform Royal Society of Chemistry (RSC).

From figure 5, it is possible to observe the difference in polarity promoted by the long apolar chain of carbons linked to the carboxyl and the other binders. The long apolar carbonic chain brings properties like miscibility and interaction with the also apolar molecules of hydrocarbons, allowing the addition of biodiesel in fossil diesel. The polar section presents amphiphilic structure, possessing both hydrophilic and lipophilic properties. Table A3 (see Appendix A) summarizes the most common types of FAs, a topic also discussed by Knothe et al., (2005).

2.3.1.2 Raw Material Pre-Treatment Processes

As previously mentioned, biodiesel can be produced from a wide variety of FAs. In Europe, colza, rapeseed, and sunflower are the most common raw material (RM) used in biodiesel production, which do not need treatment before reaction. Table A4 (see appendix A) presents the FA composition of the major RM for biodiesel production in Europe. Due to social, economic, and environmental constraints, however, there is an improved search for WFO and AF in biodiesel production (Predojevic, 2008). In Europe, more than 17 million tons of vegetable oil are consumed every year, but only 2.3% of this total amount is transformed into biofuel (Canakei, 2007).

There are not as many studies related to biodiesel production from AF, but Sharma et al.'s study has shown that the production of 5.2 million tons of biodiesel produced from AF can substitute 35, 714 barrels of fossil fuel (Sharma, Singh, & Upadhyay, 2008). Many chemical reactions take place during the frying process of vegetable oils, which alter their viscosity, FFA content, and acidity, leading a RM that is not as pure and, therefore, needs pre-treatment before going through transesterification reaction (Predojevic, 2008).

This pre-treatment process can be divided into two main steps: mechanical cleansing and chemical treatment, respectively. It starts with the removal of solid particles, the WCO is then heated to about 50 ^{o}C, following the removal of soluble particles like salt, NaCl, with liquid or vapor water. After that, WCO is neutralized with alkaline matter and reduction of FFA content through distillation; finally, WCO is dried through a vacuum (Sharma, Singh, & Upadhyay, 2008). The pre-treatment of AF starts with the removal of FFA through a saponification process in an alkaline environment and then a centrifugation process to remove the formed soap; the whole process can be disadvantageous because some of the RM is lost in the process (Chakraborty et al., 2014).

Overall, it is essential to consider the amount of water present, FFA content, and the saturation level. These characteristics are significant enough to raise technological problems, especially with the use of catalytic alkalis, such as the formation of soaps, with consequent loss of catalyst, and can also lead to the formation of solids, a significant presence of water in the raw material may also make it difficult in the separation process between glycerine and biodiesel (Sharma, Singh, & Upadhyay, 2008).

2.3.1.3 Alcohols

Methanol and ethanol are the most preferred types of alcohol used in biodiesel production (Chakraborty et al., 2014). Ethanol can be obtained through biomass fermentation, being, therefore, renewable, and more environmentally sustainable when compared to methanol, which comes mostly from petroleum products. However, ethanol leads to high miscibility between biodiesel and its by-products, making it hard to separate them after the reaction.

Despite being toxic and non-renewable, methanol is, in this case, more advantageous due to its cheap cost and favourable physical and chemical conditions. A combination of both is seen as a solution to reduce the issues raised with each one of the alcohols (Aransiola et al., 2014).

2.3.2 Biodiesel Production Pathways

2.3.2.1 Transesterification

The discovery of transesterification process aimed, at first, to simplify the extraction of glycerine during saponification since that was heavily used to produce explosives during periods of war (Gerpen, 2005). Nowadays, according to the European and American norms, EN14214 and ASTM 6751, respectively, transesterification is one of the most viable processes to obtain biodiesel.

Transesterification consists of a chemical reaction between fat (triglycerides) and alcohol (methanol or ethanol) in the presence of a catalyser. Glycerine, and fatty esters are obtained as a product, as seen in figure 6.

First, triglycerides are converted into diglycerides, then into monoglycerides, and finally yielding glycerine and fatty esters. Figure A1 (see Appendix A), presents a thorough explanation of the process, specifically in an acid medium. Due to the reaction's reversibility, excess alcohol is used. That alcohol acts as a nucleophile and, in series of reversible steps, eventually replaces the alkoxide in the ester. For each mol of triglyceride, 3 mols of methanol are consumed and 3 moles of esters are obtained (Ma & Hanna, 1999). In figure 6, R indicates different radicals composed of carbon atoms, namely CH_3.

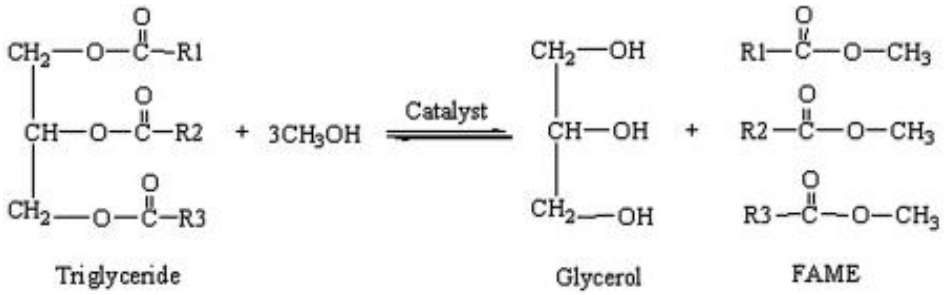

Figure 6 – Overall transesterification reaction process. Adapted from: Koberg & Gedanken (2013).

The transesterification reaction is characterized by a kinetics mathematically described by a sigmoidal function, that is, an S-curve, as seen in figure A2 (see Appendix A) resulting from the variation of the control of the reaction rate along it. The transesterification of vegetable oils as well as WCO and animal fats, starts with diffusional control due to the limitations in the mass transfer, mainly in heterogeneous catalysis, where there are three reaction phases (Puna et al., 2013). On the other hand, biodiesel itself works as a co-solvent in the reaction mixture, increasing its miscibility, and thus, after some FAME production, it is verified that the reaction proceeds at a higher speed, entering a kinetic control phase. In the final phase, the biodiesel production rate slows down again as the reaction becomes complete (Man & Hanna, 1999).

2.3.2.2 Esterification

In esterification reactions, an alcohol, most often methanol, and a FA molecule react to produce

an ester and a water molecule. Organic Chemistry LCC (2022) provided a thorough explanation of the reactional process shown in figure A3 (see Appendix A), which was first postulated by Fischer & Speier in 1895.

Basically, the process of Fischer esterification, which replaces the OH group with the OR, is an illustration of nucleophilic addition-elimination, where a strong acid like sulfuric or phosphoric acid is used in a gradual reaction carried out in reflux. According to the Le Châtelier's principle, all the processes in Fischer esterification are reversible, and the process is frequently carried out in significant alcohol excess. Depending on the physical characteristics of the constituents, the removal of water from the reaction mixture is another method to move the equilibrium forward.

From figure A3 (see Appendix A), in the first step, the electrophilic carbonyl group is activated by protonation of the C=O oxygen, thus making it more reactive towards the nucleophilic attack of the alcohol. In the second step, there is the nucleophilic addition, followed by the proton transfer in both third and fourth steps. Finally, in the fifth step the elimination of the water molecule takes place. The color-coded atoms indicate that the oxygen of the RO in the ester comes from the alcohol. In fact, it is confirmed, through the isotope label method, that the ester inherits the oxygen from the alcohol (Organic Chemistry LCC, 2022).

Simply put, figure 7 depicts the overall esterification reaction. Where, R represents the methyl groups (CH_3) attached to the end of each chain.

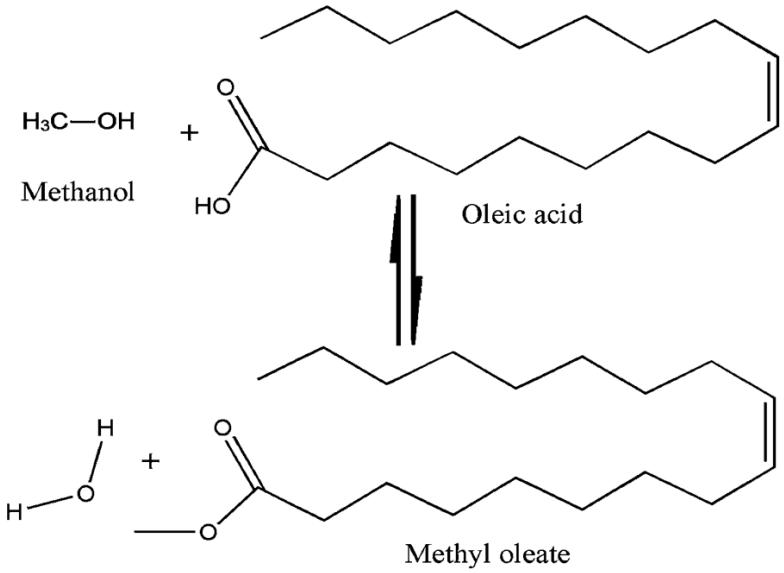

Figure 7 - Overall esterification reaction with oleic acid. (Organic Chemistry, 2022)

Sendzikiene's et al., (2004) studies have concluded that the quantity of the catalyst and the amount of oleic acid in the oil affect how quickly the esterification reaction occurs and that the ideal amount of the catalyst depends on the concentration of oleic acid.

2.3.3 Biodiesel Separation and Purification

The manufacturing of biodiesel involves two stages: a reactional stage intended to precisely alter the raw materials and produce FAMEs; and a purification step intended to produce biodiesel in accordance with the previously mentioned standards. The major goal of this procedure is to get rid of impurities that can harm the final biodiesel's quality, such as unreacted alcohol, catalysts, TGs, glycerine, FFAs, and water.

Conventional methods for separating biodiesel, including gravitational settling, decantation, filtration, and purifying it with ether and absorbents have been shown to be ineffective, time- and energy-consuming, and less economical, Atadashi et al., (2011) conclude. For the separation and purification of biodiesel, the use of separative membranes and membrane reactors holds great potential. To get beyond the typical challenges involved in both processes, membrane technology needs to be investigated and, thereafter, implemented in the industrial scale. Both traditional and cutting-edge membrane technologies utilized in biodiesel refinement have been critically analysed by Atadashi et al. (2011), Fonseca et al. (2022); Leung, Wu & Leung (2010).

2.4 Catalysis in Biodiesel Production

To increase the reaction rate, the biodiesel production, methanolysis, needs to be catalysed. In fact, catalysts can offer a different route for a certain reaction to take place with a substantially lower activation energy. Thus, affecting how quickly a reaction occurs. Since the catalyst is neither consumed nor created during the entire process, it is technically not a part of a chemical reaction. Therefore, theoretically, it should be feasible to recover completely at the end of the reaction without experiencing any mass losses or gains. To emphasize the idea that catalysts are not a part of the reaction, it is frequently stated that they are both a reactant and a product of a chemical reaction.

Catalysts can differ in their physical and chemical properties as well as how they behave under various operating conditions, as it will be explained in more depth in later in this chapter. Figure 8 presents the most common types of catalysts used in the methanolysis process. There are still many research avenues being pursued to create catalysts of different types that will favour higher yields and solve some of the primary problems the biodiesel industry is currently facing with product separation and purification.

The most common catalysts used are the homogeneous and heterogeneous depending on the production pathway. In both cases, rregardless of the catalyst's fundamental nature, the process it facilitates is controlled by the amount of acidic or basic strength present, which, in the end, determines how the reactional mechanism will take place. There are two main modern acid-base theories that can be used to evaluate and categorize a catalyst as acidic or basic: the Brønsted-Lowry theory, developed by scientists Johannes Nicolaus Brønsted and Thomas Martin Lowry, and the Lewis theory, developed by scientist Gilbert Newton Lewis and since each has its own presumptions and definitions, they can coexist.

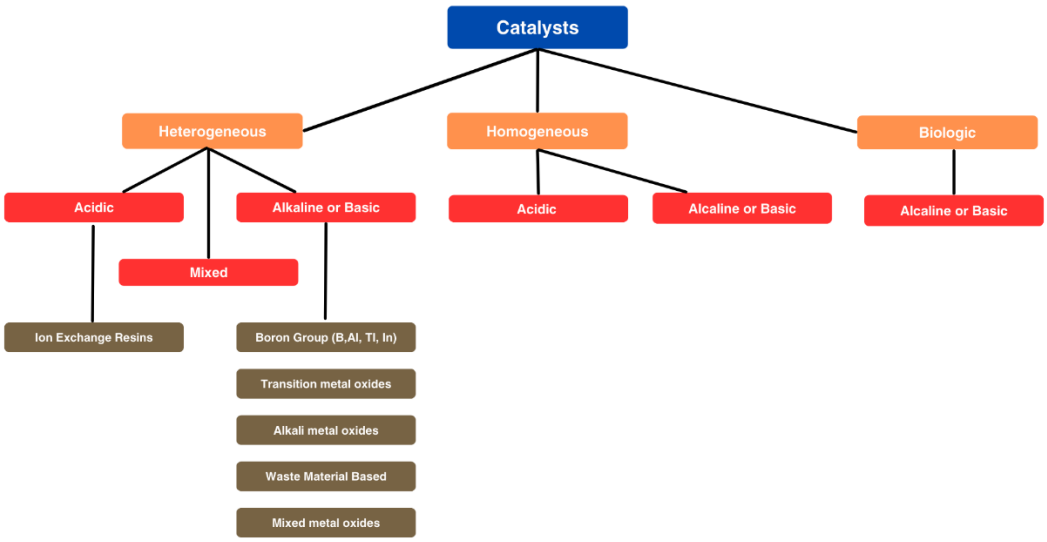

Figure 8 - Types of catalysts used in biodiesel production. Adapted from: Ruhul et al. (2015) and Ramos et al. (2019).

2.4.1 Homogeneous Catalysis

In reactions with homogeneous reactions, the catalyst is in the same phase as the reactional media, that being solid, liquid, or gaseous. By definition, the catalyst and reagents combine to create a single phase, which they do in a single phase media. According to Abdullah et al. (2017), Sharma, Singh & Korstad (2011), and Ruhul et al. (2015), homogeneous catalysts are known for potentially favoring purification and/or separation processes intended to remove it from the product stream; additionally, all those effects could be potentialized if there is an excess of catalyst in the reactional medium.

One of the greatest advantages of homogeneous catalysts is the resistance reduction of mass transfer, yielding a more efficient reaction with also higher biodiesel yield in less amount of time, Ahvad & Marchetti (2016) suggest. Nonetheless, Chouhan & Sharma (2011) argues that homogeneous environments lead to a high cost of production because they require more complex purification and separation processes and spend more energy and water for the cleansing during and after production phases.

2.4.1.1 Acidic Catalysis

In homogeneous acidic catalysis, acidic species are used to carry out the reaction, typically powerful acids like para-toluene-sulfonic acid (PTSA), hydrochloric (HCl), sulfuric (H_2SO_4), hydrofluoric (HF), and phosphoric (H_3PO_4). Its ability to catalyze both esterification and transesterification reactions is one of its key advantages, as noted in table A5 (see Appendix A) in the work of Abdullah et al. (2017) and by many other authors including Avhad & Marchetti (2015); Demirbaş (2008); Knothe, Van Gerpen & Krahl (2005); Ma & Hanna (1999).

In biodiesel production, acidic homogeneous catalysis occurs in a liquid phase and this method tends to be faster in esterification reactions than in esterification ones. In fact, acidic catalysts are preferred when transforming RM of low quality like WCO and AF, yielding final products of superior value than those of basic catalysis. However, acidic catalysis is around 4000 times slower than the basic one, needing higher temperatures, more expensive equipment, higher methanol: fats ratios, higher catalyst quantity, and higher reaction time (Ahvad & Marchetti, 2016). A study conducted by Leung & Leung (2010) shows that it is needed 30 times more methanol to oil to yield the same amount of product through acidic catalysis.

Additionally, acidic homogeneous catalysts can effectively deal with the FFA and water content in feedstocks without impairing their activity and do not promote soap formation during reactions. However, corrosion of the equipment, difficulties in recovery and reuse, and the requirement for post-reactional operations like washing and cleaning to alkalinize the medium and erase signs of its use are also considered negative characteristics of acidic catalysts.

Due to the catalysts propensity to split into ions in an aqueous media, all the aforementioned examples of acidic catalysts are known as strong acids and are, hence, Brønsted-Lowry acids. This property is important for the generation of biodiesel since the acidic reactional mechanism depends on the proton H+ initiating the reaction.

According to Di Serio et al. (2005), homogeneous Lewis acidic catalysts are coordinatively unsaturated cationic sites, which leave the exposed M+ ion to interact with guest molecules and act as the acceptor of the electron-pair. They are typically metal complexes, stearates, and acetates of calcium (Ca), barium (Ba), magnesium (Mg), cadmium (Cd), lead (Pb), zinc (Zn), cobalt (Co), and nickel (Ni). M. Di. Serio et al. (2005) also states that because acidic homogeneous catalysts particularly target the carboxyl, esterification and transesterification pathways essentially mirror one another.

For acidic catalysis, the proton H+ released from the acid attacks the carboxyl's nucleophilic oxygen, bonding with it to cause the double bond between the carbon and oxygen to break. By doing that, the carbon, which only has three bonds, becomes electrophilic and is then accessed by the oxygen from the electron-rich alcohol molecules, establishing a fourth bond. This results in the formation of an unstable tetrahedron intermediate, which is released from the TG along with a proton H+ by moving a proton from the previous carboxyl oxygen to the other one linked to the same carbon. Additionally, the entire procedure is repeated until all three FAs have been eliminated and a glycerol molecule has been released.

2.4.1.2 Alkaline or Basic Catalysis

Alkaline homogeneous catalysis occurs in the same medium as the primary reaction, liquid for biodiesel. As the name implies, this kind of catalysis uses basic species to drive the reaction, primarily strong bases like sodium (NaOH) and potassium (KOH) hydroxides, two strong bases, and basic Brønsted-Lowry catalysts. Some authors including Helwani et al. (2009), Knothe, Gerpen, and Krahl (2005), Ma & Hanna (1999), and many others have referenced these two catalysts as the most commonly used worldwide.

Homogeneous alkaline catalysts include a catalysis speed times higher than that of an acid catalyst, under alike process circumstances (Moser, 2016). However, Maleki, Ashraf Talesh, & Mansouri (2022) affirm that such catalysts can lead to soap formation if the FFA amount of the triglyceride sources is >2%. This may reduce the amount of final product available and even hinder post reactional procedures like separation and purification. Overall, homogeneous alkaline catalysts are very hard to be recovered and reused, and lead to huge amounts of waste water for catalyst removal and cleaning.

In homogeneous alkaline reactions, OH^- or RO^- are the active species (Dharma et al. 2016), in which, at the beginning of the reaction, the alkaline generates alkoxide ion RO^-, allowing nucleophilic raid on the carbonyl functional group of the triglyceride through alkoxide ion to occur, making a tetrahedral intermediary carried via rearrangement of the intermediate creating fatty acid alkyl ester. This procedure is then duplicated twice generating three molecules of fatty acid alkyl ester or biodiesel and one molecule of glycerol or water, depending on the type of reaction, as the by-product (Maleki, Ashraf Talesh, & Mansouri, 2022).

Investigations conducted by Deng, Fang, & Liu (2010); Deshmane, Gogate, & Pandit (2009); Georgogianni et al., (2009); and Thanh et al., (2010) revealed that biodiesel yields catalyzed by homogenous alkaline catalysts are above 90% despite the type and source of raw material; adding that

the optimal catalyst amount differed from 0.2 to 2 wt% through various reaction times. The studies also reaffirmed that this type of catalysis decreases the reaction times, as compared to acid catalysis to acquire a similar yield.

2.4.2 Heterogeneous Catalysis

Heterogeneous catalysis is distinguished by the presence of a catalyst and reagents that take place in a separate media. Theoretically, this catalysis occurs at the interface between two phases, such as solid-liquid, solid-gaseous, or liquid-gaseous, and for that, active sites are required since molecules must adsorb on them in order to initiate reaction. The coexistence of three phases in the reactional medium, one solid, from the catalyst, and two liquid, from the two reagents, alcohol and FA or TAG, initially immiscible lead to a more complex environment that can bring issues related to diffusion and mass transfer (Leung, Wu & Leung 2010). Adsorption of reagents and desorption of products must, therefore, take place on the surface in order to achieve a quicker reactional process. According to Sharma et al. (2011) and Helwani et al. (2009), this sort of catalyst is made up of active sites of two types, Brønnsted-Lowry or Lewis, and can thus be acidic, alkaline, or even bifunctional.

Although heterogeneous catalysts have lower activity and higher reaction time than homogeneous catalysts, they are still very relevant in catalysis because they, after reaction, can be easily separated and even recycled, as addressed by Piker et al. (2016) and Sharma, Yogesh, Singh, and Korstad (2011). This may lead to minimizing post-reaction procedures, such as washing and neutralization as well as preventing side reactions such soap formation and emulsions. Filtration makes it simple to separate them from the liquid medium.

Heterogeneous catalysts can have low corrosivity and toxicity rates compared with homogeneous catalysts. Also, in transesterification reactions, heterogeneous processes can yield glycerine with purity levels greater than 98% while homogenous processes yield glycerine with only an 80% level of purity. Despite all the advantages of heterogeneous catalysts, their high complexity and long reaction time lead to the use of homogeneous catalysts in the industrial setting, however, new research is being done to effectively transition industrial production to the use of heterogeneous catalysts that also lead to the valorisation of crude glycerine (Ahvad & Marchetti, 2016). For example, the use of heterogeneous nanocatalysts, which have a large surface area and suitable catalytic properties, can overcome the drawbacks of such catalysts.

2.4.2.1 Acidic Catalysis

In the context of heterogeneous acid catalysis, a carbocation is formed which because of the assault of alcohol provides promotion to the tetrahedral intermediary which deprives glycerol and forms a novel alkyl ester, leading to regeneration of the catalyst (Maleki, Ashar, & Mansouri, 2022). Considering the outline, adsorption of triglyceride or alcohol under certain circumstances takes place at the energetic sites of the solid catalysts depending on the kind of heterogeneous catalysts (Booramuthy, 2020).

Heterogeneous acidic catalysts are usually made up of heteropoly acids, zeolites, and modified transition metals like silica, alumina, zirconium, and molybdenum (Gupta & Singh, 2023). In fact, metal oxides like pure and sulfated tin oxide (SnO_2) supported on alumina or silica, Beta zeolite (β) promoted with Lanthanum (La), rich in Brønsted-Lowry sites, ZSM-5 zeolite, rich in Brønsted-Lowry and Lewis acidic sites, and mordenite zeolite reached relevant conversions in methanolysis reaction (Cruz et al. 2019). These catalysts are more stable and environmentally benign than homogenous acid catalysts (Ahmad & Muraza, 2014).

Under mild conditions, solid acid catalyst is discovered by Mardhiah et al. (2017) to be a viable catalyst for the esterification process. Moreover, in order to avoid diffusional problems, a heterogeneous acid catalyst should have significant active sites, be porous, and be water-repellent (Ahvad & Machetti, 2015).

Heterogeneous acid catalysts convert microalgal lipids into biodiesel via a one-step method, and have a lower environmental impact than homogeneous catalysts. Yuan et al. (2019) synthesized a $SO_4$2-/TiO_2 – SiO_2 catalyst, Guldhe et al. (2017) synthesized a WO_3/ZrO_2 catalyst for microalgal biodiesel production, and Xie & Yang (2012) synthesized a WO3/AlPO4 catalyst for transesterification of soybean oil. Ibrahim et al. (2020) used a sulfonated carbon-based catalyst to catalyse the esterification of palm fatty acid distillate with the conversion efficiency of 85%, and Endut et al. (2017) used a solid acid catalyst derived from coconut shell for transesterification of palm oil, but despite the positive results, these catalysts were expensive to prepare. Therefore, there is still a need to investigate more affordable and equally efficient solid catalysts.

2.4.2.2 Alkaline or Basic Catalysis

Heterogeneous alkaline catalysts can be classified into five main types: single metal oxides, doped and mixed metal oxides, zeolites, supported alkali and alkaline earth metal oxides and hydrotalcites (HT). Examples of this type of catalysts are present in table A5 (see Appendix A). Basic zeolites and single and mixed oxides not supported or supported on γ-alumina (Al_2O_3) are commonly applied as catalysts for biodiesel (Prestigiacomo et al., 2022).

In heterogeneous alkaline catalysis, first, there is an adsorption of alcohol to the alkaline sites on the catalyst surface, then there is a reaction of the carbonyl group with alcohol molecules, generating mono-alkyl esters and glycerol, and finally, re-accessibility of the alkaline site on the solid catalyst surface occurs. Consequently, in moderate reaction conditions, shorter time, and lower alcohol concentration is required for the transesterification process in the attendance of heterogeneous alkaline catalysts make them potential catalysts to be used in industrial scale (Maleki, Ashraf Talesh, & Mansouri, 2022). The Brønsted-Lowry basic sites, oxygen species, and Lewis acidic sites, metal species, are both present in the structures of alkali and alkaline earth metal oxides (Endalew, Kiros, and Zanzi, 2011b). Alkaline heterogeneous catalysts, however, are not suitable for esterification reactions.

Mootabidi et al. (2010) investigated the transesterification of palm oik in the presence of alkaline earth metal oxide catalysts, where the catalytic activity was in the sequence of CaO < SrO < BaO. Jamil

et al. (2021) reported the synthesis of carbon-based catalyst modified by alkaline earth metal oxides for biodiesel production with a FAME yield of 94.27% at normal conditions. Sarkar et al. (2023) studied the calcination of biomass *Parkia speciosa* to act as an alkaline catalyst for the biodiesel production with a FAME yield of 96.4% at mild conditions. Overall, alkaline heterogeneous catalysts are very promising through much more research needs to take place for the optimization and implementation of them in the biodiesel industry.

2.4.2.3 Bifunctional Catalysis

Alkaline catalysts and high FFA feedstocks contribute to soap formation and emulsification in biodiesel production. For such reason, it is important to study a new catalyst that can facilitate both FFA esterification and triglyceride transesterification reactions at the same time. Hence, bifunctional heterogeneous catalysts offer many desired characteristics, including the ability to process high FFA feedstocks in a single reaction step and possibly reducing production costs while increasing efficiency (Mulyatun et al., 2022).

Bifunctional catalysts have both acidic and basic active sites. Lee, Juan, & Taufiq-Yap (2015) and Endalew, Kiros, and Zanzi (2011a) explain that a bifunctional catalysts can be made up of a metal oxide with Brønsted-Lowry and/or Lewis acidic sites derived from transition metals like zirconium (Zr), zinc (Zn), iron (Fe), and tin (Sn) and a metal oxide that has Brønsted-Lowry basic sites from earth metals like Ca and Mg.

Overall, a catalysis that is capable of carrying both esterification and transesterification due to the presence of acidic and basic active sites is very advantageous since it has both economic and environmental benefits. Several bifunctional catalysts, such as bismuth oxide (Bi_2O_3) supported on lanthanum oxide (La_2O_3), and La_2O_3 supported on CaO, zinc oxide (ZnO) and alumina, are reviewed in the work of Mardhiah et al. (2017). Further examples are found in Table A5 (see Appendix A).

2.4.3 New Technologies

Given all the aspects previously covered on catalysts, biodiesel, and their benefits and drawbacks, there is definitely a movement toward new or improved types of catalysts. With aims to lower costs, decrease environmental impact, and improve properties, new technologies have been investigated. Most of them are focussed on sustainability and waste valorisation, using the available resources and/or wastes produced in various economic sectors.

The search for new heterogeneous catalysts for the production of biodiesel from source residues is at the forefront of a new wave of technological developments studies in many universities and research institutions across the world. Later in this chapter, low-cost catalyst alternatives will be discussed.

2.4.3.1 Alternative Catalysts

Low-cost catalysts are usually derived from industrial residues or from dwelling wastes, discerning from the most traditional sources of catalysts, which come from industrial processes and are well established on a commercial scale. In fact, there are several research papers and reviews on this topic, e.g. Li et al. (2019); Do Nascimento et al. (2011); Alsaiari et al. (2023); Catarino et al. (2017); Clohessy & Kwapinski (2020); Aransiola et al. (2013); and Lee et al. (2014).

As an example, Li et al. (2019) studied Li/NaY zeolite catalysts with different molar ratios of Li_2CO_3 to NaY zeolite synthesized from fly ash residues by hydrothermal and microemulsion-assisted co-precipitation method. Under the normal conditions of molar ratio of Li_2CO_3 to NaY zeolite of 1:1, calcination temperature of 750 °C and calcination time of 4 h for catalyst preparation, there was a fatty acid ethyl ester (FAEE) yield of 98.6%, showing that the catalyst has excellent stability, including air tolerance and reusability, and a regenerative capacity, which are crucial for industrial applications.

Do Nascimento et al. (2011), investigated catalysts for the esterification of oleic acid with methanol prepared from two Amazon kaolins (Century and *flint*) and two standard kaolins (KGa-1b and KGa-2) that were thermally treated at 950 °C and leached with 4 M sulfuric acid solutions. After the experiment, kaolin was found to be a promising raw material to produce new solid acid catalysts while Amazonian *flint* kaolin was found to be amenable to production. These are low cost catalysts that have a huge potential in the industry however, geographic availability of the RM may be a drawback.

Moreover, a newly novel hydroxyapatite heterogeneous catalyst was investigated by Alsaiari et al. (2023). The catalysts were obtained from waste camel bones. The waste bones were dried to remove moisture and then calcinated. A FAEE yield of 89 wt% was achieved after transesterification with normal reaction conditions; that is, 4 wt% catalyst, oil to ethanol molar ratio of 1:7 and temperature 75 °C, and 3 h reaction time. Fuel properties of FAEE complied with ASTM D 6751 – as described on table A3 (see Appendix A) - proving that it would be a feasible alternative form of fuel. Overall, producing biodiesel from waste and untamed resources promotes a sustainable energy strategy.

Catarino et al. (2017), also researched the production of biodiesel with calcium rich food wastes, such as mollusc, shrimp, egg shells, derived alkaline heterogeneous catalysts. The catalysts were considered to be effective in catalysing the methanolysis of soybean oil, with a FAME yield of 96% after just 2.5 hours of reaction. When using WCO, however, the FAME yield was only 65% with simultaneous production of soap. The study indicated that the use of WCO and soybean oil mixtures attenuates the loss of catalytic performances.

Some research is also taking place in the biodiesel sector to devise acidic heterogeneous catalysts, which can be advantageous in biodiesel production. Clohessy & Kwapinski (2020); Aransiola et al. (2013); and Lee et al. (2014) reviewed the use of carbon-based catalysts prepared from wastes of different sources, such as agricultural crops, algae and biodiesel production by-product (glycerine). These RM, after partially carbonized and treated with a H_2SO_4 turned into a high quality material for FFA esterification. These particular studies led to a more in-depth investigation, in the next section, of glycerine, a biodiesel by-product, and alike carbon hydrates as RM for acidic heterogeneous catalysts.

2.5 Carbon Sulfonated Catalysts

Sulfonated carbons are a group of metal-free solid acidic catalysts that can be described as having SO_3H – functionalized acidic carbon materials with Brønsted acidity equivalent to concentrate H_2SO_4 while maintaining their original carbon structure (Changmai et al., 2020).

Additionally, sulfonated catalysts' elements are disposed in an amorphous structure of turbostratic polycyclic aromatic layers. In general, short chain carbohydrates of various sources, including sugars, are considered to be great precursors for preparation of these catalysts. Figure 9 illustrates the synthesis of sulfonated carbon derived from sucrose. The reaction mechanism involved in this process consists of partial carbonization accompanied by dehydration of the precursor and dissociation of the -C-O-C- bonds, forming aromatic polycyclic carbon rings, obtaining amorphous carbon; -SO3H groups are simultaneously introduced into the carbon rings by sulfonation. In the sulfonation reaction, oxidation of the aromatic carbon rings occurs, so that the sulfonic groups are covalently bound to the carbon-based and other oxygenated groups are formed during sulfonation (Fonseca et al., 2022).

Moreover, the acid feature is due to the presence on its surface of three main acidic groups with different strengths: carboxylic acid (–COOH), phenolic acid (– OH) and sulfonic acid (–SO_3H), as seen in figure 9. Sulfonated carbons differ from other acid catalysts by the presence of yet another acid group on their surface. These materials can incorporate hydrophilic molecules, such as water, on their surface due to the presence of hydrophilic groups (–COOH and –OH). Therefore, the reaction reagents have easy access to the sulfonic group, responsible for the catalytic activity, increasing the reaction rates, even in materials with a small surface area (Fonseca et al., 2022).

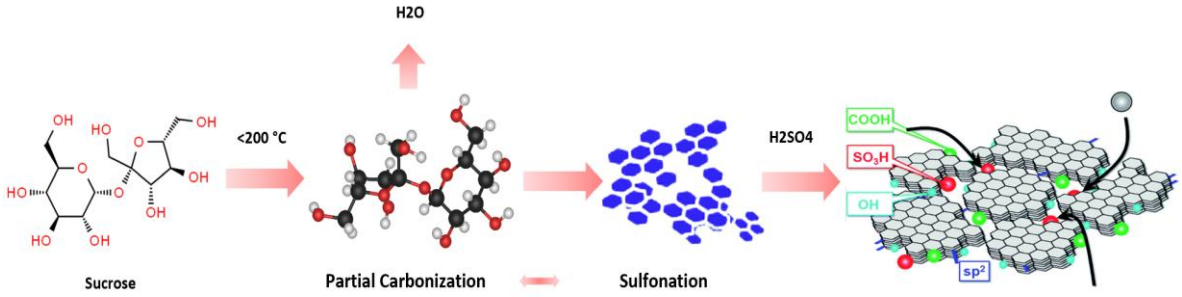

Figure 9 – Synthesis of sulfonated carbon catalysts from sucrose. Adapted from: Toda et al. (2005).

Segunuma et al. (2008) prepared a carbon material functionalized with –SO_3H groups by fuming sulfuric acid as the –SO_3H source, producing an amorphous carbon consisting of – SO_3H, –COOH and phenolic OH-bearing nanographene sheets in a considerably random manner. The prepared sulfonated carbon-based material exhibited much higher catalytic activity for the esterification of oleic acid with methanol than other conventional solid Brønsted-acid catalysts including niobic acid or sulfonated polystyrene-based cation-exchangeable resins. In fact, the catalyst was 60% as active as H_2SO_4 under the same reaction conditions (Su & Guo, 2014). It is argued that the strong acidity of the catalyst might be since some of the –SO_3H groups in the carbon materials are linked by strong hydrogen bonds, which

can result in strong acidity due to mutual electron withdrawal.

After research, Zong & Smith (2007) have reported that a sulfonated D-glucose-derived sugar catalyst showed higher catalytic activity towards esterification of palmitic acid, oleic acid and stearic acid with methanol compared with niobic acid, Amberlyst-15, and sulfated zirconia. Moreover, it had excellent operational stability, and after more than fifty cycles of successive re-use, it still retained a remarkably high proportion (93%) of its original catalytic activity in the methyl oleate formation reaction. Therefore, sugar catalysts are very promising to replace H_2SO_4 as a green catalyst for efficient production of biodiesel from higher fatty acids and especially waste oils with a high acid value (Nakajima & Hara, 2012).

Since it is well established the strong catalytic activity of sulfonate carbons, it is now important to investigate precursors of low cost and easily accessible for the production of these catalysts. Devi et al. (2009) suggested that glycerol is heap raw material that can be used as a base for a carbon catalyst with a high density of sulfonic acid groups (SO_3H) and it is regarded as an efficient solid-acid catalyst from its esterification activity and reusability. Therefore, in the next section, glycerol, a biodiesel by-product, will be explored as a potential precursor to sulfonated catalysts.

2.5.1 Catalyst Precursors: Glycerol

Glycerol, also known as glycerine, is an organic compound containing multiple hydroxyl groups that is an odourless, colourless, viscous liquid, with a sweet taste, and non-toxic and can be obtained as a biodiesel production by-product. With the increase of biodiesel production, glycerine from biodiesel has become the main source of glycerine in the world (Ciriminna et al. 2014). As seen in figure 10, as of 2024, more than 4 million tonnes of glycerol will have its source from biodiesel production alone.

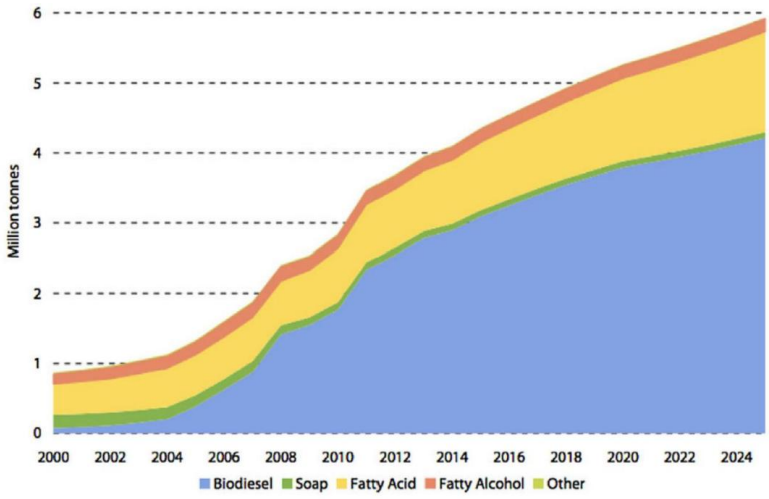

Figure 10 – World crude glycerol production by sector from 2000 to 2024. (Ciriminna et al. 2014)

The global production of glycerol from biodiesel has flooded the market and has diminished its economic value (figure 10). As of 2020, crude glycerol's was expected at $0.20 per pound while it was commercialized at $0.70 before the biodiesel production expansion in 2005 (Saifuddin, Hussein, & Ong, 2018). To put into perspective, glycerine production has climbed from 200 thousand tones in 2003 to

more than 2 million tones. Therefore, traditional market usages for refined glycerol around the world are no longer capable of absorbing this surplus, and most key players have, in fact, exited the market (Ciriminna et al., 2014).

To absorb the glycerine surplus, developing new chemical uses of glycerol has become a priority. As a matter of fact, the number of research papers dealing with new usages of crude glycerol published annually between 2005 and 2015 doubled to more than 7000, and several new catalytic routes to high added value products are in course to be discovered, improved, and applied, Ciriminna et al. (2014) affirms. For such reasons, the development of sulfonated carbons based of crude glycerine would be a great way to valorise this biodiesel by-product and promote a more circular economy in this sector. Figure A4 (see Appendix A) displays a schematic of the overall process of glycerine valorisation in biodiesel production.

2.5.2 Other Catalyst Precursors

Besides glycerol, other compounds of similar chemical composition have been considered for the production of solid acidic catalysts via partial carbonization an sulfonation. To reduce the cost of biodiesel production, several sulfonated raw biomasses have been prepared and investigated for their catalytic activities. Sugarcane bagasse, corn straw, bamboo, bio-glycerol, microalgae residue, oil cake waste, pine chip char, and biochar were reported by Changmai et al. (2020) as potential catalysts for FAME production. Researchers, including Toda et al. (2005), Devi et al. (2009), Nata et al. (2017), Zhang et al. (2020), have conducted extensive, yet individual, investigations on the referred precursors.

For instance, in a pioneering work towards the preparation of the biomass-based sulfonated carbon catalyst, Toda et al. (2005) synthesized the sulfonated carbon catalyst by partial carbonization and sulfonation of sucrose. From that, high grade biodiesel was produced by esterification of the vegetable oil constituents oleic and stearic acid.

Likewise, Nata et al. (2017) obtained carbon sulfonated catalysts by hydrothermal carbonization and sulfonation of glucose, through which esterification of WCO with methanol was easily achieved. The sulfonated carbon-based solid acid catalyst was thus designed to be an active, stable and reusable solid acid as an environmentally benign replacement for homogeneous.

Nonetheless, none of the mentioned research has combined their findings and measured the effectiveness of these catalysts among them based on same conditions including ratio, time, and type of reaction (Changmai et al. 2020). It is anticipated that a number of these catalysts will assume a key role in the near future and aid in the production of biodiesel using environmentally benign and commercially viable techniques, so it is crucial to thoroughly investigate and optimize them.

Although recent developments in the creation of various acidic heterogeneous catalysts suggests a promising future for the biodiesel industry, more work is still needed to create even more efficient and affordable catalysts, which will help resolve the current problems with all of the aforementioned catalysts and boost the effectiveness of sustainable biodiesel production.

Chapter 3

Experimental Procedures and Methodology

3.1 Experimental Procedures

3.1.1 Heterogeneous Catalyst Preparation

For the catalyst preparation, the following precursors were used: sucrose, glycerine, glucose, and xylitol. These precursors were combined with sulfuric acid (H_2SO_4) at different proportions. Table 1 presents the information on the masses and proportions used for each sample. Each sample was prepared at least two times for accuracy. Therefore, the masses of precursors presented are an average of all the used masses.

Table 1 – List of precursors and conditions used in the catalyst preparation.

Name	Chemical Formula	Structure	Molar mass (g/mol)	ratio	Mass of precursor (g)	Mass H_2SO_4 (g)	Temp. (°C)	Time (min)
Sucrose	$C_{12}H_{22}$	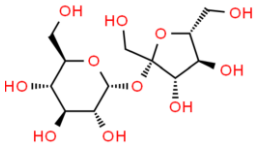	342.3	1:1	174.5	50	150	45
Sucrose				1:4	43.6	50	150	30
Glycerin	$C_3H_8O_3$	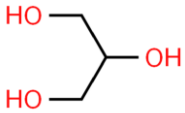	92.09	1:1	46.9	50	150	120
Glycerin				1:4	23.5	100	150	100
Glucose	$C_6H_{12}O$	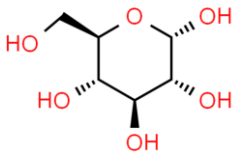	180.15	1:1	91.8	50	150	75
Glucose				1:4	45.9	100	150	60
Xylitol	$C_5H_{12}O$	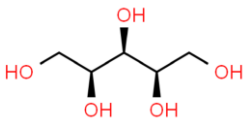	152.15	1:1	77.6	50	150	80
Xylitol				1:4	38.8	100	150	75

To prepare the catalyst, the reactants were weighted and placed in a 2L beaker. The beaker was then placed on a heating source and stirred with a glass rod. The temperature increased gradually (to avoid rapid decomposition) on the hot plate. When the temperature reached a certain degree, depending on the precursor used, carbonization started to occur, resulting in the formation of a black gelatinous and foamy carbonaceous material. As carbonization took place, at a relatively constant temperature, sulfonation also took place.

After some time, depending on the type of reactant, the carbonaceous material became sandy in texture, like a black powder, as seen in figure 11a.

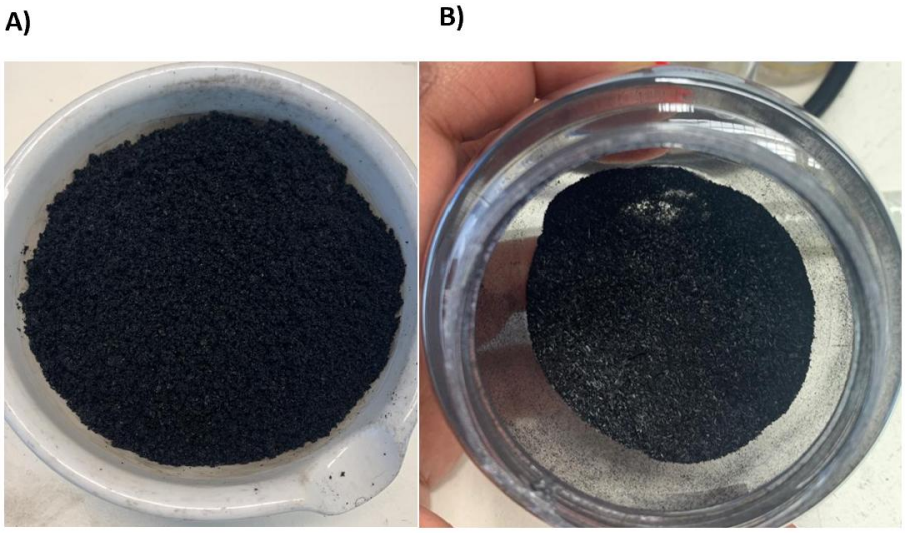

Figure 11 - A) Partially carbonized and sulfonated catalysts before drying. B) Heterogeneous catalyst after drying and ready to use.

The mixture was cooled to room temperature. Then, the product was washed and filtered with distilled water to separate the solid carbonized and sulfonated material from the remaining solution and to remove any residual reactants or by-products. The filtered carbonized and sulfonated product was dried in oven for 24 hours at low temperature to remove any remaining moisture. The final product is seen on figure 11b.

3.1.2 Biodiesel Production: Experimental Conditions

3.1.2.1 Oleic Acid Preparation

Oleic Acid, 99% pure, was used for the esterification reactions. In fact, oleic acid was dried, to remove the 10% moisture, in 200 mL batches in a *Rotavapor® R-100* with reduced pressure (around 160 mmHg) for about 1 hour, as seen in figure 12. Some reactions took place with oleic acid 90% for comparison reasons.

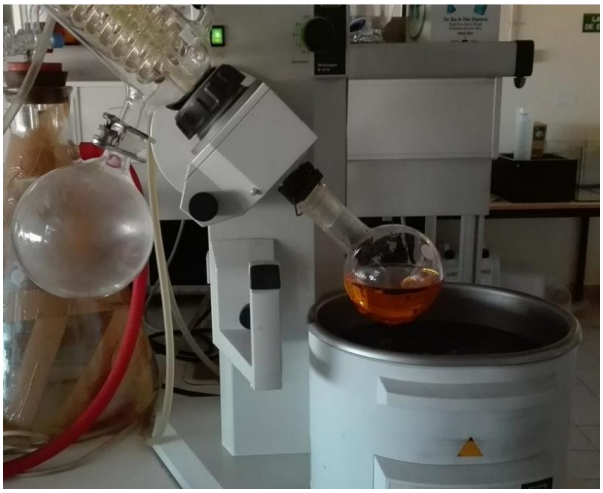

Figure 12 – Rotavapor® with reduced pressure used for oleic acid drying.

3.1.2.2 Esterification: Experimental Conditions

The biodiesel production was done with treated oleic acid. The raw material was used for a esterification methodology in a laboratory scale scheme, as described in Figure 13.

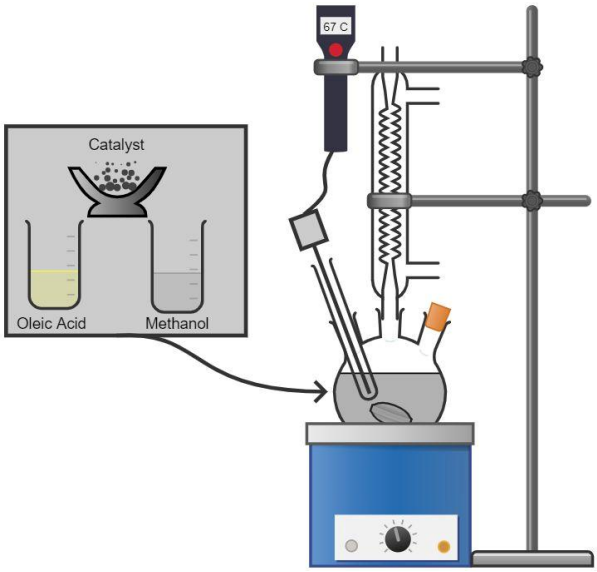

Figure 13 – Biodiesel production setup. Source: Author and Chemix Lab Diagrams

The reactional parameters and conditions were defined and standardized throughout all the experiments. It was defined a pre-conditioning step for the raw material of 50g for 30 minutes at 70°C and a reactional temperature at 67 °C – methanol total reflux condition – under vigorous mixing, around 1000 rpm. The methanol: oleic acid molar ratio is 12:1 (molar excess of 200%). The catalyst amount in % wt. was 5 for all samples and the reactional time was 3 hours. Also, a preconditioning step, contact step, at 65 °C for 30 minutes between methanol and the catalyst was used to promote the formation of methoxide ionic species. Each experiment was repeated at least 2 times to evaluate and confirm the repeatability of the results. The Standard conditions for the esterification reaction is summarized in table 2.

Table 2 – Standard conditions for the experimental esterification reactions.

Mass of oleic acid (g)	50
Methanol:oleic acid ratio	12:1
Mass of catalyst (% wt.)	5
Temperature (°C)	67

After each transesterification reaction experiment, the medium was vacuum filtered with a Büchner funnel to remove the catalyst and transfer the liquid phase to a decantation funnel to promote the segregation of water and the esterification liquid product. After certain time, 12-24 hours, the water and the possible methyl oleate were separated and safely stored for further characterizations. Figure 14 presents a sample of esterification product and water in separation funnel.

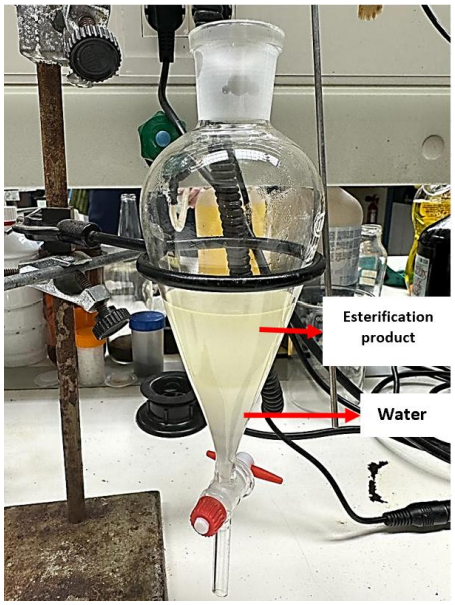

Figure 14 – Esterification product during separation process.

The heterogeneous catalyst after filtration was dried in a laboratory oven at 60°C during 24 hours to promote the evaporation of unreacted reagents (e.g. methanol) and water. After that, it was stored for further analysis to evaluate its physical aspect, loss of crystallinity and the possible reuse after a simple cleaning procedure to remove any retained residues, such as water, oil, and ester.

3.2 Methodology

3.2.1 Fourier Transform Infrared (FTIR) Spectrometry

The Fourier Transform Infrared Spectroscopy (FTIR) is a simple method in which information about many functional groups can be identified in a given sample. FTIR Spectroscopy is applied in micro analysis where high sensitivity is required, in the analysis of aqueous solutions or dark, solid state samples, which is the case of chars, that requires the use of special reflectance techniques. In contrast to a dispersive instrument, where the interacting energy takes on a certain wavelength range, FTIR spectroscopy involves the interaction of an interference wave with the material where the interferometer is managed by a computer, which is also used to gather and store data and carry out the Fourier transformation. The computer also carries out post spectroscopic tasks like spectrum display, resolution improvement, calibration, and correlation equation calculation (Faix, 1992).

In this study, the absorption spectroscopy experiments involve the mid range of infrared radiation (MIR), between approximately 400 and 4000 cm^{-1}. This is the range where most of the molecular vibrations absorb light, and the most commonly used in biodiesel and catalyst characterization (Zaera, 2014). In fact, raw oils and the methyl esters are noted as very strong absorbers in the infrared region of the electromagnetic spectrum (O'Donnell, 2013). On the other hand, this very nature of the bonds, together with the molecular environment in which they are insert, results in obtaining a unique spectra for each molecule or adsorbate, giving them a "fingerprint" information (Zaera, 2014).

For the characterization of the biodiesel and catalyst samples, before and after the reaction, a single horizontal reflection equipment, HATR, was used with an Attenuated Total Reflection, between 4000 cm^{-1} and 400 cm^{-1}, in most cases. For this study, the integration of the side (1750 – 1760 cm^{-1}) of the carbonyl peak is used to monitor the progress of the biodiesel reactions (O' Dannell, 2013). In theory, the presence of a board band signal between 2500-3300 cm^{-1} indicates the presence of FFA and moisture in oleic acid. The peak at around 1436 cm^{-1}, of the methyl ester (OCH_3) is very narrow and moves along the raw oil peak, making it unattractive for monitoring the progress of the biodiesel reactions; however, this measurement gives a direct indication of the attachment of the alkyl groups of the alcohol with the fatty acids of the triglycerides without the influence of the alkyl group (- CH_3), as explained by Ivanoiu et al. (2011), which can also be significant for the purpose of this study.

Despite the fact that this method is highly used in laboratorial routine, there are still some setbacks related to its sensitivity due to background "noise" (Zaera, 2014). For such reason, all FTIR data were treated by the *Kubelka-Munk* method, expressed by Equation 1, with R corresponding to *Reflectance* and I corresponding to *Intensity*. This method allows noise attenuation, improving the reading of the spectra.

$$I_{correct} = \frac{(1-R)^2}{2R} \qquad \textbf{Equation 1}$$

The *Kubelka-Munk* model has been widely used in many industries for many years due to its explicit form, simple use and its acceptable prediction accuracy. It is used for multiple-scattering calculations in biodiesel and catalysts among many other liquid or solid samples (Džimbeg-Malčić, 2011).

3.2.2 FAME Yield

In this study, the FAME yield was done by an analysis of the FTIR spectra produced based on the differences between the oleic acid spectrum and the esterification product, methyl oleate (ME), spectrum. There are existing technical standards from ASTM International (2014) and DIN (2014) that outline the process for FAME determination using FTIR. These standards are known as "ASTM D7371-14 – Standard Test Method for Determination of Biodiesel (FAME) Content in Diesel Fuel Oil Using Mid Infrared Spectroscopy (FTIR-ATR-PLS Method)" and "DIN 14078 – Liquid petroleum products – Determination of fatty acid methyl ester (FAME) content in middle distillates – Infrared spectrometry method," respectively. Nonetheless, in this work, the methodology used for measuring FAME yield differs somewhat from the two methods described above in terms of the spectrum range and procedure employed. Moreover, there are several researchers invested in devising new techniques to optimize the FAME yield determination including Vergas et al. (2020), Mello et al. (2008), Cruz et al. (2019), and Aliske et al. (2007).

A disadvantage of FAME determination by FTIR is the lack of capacity for quantifying MAG and DAG separately. Nevertheless, every section chosen is directly connected to the molecular vibration patterns of each species involved in the analysis, not only FAME molecules, but also glycerol, MAG, DAG and TAG since the esterification reaction incurs molecular modifications that influence the FTIR spectrum.

The FAME yield quantification was evaluated by using the spectrum range between 1775 cm^{-1} – 1725 cm^{-1}. The calculation methodology was based on the area ratio of a specific peak at 1741 cm^{-1} . Gaussian functions were used to fit the sole peak at 1741 cm^{-1} as well as to cover the whole 1775 – 1725 cm^{-1} FTIR spectrum at maximum to obtain a very precise area value when compared to the area calculated using integration techniques, Trapezoid rule, with experimental data existent. Figure 15 presents the obtained curve for FAME yield calculations.

To obtain the FAME yield result an exponential equation holding parameters obtained from a calibration curve for biodiesel FAME yield using biodiesel patterns in different ratios, 0% up to 100% for FTIR FAME yield measurements.

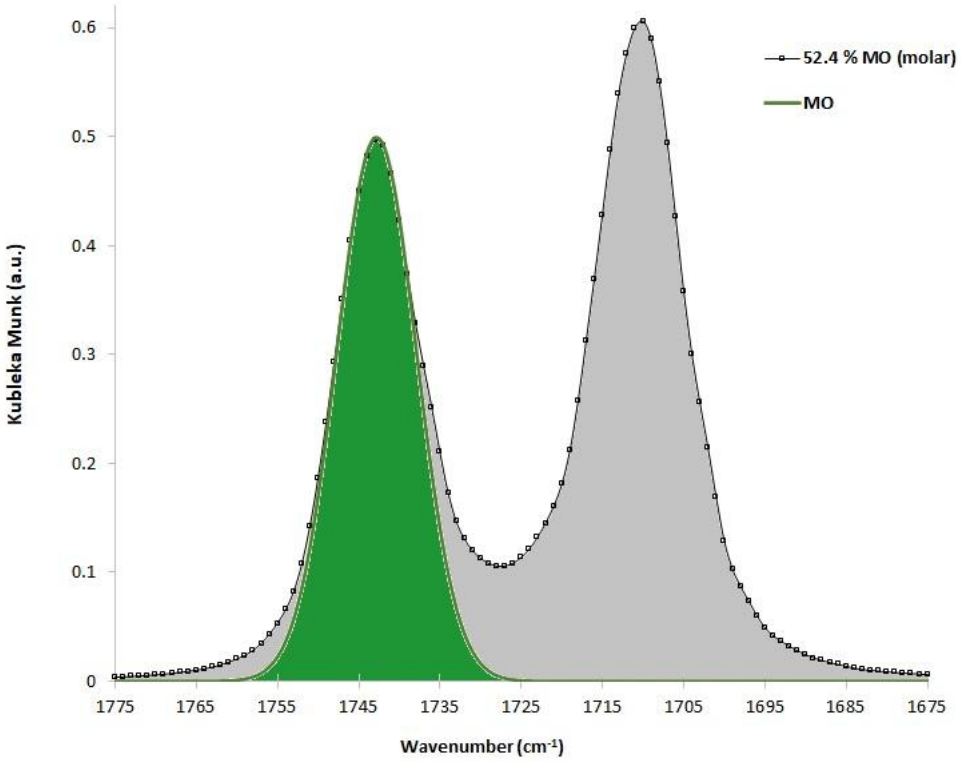

Figure 15 – Gaussian calibration curve for methyl oleate determination by FTIR.

3.2.3 X-Ray Powder Diffraction (XRD)

The ability to catalyze chemical reactions is a surface phenomenon and is often considered since the internal structure of the catalyst does not affect it. However, the catalytic surface and the reactivity of solids are also determined by its interior. The internal structure decides the integrity and stability of the catalyst under the reaction conditions (Che and Vedrine, 2012).

X-ray diffraction techniques, XRD, constitute one of the main means of characterizing the internal structure of solids (Perego, 1998). The choice for this type of radiation relates to its energy and, consequently, to its wavelength, which is located in the same order of magnitude as the interatomic distances. Through this method of characterization, it is possible to find out the degree of crystallinity of the sample under study, which phases are present in that and at what concentrations these phases are found (Che and Vedrine, 2012); (Leofanti et al., 1997).

A diffractogram contains structural information in the intensity of the lines about the symmetry of the crystal lattice and the electronic density inside of the cell, depending on the position and type of atoms present in the sample (Perego, 1998). Additionally, Hargreavens (2005) stated that the that the intensity has a relative scale, with 100% being attributed to the most intense line. Moreover, X-ray wave has a determined wave length (λ) between 0.01 nanometer (nm) and 10 nm, and, while reaching a solid material, energy is transferred to the atoms, more specifically, to the electrons. Although this increase of energy is not enough to excite and remove the electrons out of the atoms, two patterns may occur: diffraction of

part of this extra energy as other x-rays in a process named scattering, or transmission of the electrons through the material entirely. These scattered waves are, what is captured, measured and interpreted by an XRD equipment (Leofanti et al., 1997).

The phase identification is done by comparing the positions and intensities obtained for the crystalline phases. If the reference phase is not sufficient to explain the experimental pattern, a mixture of phases may be present. However, the identification of all the peaks of a sample does not exclude the hypothesis that there are impurities since they can be amorphous or be below the detection limit. Also, it is important that all lines of greater intensity of the reference phase, in the range of measured angles, are present in the experimental pattern, as this guarantees that there is no ambiguity in the identification of sample phases (Che and Vedrine, 2012).

Additionally, there are two major ways that the diffracted x-rays can behave: destructive interference or constructive interference. The former is frequently seen in x-ray analysis because many waves interact indistinctly before partially canceling or not, leaving little room for equipment to detect it. The synchronism of two waves that arrive at the material in phase, on the other hand, necessitates that they have a specified wavelength, amplitude, frequency, angle of incidence, and separation to result in a constructive interference of x-rays. As a result, the signal picked up by the x-ray apparatus is amplified appropriately, creating an XRD diffractogram (Hargreavens, 2005).

Bragg's law is a fundamental principle in X-ray crystallography that explains the interaction of X-rays with crystalline materials. It describes the relationship between the angle of incidence of X-rays on a crystal lattice and the resulting diffraction pattern observed. Bragg's law, which is shown in Equation 2, expresses this constructive interference of the waves quantitatively. Where, n is an integer representing the order of the diffraction peak; λ is the wavelength of the incident x-ray beam; d is the spacing between the lattice plane; and θ is the angle of incidence or diffraction.

$$n\lambda = 2dsin(\theta) \qquad \textbf{Equation 2}$$

According to Bragg's law, the X-rays will undergo constructive interference when the path difference between the waves scattered from different lattice planes is equal to an integer multiple of the X-ray wavelength. This condition leads to the formation of a diffraction pattern. In a graphical representation of Bragg's law, we can visualize a crystal lattice as a set of evenly spaced planes stacked in three dimensions. The planes can be depicted as parallel lines or as layers within the crystal structure. The incident X-ray beam, as seen in Figure 16, shown as a straight line or arrow, strikes the crystal at a specific angle, known as the incident angle or the angle of incidence. This angle is typically measured relative to a reference plane, such as the surface of the crystal. Figure 16 shows a beam of parallel X-rays penetrating a set of parallel lattice planes with indices *h,k,l* of spacing *d* and at an angle of incidence *θ*. The lattice planes are represented behaving as a mirror and A and B represent the path difference between the scattered waves.

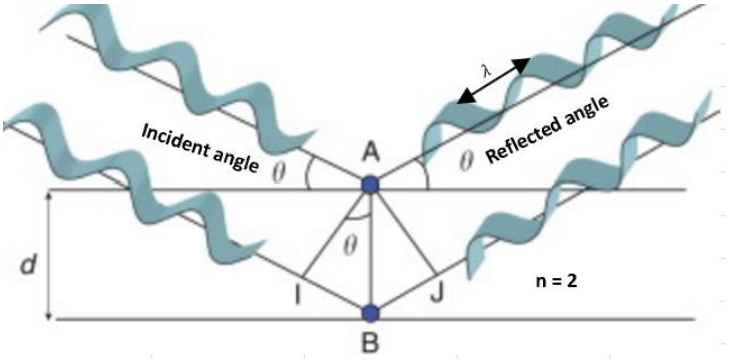

Figure 16 – The condition for reflection – the Bragg's law. Adapted from: Pevelen, 2010.

As the X-rays interact with the crystal lattice, they are scattered or diffracted by the atoms or ions within the lattice planes. The diffracted waves propagate in various directions, forming an interference pattern. To represent the constructive interference described by Bragg's law, figure x shows diffracted waves emanating from multiple lattice planes and intersecting at specific angles. These angles are known as the diffracted angles or the angles of diffraction. They are measured relative to the same reference plane as the incident angle. The key aspect of Bragg's law is that the incident angle, the angle of diffraction, and the spacing between the lattice planes are all related, expressed in Equation 2. Therefore, it provides a visual framework for comprehending the fundamental principles underlying XRD and the analysis of crystalline materials (Prevelen, 2010).

For the XRD experiments developed throughout this work, after obtaining the data, baseline adjustment was used to correct for background signals and improve the accuracy of peak identification and intensity determination. The data was loaded, into Excel, then unwanted noise was removed by normalizing the intensities. The region were signals we minimal (low intensity range) served as the baseline reference. Based on the selected baseline region, the general shape of the baseline was selected. The baseline parameters, including slope and curvature were used to minimize deviations from the experimental data in that region.

3.2.4 Scanning Electron Microscopy (SEM) with Energy Dispersive Spectroscopy (EDS)

The Scanning Electron Microscopy (SEM) is a well-known technique that uses an accelerated electronic beam to enable the superficial analysis of solid materials, including morphology, chemical composition, with Energy Dispersive Spectroscopy (EDS), and crystallographic information, and direction. The lens of the optical microscope is limited in terms of lens magnification (up to around 1000 times) and the wavelength of the light beam used to illuminate the sample. Therefore, with the need to evaluate new materials in micro or nano scales or to obtain more detailed information of surfaces, the optical microscope became limited and SEM used to fulfil these characteristics (Lim et al., 2023).

The SEM – EDS is a powerful combination of techniques used for high-resolution imaging and

elemental analysis of solid samples. Figure 17 presents a graphic representation of the SEM-EDS setup, in which the diagram begins with the main component of the SEM, the column, an electron gun that emits a focused beam of high-energy electrons; this electron is accelerated towards the sample using electromagnetic lenses. Then, the sample of interest is placed within a sample chamber, which is typically under a high vacuum to prevent electron scattering. The focused electron beam scans across the sample's surface in a raster pattern.

As the electron beam interacts with the sample, several interactions occur, leading to the generation of various signals. Then, the focused electron beam scans across the sample's surface in a raster pattern. As the electron beam interacts with the sample, several interactions occur, leading to the generation of various signals (Giurlani and Berretti, 2020).

One type of signal generated is secondary electrons. These low-energy electrons are emitted from the sample's surface due to the interaction with the primary electron beam. They provide topographic information about the sample's surface. Another type of signal is backscattered electrons. These higher-energy electrons are scattered back towards the detector, primarily depending on the atomic number of the sample's elements. Backscattered electrons provide compositional and contrast information.

Integrated within the SEM column is an EDS detector. The EDS detector captures X-rays emitted by the sample when it is bombarded with the electron beam. When the primary electrons collide with the sample's atoms, inner shell electrons can be ejected, leaving vacancies. Electrons from higher energy levels then fill these vacancies, emitting characteristic X-rays that are unique to the elements present in the sample. The EDS detector collects and measures the energy and intensity of the emitted X-rays. Each element produces X-rays at specific characteristic energies, allowing for identification of the elements present in the sample (Rades et al., 2014).

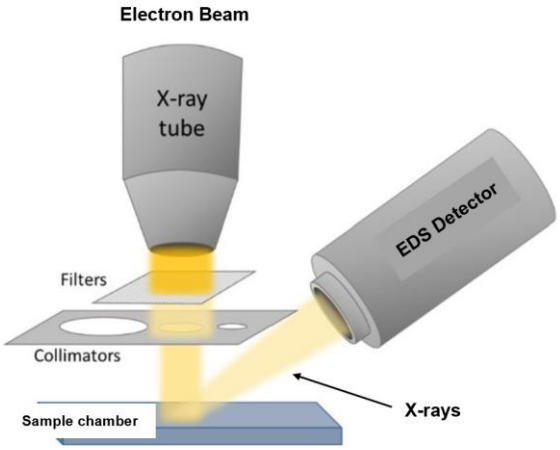

Figure 17 – Scheme of the principal components of SEM – EDS. Adapted from: Giurlani and Berretti, 2020).

The collected X-ray data is analysed using specialized software, generating an energy spectrum. This spectrum shows peaks corresponding to the characteristic X-ray energies emitted by the elements

in the sample. The intensity of each peak provides quantitative information about the elemental composition and concentration. Simultaneously, the SEM scans the electron beam across the sample's surface, generating an image based on the detected signals (secondary electrons or backscattered electrons). This results in high-resolution imaging of the sample's topography and morphology. Additionally, EDS data can be collected at specific locations or continuously during imaging to create elemental maps, visualizing the distribution of elements across the sample's surface (Giurlani and Berretti, 2020).

The SEM is a non-destructible analysis, so it is possible to carry it several times using the same sample material. Nonetheless, it is important to emphasize that it is a mere qualitative technique in terms of superficial analysis. The EDS tool, on the other hand, is a semi-quantitative technique, as explained by Makhlouf & Aliofkhazraei (2016), for its capability of detecting amounts higher than 10% wt. and amounts between 1% wt. and 10% wt., but has a minimum detection limitation of 0.1% wt. Therefore, it is not capable of identifying trace elements.

3.2.5 Thermogravimetry

Thermogravimetric Analysis, TGA, is an analysis technique that is based on the thermal stability of the materials, registering the mass loss felt by the sample in function of temperature increase. This technique allows determining the yield of the reaction of esterification, however, does not allow to evaluate the quality of the product obtained (Chand et al., 2009). The temperature increase rate is an extremely important operating parameter, as it dictates the quality of the analysis. Low rates ensure better resolution of peaks, making them wider (Leofanti et al., 1997). When carrying out thermograms for biodiesel, it is still essential to have special care in relation to the glycerine present in the system, this must be minimal since the thermogravimetry does not allow distinguishing between this compound and the methyl esters that constitute the methyl oleate (Chand et al., 2009).

Applying thermogravimetric methods for the study of the efficiency of the esterification reaction, despite not being the common practice, this technique presents advantages, both from the economic point of view and from the environmental point of view, since it does not imply the use of solvents or standard solutions, therefore, producing less waste. This study It is possible since the thermal degradation process of biodiesel starts around 150°C while that of oleic acid starts at practically over 200°C (Chand et al., 2009); (Chand et al., 2008).

Moreover, Thermogravimetry (TGA) is a thermal analysis technique used to study the weight changes of a sample as a function of temperature or time. As seen in figure 18, the TGA begins with a sample holder or crucible, where the sample of interest is placed. The crucible is usually made of a heat-resistant material, such as ceramic or metal. The sample holder with the sample is then placed inside a thermogravimetric analyser, which contains a heating system. The heating system can be an electric furnace or a heating element that provides controlled temperature ramping or isothermal conditions. The temperature is precisely controlled and increased at a defined rate, typically in a stepwise or continuous manner. The temperature range can vary depending on the analysis requirements and the thermal stability

of the sample (Granados et al., 2014).

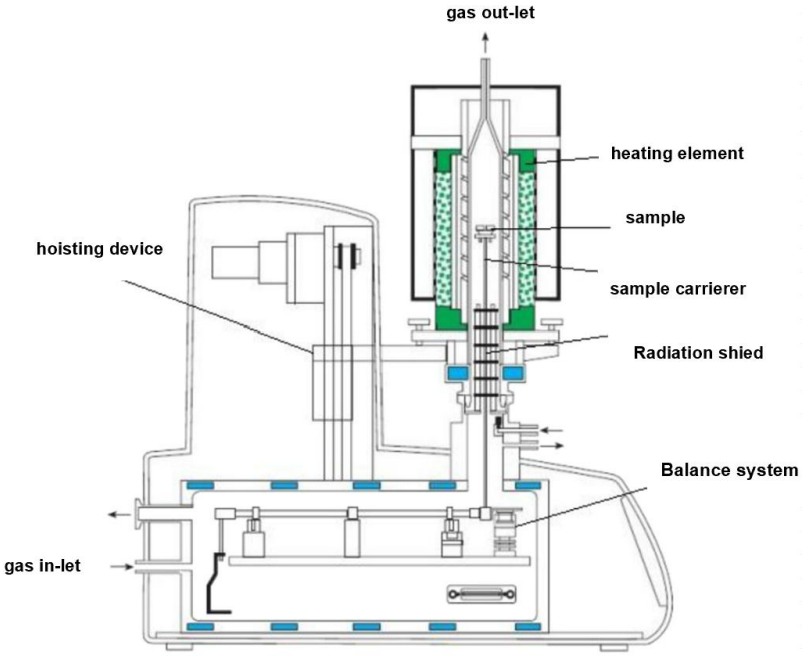

Figure 18 – Schematic of TGA. Adapted from: Granados et al. (2014).

Also, the thermogravimetric analyser is equipped with a highly sensitive balance that continuously measures the weight of the sample during the heating process. The balance can detect even small weight changes, typically in the microgram or milligram range. As the temperature increases, the sample undergoes thermal decomposition, phase transitions, or other chemical reactions.

These changes result in the evolution of volatile components, release of gases, or weight loss due to sample degradation (Alves et al., 2022). The balance continuously records the weight change of the sample as a function of temperature or time. The data is then plotted on a graph, with weight loss on the y-axis and temperature on the x-axis, this plot is known as the thermogravimetric curve, which provides valuable information about the thermal stability, composition, and decomposition behaviour of the sample. Finally, the thermogravimetric curve is analysed to determine important parameters such as initial weight, final weight, onset temperature of decomposition, weight loss rate, and decomposition kinetics. This analysis helps in understanding the thermal behaviour, degradation mechanisms, and composition of the sample; Vega – Lizama et al. (2015) explain this procedure in the study of the degradation of soy biodiesel.

In this work, the thermograms were acquired on a Netzsch STA 490 PC thermobalance using heating rates from 10 to 50 C/min. For each test 30 - 70 mg of grounded sample were placed in a 100 mL alumina crucible. During the TG tests, the thermobalance oven was flushed with air (18 L/h).

3.2.6 Raman Spectroscopy

Raman spectroscopy is a technique used to study molecular vibrations by analyzing the inelastic scattering of light. It provides valuable information about the molecular structure, chemical composition, and bonding characteristics of a sample. Raman spectroscopy can identify the crystalline phases that are

present in a material based on the quantity of bands that are observed and their wavenumbers, which are correlated with the space group and the force constants of the bonds, respectively (Loridant, 2021).

Because Raman spectroscopy is sensitive to the short-range order and to the chemical bond itself, it can be used to characterize disordered materials like nanomaterials. Typically, the Raman spectrum of a nanomaterial remains sufficiently similar to the corresponding single crystal spectrum to allow unambiguous identification. Therefore, it is frequently employed to describe nanomaterials like heterogeneous catalysts (Gouadec and Colomban, 2007). This was a particularly important tool to investigate the spectral alterations seen for the hydrochars.

In Raman spectroscopy, a laser was used to irradiate the sample. When the laser light interacted with the sample, a small fraction of the scattered light underwent an energy shift due to the vibrational modes of the molecules in the sample. This energy shift, known as Raman scattering, was then detected and analyzed to provide information about the molecular vibrations. It is important to note that the spectrometer only detected the scattered radiation of lower energy and generated a plot of frequency of scattered radiation versus intensity. This plot, the Raman spectrum, and the peaks present are due to vibrational excitation; as a matter of fact, it is for this reason that Kirkbride (2000) referred to Raman spectroscopy as the complement of infrared spectroscopy.

To separate overlapping peaks in the spectrum and extract individual component information, a deconvolution was performed using Excel. In the data was loaded and pre-processed by subtracting the background signal, applying baseline corrections, and normalizing the spectrum. The Gaussian model was used as the peak model and the peak parameters including position, widths, and intensities were also defined (as these provided valuable insights into the composition and molecular structure of the hydrochars). The quality of the deconvolution fit was accessed by examining the difference between the experimental data and the fitted model and calculating the root mean square error (RMSE).

Chapter 4

Results and Discussion

4.1 Characterization of the Catalysts

4.1.1 Before Reaction

The ATR-FTIR spectra of the catalysts obtained with low concentration of H_2SO_4, namely the ones with ratio 1:1, in figure 19, show that all activated carbons presented reflectance bands belonging to the sulphur dioxide, SO_2, asymmetric and symmetric stretching modes of sulfonic active sites (-SO_3H groups). The stretching modes represent the vibrations of the chemical bonds within the sulfonic acid groups where the asymmetric stretching mode is observed at a higher wavenumber (1100 -1200 cm^{-1}) and it is as intense as the symmetric stretching mode. This mode is attributed to the stretching vibration of the sulphur-oxygen bonds in the sulfonic acid group. As seen in figure 19, the asymmetric part lies in bands between 1150 com^{-1} and 1175 com^{-1} for sucrose1 and xylitol1, while for glucose1 and glycerol1, the mode is broader, ranging from 1125 cm^{-1} and 1200 cm^{-1}. On the other hand, the symmetric stretching mode appears at a lower wavenumber (1000 -1100 cm^{-1}), corresponding to the simultaneous stretching of the sulphur-oxygen bonds in a symmetric manner within the sulfonic acid group. The symmetric mode lies in bands between 1005 cm^{-1} and 1025 cm^{-1} for glucose1, whereas in sucrose1, xylitol1, and glycerol1, the curve has a broader and higher peak in this area, ranging from 970 cm^{-1} and 1025 cm^{-1}. As speculated by Goncalves et al. (2016) and Correa et al. (2023), the intensity and position of both modes can be influenced by factors such as the hydrogen bonding and the neighbouring functional groups.

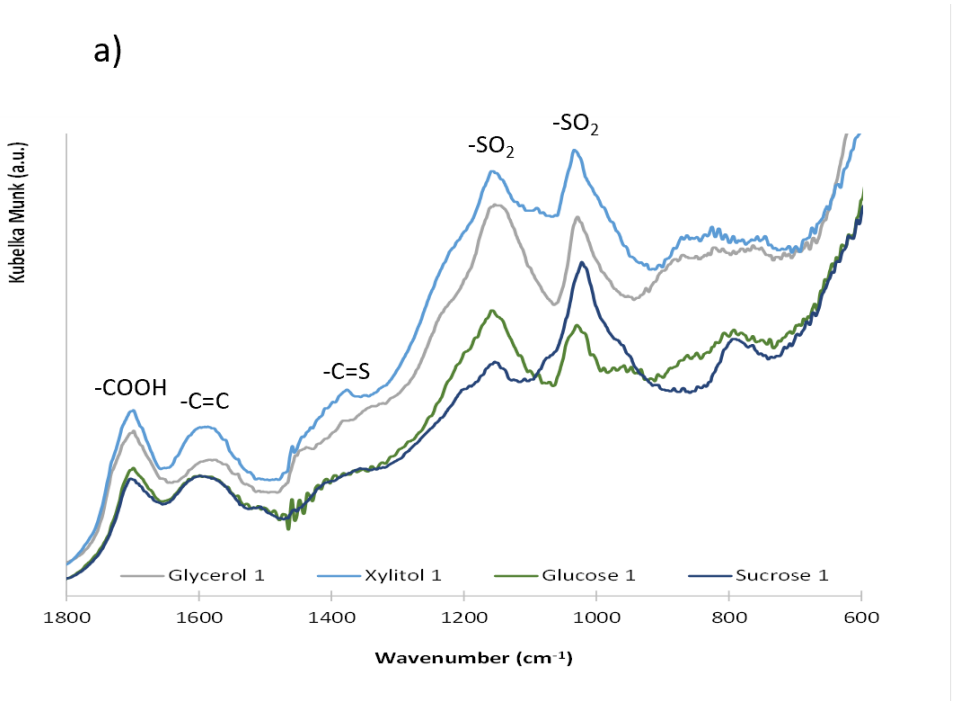

Figure 19 – ATR – FTIR spectra of fresh catalysts with 1:1 ratio.

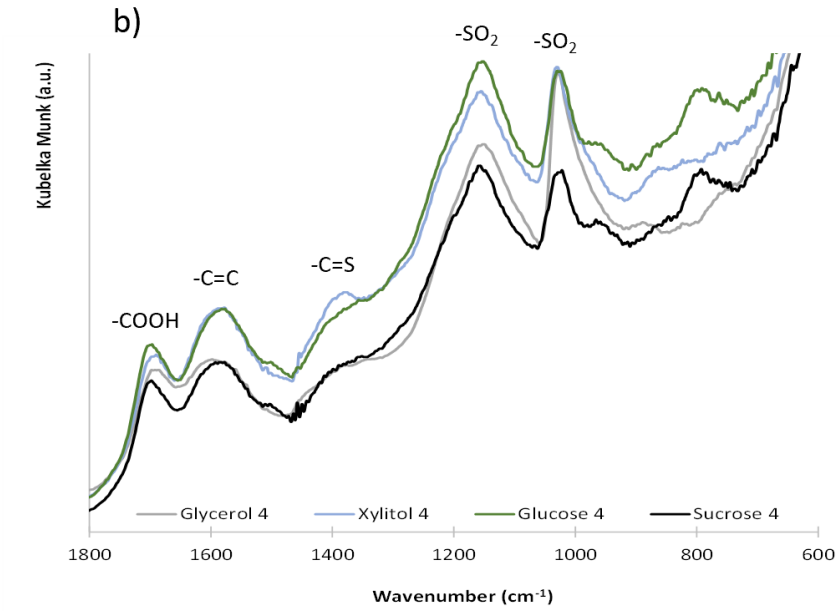

Figure 20 – ATR – FTIR spectra of fresh catalysts with 1:1 and 1:4 ratio.

Another band at 1370 cm^{-1}, attributed to the thiol-carbonyl stretching modes (Ngaosuwan et al., 2016), (-C=S) appeared in both xylitol1 and glycerol1 and is very settle, almost inexistent, for sucrose1 and glucose1. Other characteristic bands of components generated in the carbonization of sugar derived catalysts are identified, such as at 1600 cm^{-1} referring to the normal vibrational mode (NVM) of the stretch associated with the -C=C bond of aromatic rings, and at 1705 cm^{-1} attributed to the MNV of the stretch referring to the -COOH bond of carboxylic groups (Zhang et al., 2021). Since all of the catalysts present a significant absorption in this area, it is plausible to say that they all are abundant in carboxylic groups (Correa et al., 2023), probably due to the short time and low temperature of carbonization-sulfonation; as sucrose1 being the most oxygenated and oxidation-prone catalyst.

As for the -C=C bond, xylitol1, followed by glycerol1, have a higher reflectance compared to the other two catalysts, sucrose1 and glucose1, suggesting that the former two catalysts have a higher degree of graphitization, which explain that, given that they were all partially carbonized at a relatively same temperature, materials carbonized for longer tend to be composed of more extensive polyaromatic layers of carbon, -C=C.

Similarly, for the sugar derived catalysts with higher concentration of H2SO4, ratio 1:4, presented in figure 20, the presence of bands at 1000 cm^{-1} and 1200 cm^{-1}, typical of normal vibration modes associated with symmetrical and asymmetric stretches of the O=S=O bonds of the sulfonic groups is evident for the four types of catalysts (Scholz et al., 2018), with sucrose 4 being the less intense compared to the other three catalysts.

The spectra in figure 19 and 20 demonstrates that the catalysts with the molar proportion of 1:4 between sucrose, glycerol, glucose, or xylitol, and H_2SO_4 are the ones with higher intensity of the SO_2 bands, both symmetric and asymmetric. Besides, when the sulfuric acid proportion increases, the intensity of the band attributed to the $-SO_3H$ groups increases too, which indicates a higher amount of

these groups. Similar results are described by Spataru et al. (2021). For these catalysts, the asymmetric part lies in bands between 1000 com^{-1} and 1010 com^{-1}, whereas, the symmetric stretching mode lies in bands between 1110 cm^{-1} and 1191 cm^{-1}. It is important to notice that for sucrose4 and glucose4, there is a noticeable absorption in the 762 cm-1 band, which could be the stretching vibration of carbon-sulphur (C-S) bonds. The -C=S bonds in the 1998 cm^{-1} band is almost unnoticeable for all the catalysts except for xylitol4, indicating that, despite the high sulphur content, there is a stronger infrared absorption of carbon structures with a high degree of graphitization for all of the three catalysts, specially for sucrose4 and glycerol4.

The bands between 1698 and 1747 cm^{-1} of the catalysts are also present and represent the carboxylic groups (-COOH) stretching modes (Khayoon et al., 2014); (Gonçalves et al.,2016). The presence of this band suggests that the sulfonation with H_2SO_4 not only created -SO_3H acid groups but also induced the formation of some weak acid groups, as -COOH (Kastner et al., 2012) more accentuated in the xylitol4 catalysts, proving their highest content of sulphur (based on the EDS elemental analysis discussed later in this paper). Also, all these sugar catalysts also showed a band at 1586 cm$_{-1}$ which can be attributed to -C=C stretching, corresponding to the bonds formed during the carbonization process (Spataru et al., 2021).

SEM technique was used to characterize the morphology of the catalysts. When analysing the SEM micrographs, in figures 21 and 22, it is noticed that the sugar catalysts with 1:4 ratio present pore increment compared to the catalysts with 1:1 ratio because of the corrosion and oxidation of concentrated sulfuric acid that occurred during sulfonation (Chen et al., 2022). This increase in the number of interconnected pores on the catalysts surface is extremely beneficial, since it favours contact between reagents and active sites in the catalytic process (Zhang et al., 2021).

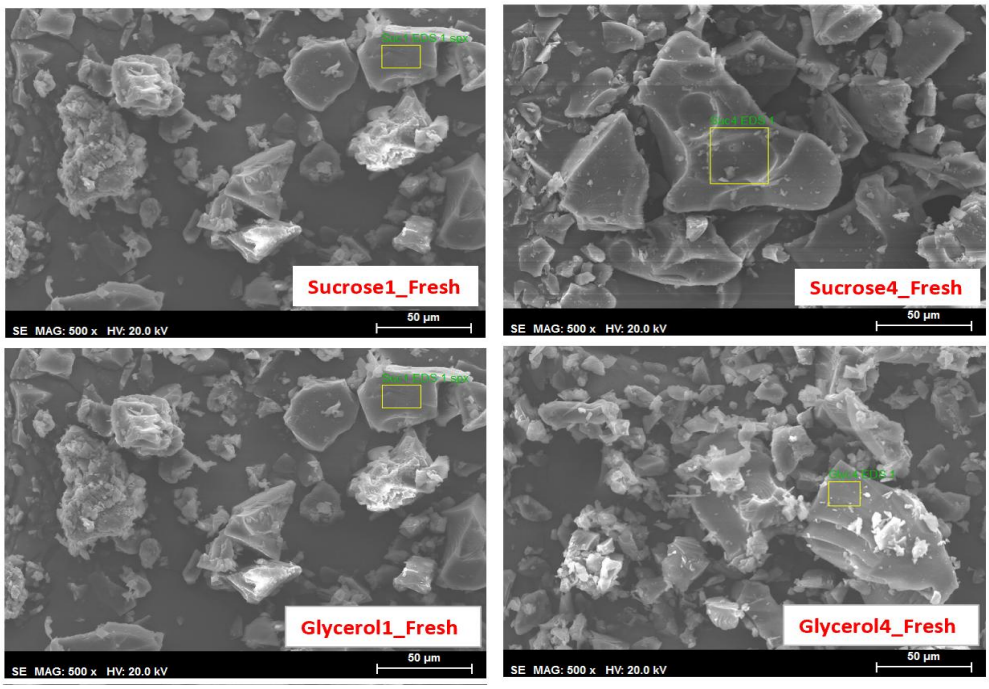

Figure 21 – SEM micrographs, at 500x magnification, for fresh glucose and xylitol, ratios (1:1) and (1:4).

From figures 21 and 22, it is possible to observe that all of the catalysts are not as porous as if they were if carbonization took place at a much higher temperature (Correa et al., 2023). The images also present no fibrous structure given that the precursors are hydrocarbons of short chain. Agglomeration of catalysts clusters with angular nature could also be observed. The samples of glucose1 and xylitol1 showed large crystallites surrounded by fine material (Spataru et al., 2021). On the other hand, samples of sucrose1 and glycerol1 showed much smaller crystallites, like the samples with ratio 1:4, indicating that the sulfuric acid attack was more aggressive to grains size in these catalysts. The sample of glycerol4 seems to be the most porous and mostly attacked by the sulfuric acid.

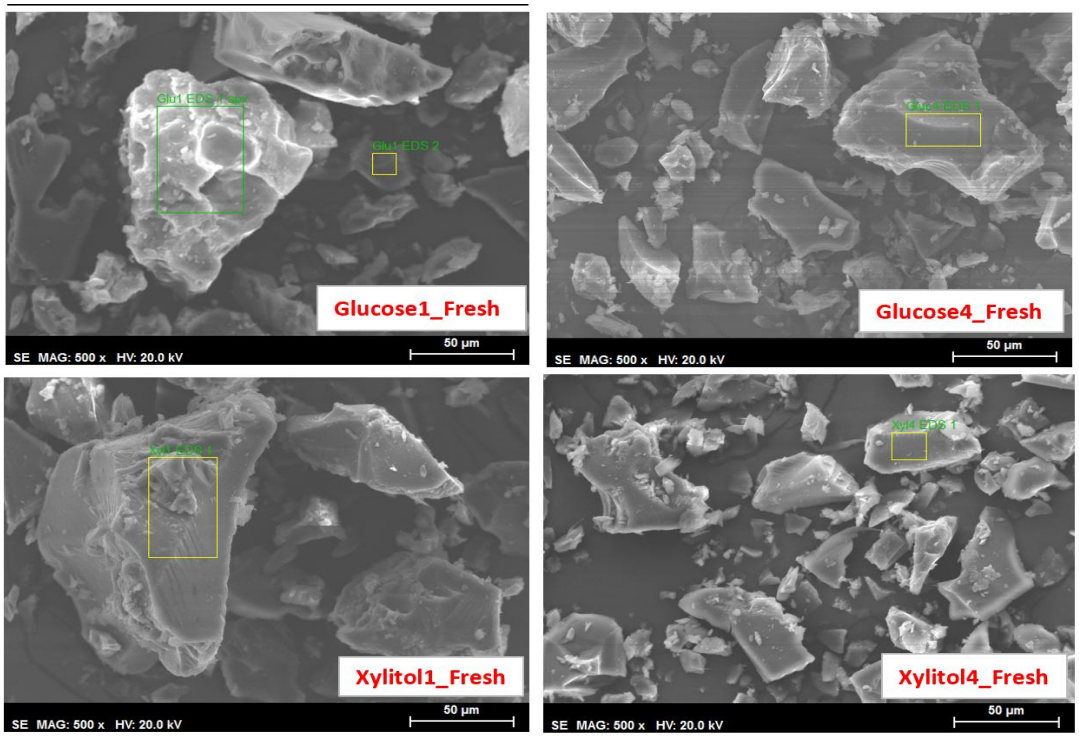

Figure 22 - SEM micrographs, at 500x magnification, for fresh glucose and xylitol, ratios (1:1) and (1:4).

The EDS analysis show that all catalysts have carbon as the main element, a common characteristic resulting from the carbonization process. The second most predominant element is oxygen probably due to the low temperature at which the samples were partially carbonized, meaning that the increase in carbonization temperature has a positive correlation with the amount of fixed carbon and a negative correlation with the number of oxygenated species (Zhao et al., 2018). It is also important to note that the sulfonation process favoured the formation of oxygenated groups giving that concentrated sulfuric acid used in functionalization is a powerful oxidizing agent (Correa et al., 2023).

Table 3 – Elemental analysis of catalysts obtained from EDS technique.

Samples	Elemental Composition (%)			Elemental ratio
	C	O	S	O/C
Sucrose1	66.7	33	0.8	0.49
Sucrose4	74.4	29.9	0.85	0.40
Glycerol1	63.5	23.4	1	0.37
Glycerol4	76.3	22.2	2.4	0.29
Glucose1	71.7	28.3	0.6	0.39
Glucose4	71.8	27.7	0.5	0.39
Xylitol1	73.3	26.3	1.1	0.36
Xylito4	75.7	23	1.7	0.30

Moreover, the presence of sulphur element shows that the process of sulphur insertion was efficient, with a lower content (up to 1.1%) for samples with 1:1 ratio and higher content (up to 2.5%) for samples with 1:4 ratio. Therefore, it can be inferred that the introduction of the groups -SO_3H and formation of -COOH during sulfonation was effective, which was confirmed by the FTIR analysis. The catalyst that shows the higher percentage of sulphur atom is glycerol4, also confirmed by FTIR analysis, where it is possible to see that this catalyst has a high intensity of the SO_2 bands. The variation of the O/C ratio is well observed with the different sulfuric acid concentrations in the catalysts. Catalysts obtained with lower sulfuric acid concentration have a higher O/C ratio than their counterparts.

Presuming that all catalysts were obtained at the same temperature, it can be inferred that higher concentrations of sulfuric acid not only favoured the formation of the aforementioned sulfonic groups, but also promoted a more efficient carbonization of the samples with an increase in their carbon composition. It is worth noting that some elements including Calcium (Ca), Magnesium (Mg), and Aluminium (Al) were also present, in small quantities, in some of the samples. It will be assumed that they were impurities from catalyst synthesis as further investigation would be needed to fathom the presence of these elements.

In order to complement investigations into the carbonaceous structure of materials, figure 23 illustrates the Raman spectra for sucrose and glycerol catalysts as a representation of all the catalysts which can be found in figure B1 (see Appendix B). All materials have characteristic bands of carbon material located at 1350 cm^{-1}, band D – Defect, and 1600 cm^{-1}, G – Graphite.

The properties relative to the intensity of the bands can be evaluated according to the Xu et al. (2020), from the deconvolution of the Raman spectrum in a Gaussian curve to the band D and a Lorentzian curve for the Band G. The intensity values of bands D (I_D) and G (I_G) are described in table x. It was observed low intensity of the bands despite the low carbonization temperature. Xu et al. (2018) report that for carbonized materials, with the increase in the degree of structural order, the amount of aliphatic components such as C-H, C-O and C=O, and alkyls substituents of aromatic rings, becomes smaller, resulting in the disappearance of smaller bands and sharpness of bands D and G.

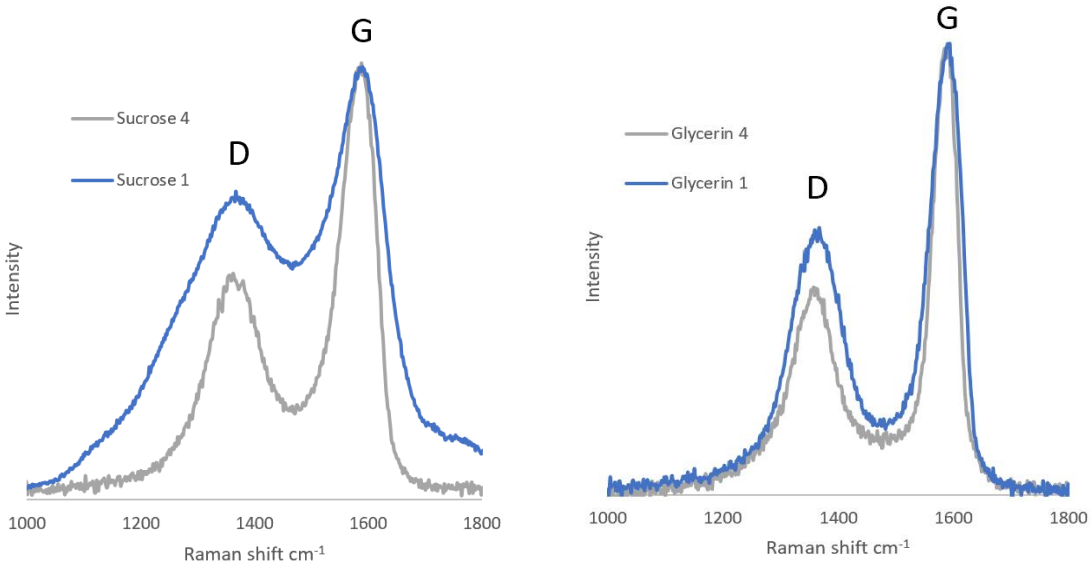

Figure 23 – Raman spectra for the sucrose and xylitol samples.

Also, Ferrari and Robertson (2000) explained that the D band of the graphite is around 1350 cm^{-1}, so the bands are shifted to higher values of around 1380 cm^{-1}, which indicates the presence of smaller aromatic clusters that have higher modes. The G band is also shifted from 1580 cm^{-1} to 1600 cm^{-1} indicating the presence of nanocrystalline graphite, indicating that the structure of the catalysts consists of a graphitic carbon structure dispersed in the amorphous carbon bulk, as described in Spataru et al. (2021) studies.

Table 4 – Raman analysis for catalyst samples: intensity of D and G bands.

Catalyst	ID	IG	I_G/I_D
Sucrose1	90.08	64.79	1.22
Sucrose4	41.79	48.74	0.59
Glycerol1	45.33	46.68	0.97
Glycerol4	25.37	39.3	0.65
Glucose1	42.9	50	0.86
Glucose4	18.4	24.7	0.74
Xylitol1	45.15	47.71	0.95
Xylitol4	71.81	52.19	1.38

By relating the intensity of band G with the intensity of band D for each material, through the I_G/I_D ratio, it was possible to obtain information to confirm the changes in Raman spectral parameters and the structure information represented by them (Xu et al., 2020). The I_G/I_D ratio decrease for all the

catalysts as the amount of sulfuric acid increased. Correa et al. (2023) explained that during sulfonation the decrease of small aromatic rings and substituting groups are limited, and the growth of polycondensed aromatic rings occur significantly, resulting in decreased I_G/I_D ratio for those with higher H_2SO_4 concentrations. Therefore, it can be assumed that sucrose4 and glycerol4 has the highest growth of polycondensed aromatic rings and lowest degree of graphitization while xylitol4 and sucrose1 have the highest degree of graphitization and a more ordered carbon structure. This may be a positive indication of glycerol4 and sucrose4 as having high catalytic activity.

Moreover, x-ray diffraction (XRD) was used to analyse the crystallographic structure of the catalysts. The notation used to label diffraction peaks followed the Miller indices system. Each set of Miller indices (hkl) represented a specific set of crystallographic planes. The numbers h, k, and l corresponded to the indices of the planes intersecting the crystal axes. The (101) reflection refers to the diffraction peak that arises from the scattering of X-rays by the crystal lattice planes defined by the Miller indices (1 0 1). This notation indicates that the planes intersect the crystal axes at a fraction of 1 along the first axis, 0 along the second axis, and 1 along the third axis. The (101) peak provided information about the arrangement and orientation of atoms along these crystallographic planes. On the other hand, the (002) reflection corresponded to the diffraction peak resulting from the scattering of X-rays by the crystal lattice planes defined by the Miller indices (0 0 2). In this case, the planes intersected the crystal axes at 0 along the first and second axes and 2 along the third axis. Thus, the (002) peak provided insights into the arrangement and spacing of atoms along these specific crystallographic planes (Edington, 1976); (Ashocroft et al., 1976).

The catalysts with lower concentration of sulfuric acid in their preparation (1:1 ratio), presented in figure 24, exhibited broad diffraction at around $2\theta = 14°$ to $25°$ and a weak peak around $2\theta = 26°$ to $45°$, assigned to graphic planes (002) and (101) (Liu et al., 2010), which can be attributed to the presence of small graphitic domains. These peaks might be broadened due to the disordered nature of the carbon structure, but its intensity and shape can provide insights into the graphitic carbon content and the degree of ordering within the catalysts. Specifically, this feature indicates that the catalysts have an amorphous 5tructure, lacking long-range order in its atomic arrangement, composed of disordered polycyclic aromatic carbon sheets containing low content low content of crystalline graphite (Singh and Vander Wal, 2022); (Karnjanakom et al., 2018) (Malins et al., 2015) (Prabhavathi Devi et al., 2009).

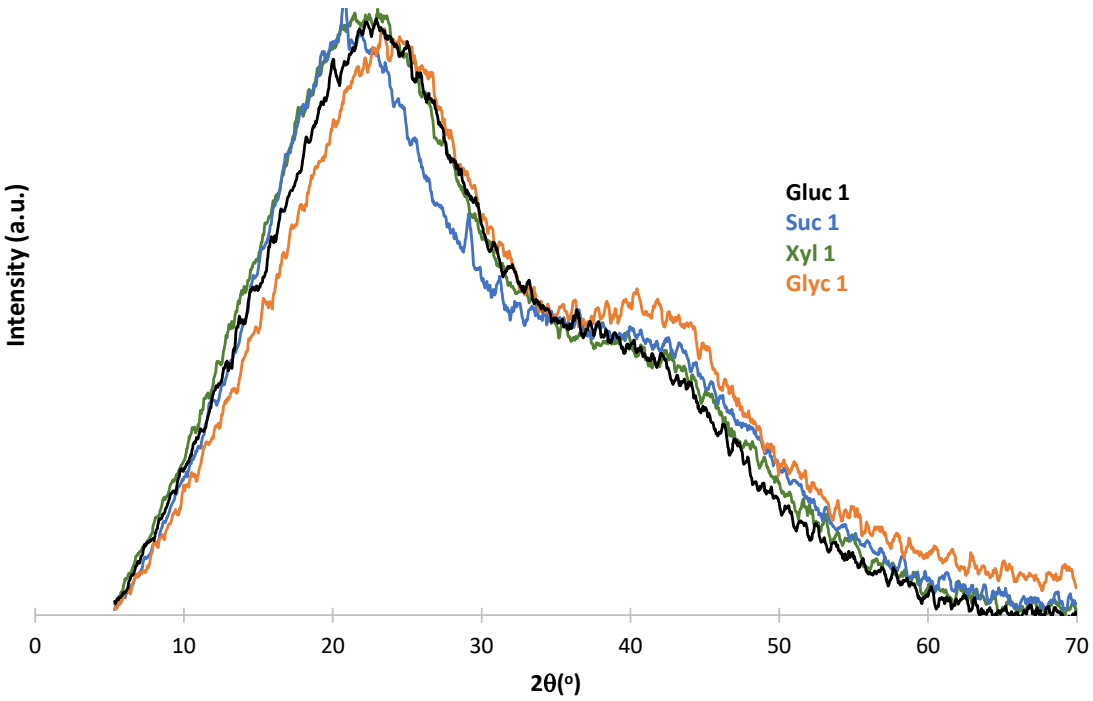

Figure 24 – XRD analysis of fresh catalysts with 1:1 concentration ratio.

Figure 25 presents the x-ray diffraction (XRD) of the catalysts with higher concentration of sulfuric acid in their preparation (1:4 ratio). For these catalysts, the (002) feature is shifted to 23, attributed to graphite oxide (Zhang et al., 2013). This means that during the carbonization process there were proper conditions for the formation of graphite oxide.

For all the catalysts, despite the presence of amorphous carbons, x-ray diffraction spectra displays graphitizing behaviour for all catalysts. They all present a similar lattice and crystallite behaviour with a somewhat high graphitic composition. They have a high intensity, sharper and more intense (002) peak, which is associated with a higher degree of graphitization. Basically, the broader peak of the catalysts is consistent with a non-graphitized, sugar derived carbon, while the weaker peak is indicative of a very graphitic phase in the composite (Singh and Vander Wal. 2022). Also, XRD provided insights into the interlayer spacing of layered materials within the catalysts. From analysis, it was possible to observe that the catalysts contain layered structures, graphene-like and intercalated sheets.

Additionally, the width of the (002) peak offered insights into the size of the graphitic crystallites present in the catalysts. Catalysts with 1:4 ratio have a narrower peak corresponding to larger and more ordered graphitic domains while catalysts with 1:1 ratio have a broader peak, suggesting smaller and less ordered crystallites, as seen in figure 24 and figure 25 (Liu et al., 2010).

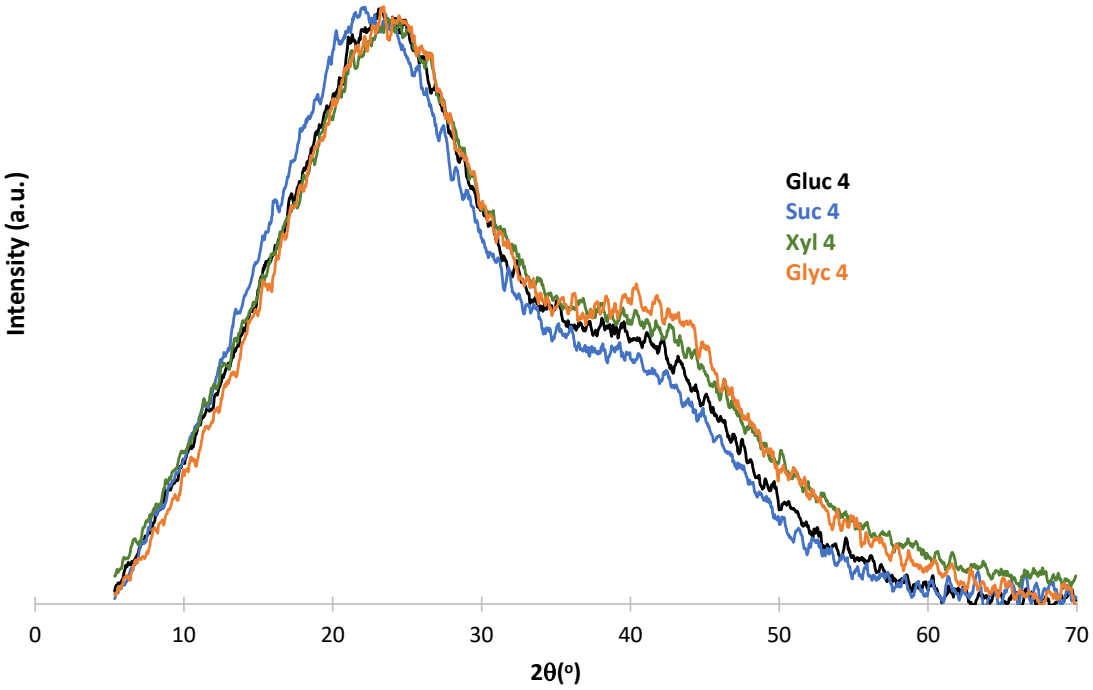

Figure 25 - XRD analysis of catalysts with 1:4 concentration ratio.

Furthermore, the prepared catalysts were also characterized by thermogravimetry under airflow. The thermograms (mass loss curve, TG) in figure 26 shows three stages of significant mass losses. The weight loss that occurred between 150 °C and 275 °C is related to the removal of water since the catalysts tend to adsorb water in an open environment. This first mass loss could be an indicator of the decomposition of volatile components, including water, residual sugars, and other organic species, from the catalyst (Correa et al., 2023).

For the range of 300 - 450 °C the catalysts exhibit other significant mass loss assigned to the decomposition of the sulfonic (-SO3H) and carboxylic (-COOH) groups (Spataru et al., 2021). Additional decomposition of the carbon structure, which consists of C-O and C-C bonds, between 450 °C and 775 °C was observed (Lokman et al., 2016). All the catalysts show a somewhat good thermal stability in the range of 25 °C to 150 °C, before the -SO3H groups start to decompose, which guarantees its application in the esterification of oleic acid that is performed at 67 °C (Kefas et al., 2018); (Correa et al., 2023).

Comparing the samples prepared with 1:4 and 1:1 ratios, the glycerol4 (glyc4) catalyst has a higher residual mass. The partial carbonization of glycerol4 might have led to the formation of carbonaceous residues including char, carbon black, or amorphous carbon (as confirmed by XRD analysis), which have a relatively high thermal stability and could have contributed to the residual mass observed (Correa et al., 2023). Therefore, glycerol4 is the most thermally stable catalysts among all of the others. The catalyst samples prepared with sucrose1 have a smaller residual mass compared to the other molar ratios.

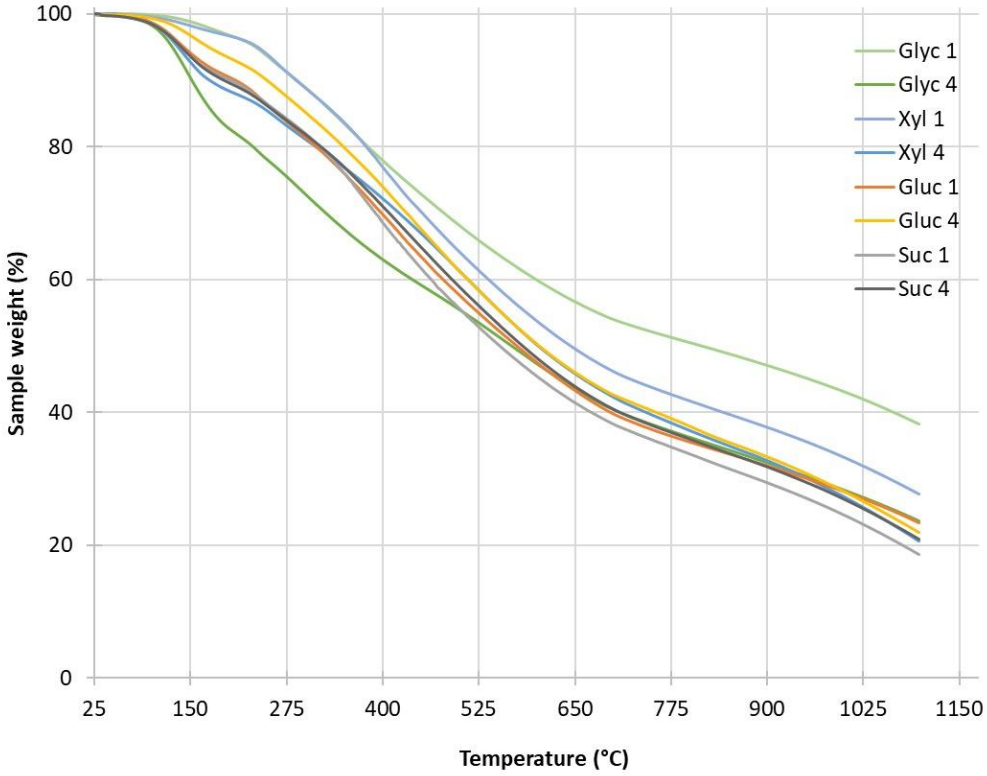

Figure 26 – TG analysis of catalysts.

4.1.2 After Reaction

ATR-FTIR characterization of the catalysts after reaction provided valuable insights into the chemical changes and functional groups present in the catalysts. Figure 27 presents the FTIR spectra of the sucrose4 catalysts, higher concentrations of sulfuric acid, as a representation of all the other catalysts. It can be observed, in bands 1700-1750 cm^{-1}, carbonyl stretching groups (C=O), indicating the esters formed during the esterification reaction. The acidic groups (SO_3H), in the bands ranging from 1100 to 1300 cm^{-1}, corresponding to the asymmetric and symmetric stretching modes, are still very prominent in the catalysts. Bands ranging from 2900 and 3200 cm^{-1} spectrum show the presence of O-H vibrations, which is a suggestion of residual hydroxyl groups and the presence of water, a methyl oleate by-product. Comparing this spectra with figure 19 and 20, all groups were still present, but with a much lower reflectance. For example, band 1600 cm^{-1}, representing -C=C is not as present in the catalysts after reaction.

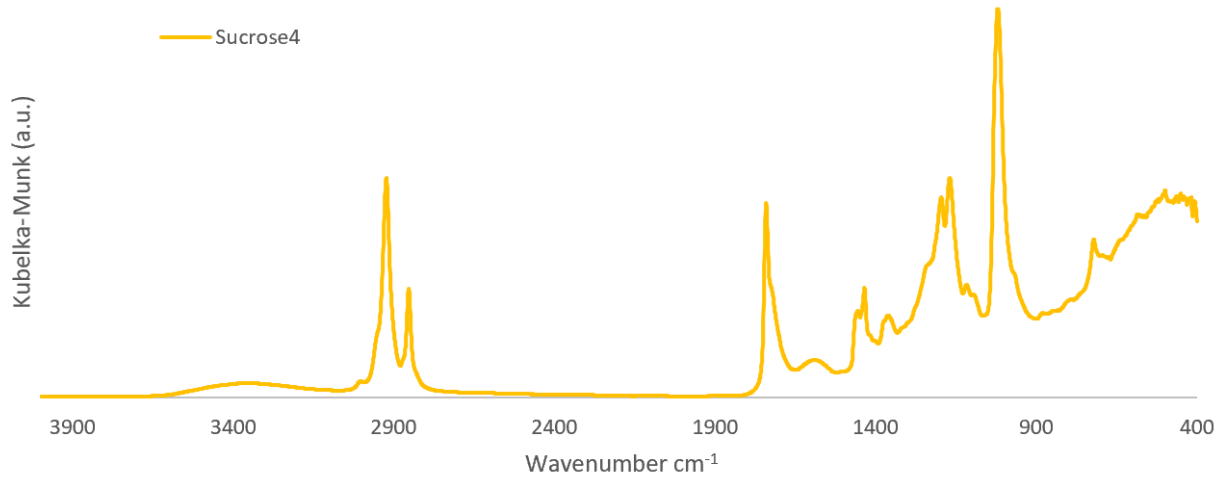

Figure 27 – FTIR spectra of sucrose with 1:4 ratio after reaction.

SEM technique was also used to characterize the morphology of the catalysts after the reaction. When analysing the SEM micrographs, in figure 28, for sucrose derived catalyst, it is noticed that the sugar catalysts with 1:4 ratio present less agglomerate behaviour compared to the catalyst with 1:1 ratio (Chen et al., 2022). In the next sections, it will be discussed if, in fact, the increase in the number of interconnected pores on the catalysts surface favoured contact between reagents and active sites in the catalytic process, as suggested by Zhang et al. (2021). In general, all catalysts present a similar morphology after reaction and present a similar cluster behaviour, with a more rounded shape and particles of similar size.

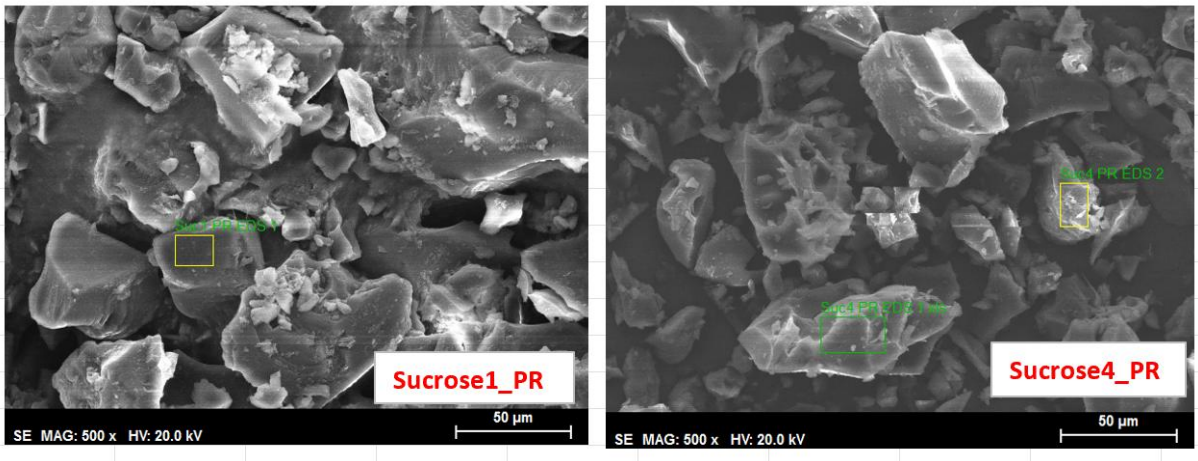

Figure 28 - SEM micrographs, at 500x magnification, for sucrose1 and sucrose4 post reaction.

Leaching of the sulfonic groups is reported as one of the main causes of catalytic efficiency reduction of sulfonated sugars (Zhang et al., 2021). That is, the sulfonic acid groups and the sulphur containing species could have leached out the catalysts into the reaction medium, resulting in the loss of sulphur from the catalysts. The elemental analysis of the catalysts after reaction, present in Table 5, revealed that glucose4 catalyst has greater leaching of the sulphur element after the reaction, which consequently may lead to a greater reduction of its catalytic activity when compared to the others.

Glycerol4 and sucrose1 catalysts have not lost a large amount of sulphur, but xylitol4 has a greater amount of sulfonic groups after reuse, which implies that they may have the best catalytic performance even though other factors such as the loss of mass after reaction, or the blocking of active catalyst sites by product residues that can also contribute to the deactivation of catalysts (Correa et al. 2023).

Table 5 - Elemental analysis of catalysts obtained after reaction from EDS technique.

Samples	Elemental Composition (%)			Sulfur percent decay
	C	O	S	(%)
Sucrose1	76.2	23.8	0.2	25
Sucrose4	73.6	26.2	0.4	47
Glycerol1	77.4	24.3	0.5	50
Glycerol4	75.5	24.5	0.6	25
Glucose1	70.1	27.2	0.3	50
Glucose4	70.6	26.7	0.4	80
Xylitol1	75.7	20.4	0.7	64
Xylito4	81.3	18.5	1.0	59

Another possible reason for sulphur loss after reaction is the decomposition of the sulphur containing compounds given the acidic environment in which the reaction occurred. This decomposition could have resulted in the release of sulphur in the form of sulphur dioxide, SO_2, or other gaseous sulphur compounds, leading to the loss of sulphur from the catalyst, as Zhang et al. (2021) and Tamborini et al. (2019) explain in their studies. It is also noticeable that carbon and oxygen has suffered a slight decrease, which is an indication of mass loss after reaction. Given that all reactions occurred at a temperature low enough, 67 °C, for thermal degradation not to occur, the loss of oxygen and carbon could be due to catalyst deactivation, because of the acidic environment of the reaction and consequent destruction of the active sites resulting in the breakdown of the sulfonic groups and loss of carbon from the catalysts. Leaching can also be a possible cause for the loss of carbon and oxygen in the catalysts.

4.2 Biodiesel

4.2.1 Determination of the Calibration Curve for FAME Yield Calculation

A calibration curve was created to determine FAME yielding from the different experimental reactions with different catalysts and conditions, including FAME different concentrations (mix1 to mix7). The biodiesel used in the calibration was obtained through the conventional esterification of pure oleic acid (99%) with a strong acidic homogeneous catalyst (H_2SO_4).

Specifically, a series of reference samples with varying FAME yields were prepared by blending known amounts of FAME with a suitable matrix. Such concentrations of FAME covered a range that was representative of the samples you intended for analysis. Then, the FTIR spectra of the reference samples were obtained using a consistent and standardized measurement protocol and the spectra over the relevant spectral range that captures the characteristic bands associated with FAME were analysed.

The ATR-FTIR spectra of the methyl oleate obtained from the esterification, from 1675 and 1775 cm^{-1}, is present in figure 29. Band 1750 cm^{-1} is a reflectance of pure biodiesel, representing the typical peak of methyl ester (OCH_3) (O'Donnell, 2013), meaning that the stronger the biodiesel concentration, the higher the reflectance in this band. Therefore, computations were carried out using the IR band centered at that point. Other authors, including Dias et al., (2020) have used the same FTIR band to characterize biodiesel both from transesterification and esterification reactions.

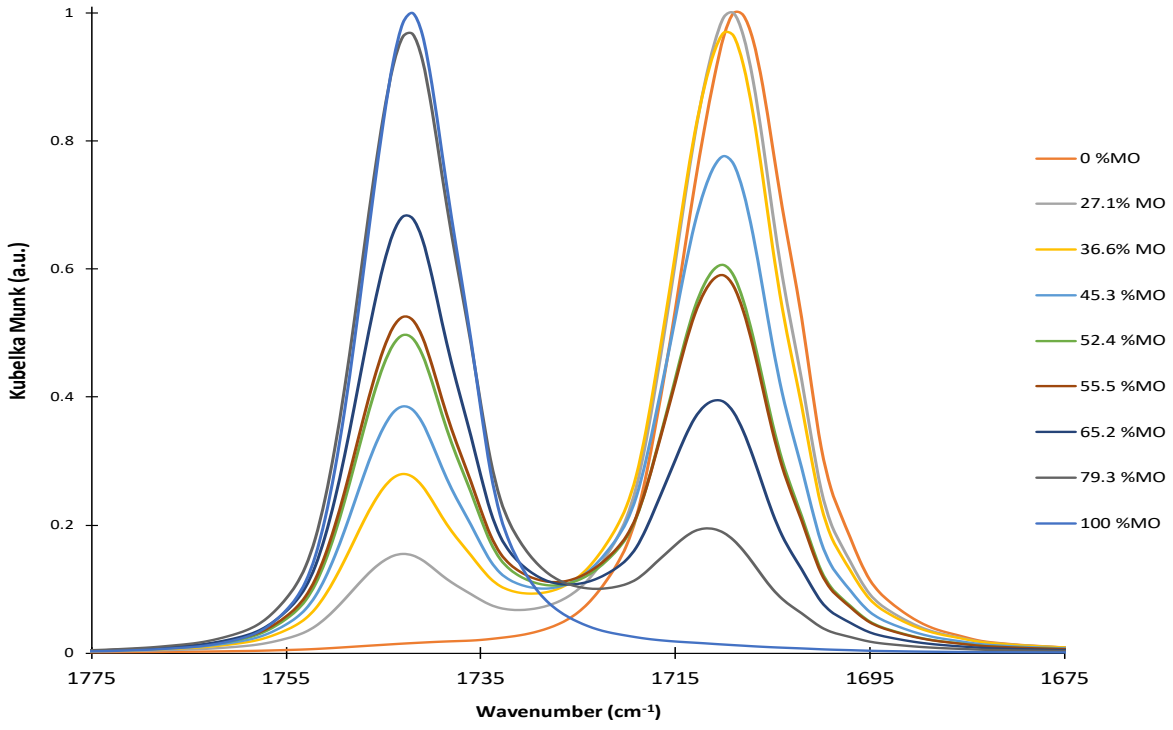

Figure 29 – FTIR spectra of methyl oleate obtained for calibration.

To determine the calibration curve, the ratio between the area attributed to biodiesel and the area of the total wavelength was used as the variable; this way, it remained constant regardless of the optical path, which is different from the experimental method since it presents variations, contrary to, for example, the band intensity. Thus, the deconvolution of the FTIR spectra was performed by adapting the spectra to Gaussian functions, one for each identifiable band in the spectrum, expressed by Equation 2, where A represents the maximum amplitude of the spike, λ is the wavelength, B is the wavelength corresponding to the maximum amplitude, and C is the width of half of the band.

$$Signal = Aexp(\frac{(\lambda - B)^2}{C^2}) \qquad \textbf{Equation 2}$$

The obtained curve, with the quadratic correlation coefficient of 0.9989 can be observed in the calibration curve (Figure 30) with the respective function expressed in the Equation 3. The FAME content obtained through this method corresponds to a mass yielding.

$$\%FAME = 7e^{-5}\left({}^{A_1}/_{A_\tau}\right)^2 + 0.0029\,({}^{A_1}/_{A_\tau}) \qquad \textbf{Equation 3}$$

An exponential curve, seen in figure 30, was established, thus, making it suitable for analysis of the unknown samples using FTIR spectroscopy. The FTIR spectrum of each sample was analysed and the calibration curve used to determine the corresponding FAME yield for each unknown sample.

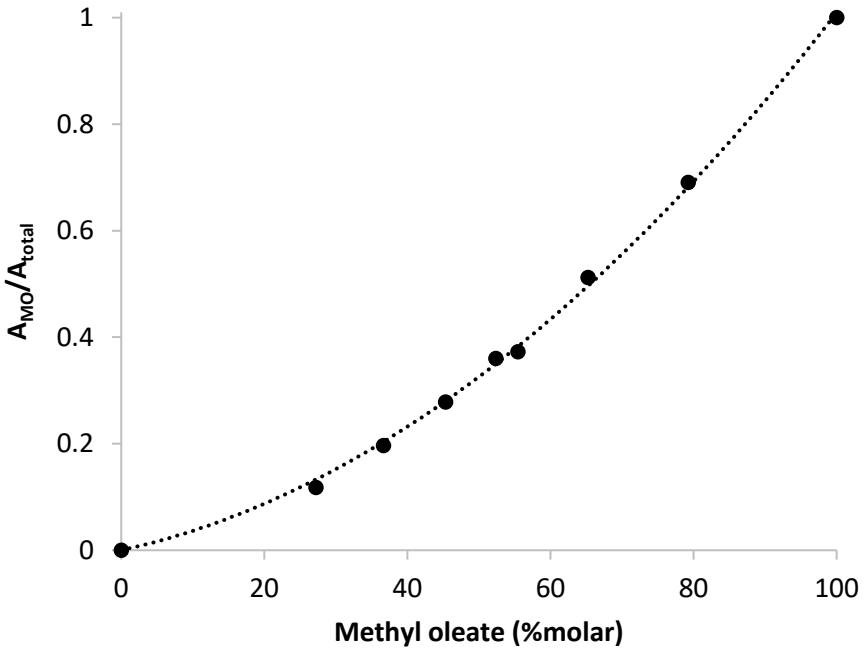

Figure 30 – Calibration curve obtained from FTIR analysis.

4.2.2 Characterization of Oleic Acid

FTIR spectroscopy is commonly used to characterize the molecular structure and functional groups present in organic compounds like oleic acid. In fact, oleic acid is an unsaturated fatty acid with a variety of functional groups, which can be observed in figure 31. The bands between 2600 and 3200 cm^{-1} present a strong reflectance, representing the carboxylic acid groups (-COOH). Specifically, the C-H stretching vibrations of the alkyl chains in oleic acid were observed in the range of 2800 and 2900 cm^{-1}. The stretching vibration of the carbonyl group (C=O) in the acid appeared as a very strong band around 1710 and 1745 cm^{-1}. Also, as oleic acid contains a carbon-carbon double bond (C=C) in its structure, a characteristic band was observed around 1400-1450 cm^{-1}, representing the stretching vibration of the double bond.

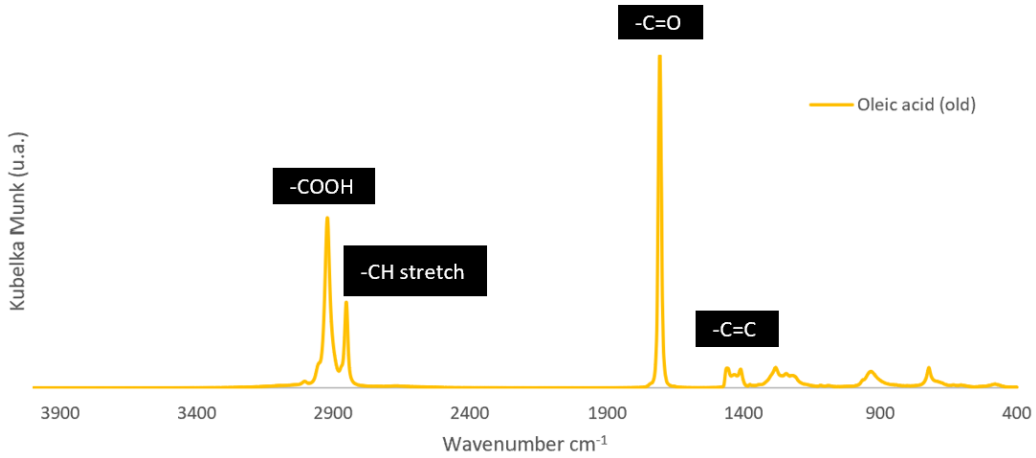

Figure 31 – FTIR spectra of oleic acid.

Moreover, oleic acid can form intermolecular hydrogen bonds, especially in its solid state or concentrated solutions. This can be observed as shifts or broadening of the stretching bands associated with functional groups like -COOH and -OH. In fact, the FTIR spectrum of oleic acid can vary depending on whether it is in the solid or liquid state. In the solid state, additional bands associated with crystal lattice vibrations may be present (Toikka et al., 2022), whereas the liquid state spectrum is dominated by the characteristic functional group vibrations mentioned above. Since this is a pure oleic acid (99%) the possibility of impurities in the spectra is neglected.

4.2.3 Catalytic Activity, FAME Yield

In order to choose the most effective catalyst, an esterification test was carried out under the standard aforementioned conditions. The yield for each reaction was evaluated according to the method explained in the last section. The FAME yield for each reaction for the different catalysts is presented in table 6. From the observation of the obtained results, it is clear that all catalysts have a significant conversion, with sucrose4 being the one with the highest yield and glucose1 with the lowest yield.

Table 6 – FAME Yield obtained through FTIR analysis of the esterification of oleic acid.

Catalyst	% FAME
Sucrose4	92.1
Sucrose1	59.1
Glycerol4	72.4
Glycerol1	61.6
Xylitol4	71.5
Xylitol1	69.2
Glucose4	68.3
Glucose1	66.3

The amount of catalyst used in the esterification reaction was the same, 5 %wt., for all reactions. Perhaps, different catalyst loadings should be tested to optimize the conversion of oleic acid to FAME, specially for those catalysts with lowest yield. Furthermore, the reaction time was the same, 180 minutes, for all the reactions, but for some catalysts, the FAME yield peak occurred before the end time and had a decline afterwards, which is the case of both sucrose1 and xylitol4 presented in figures 32 and 33, respectively.

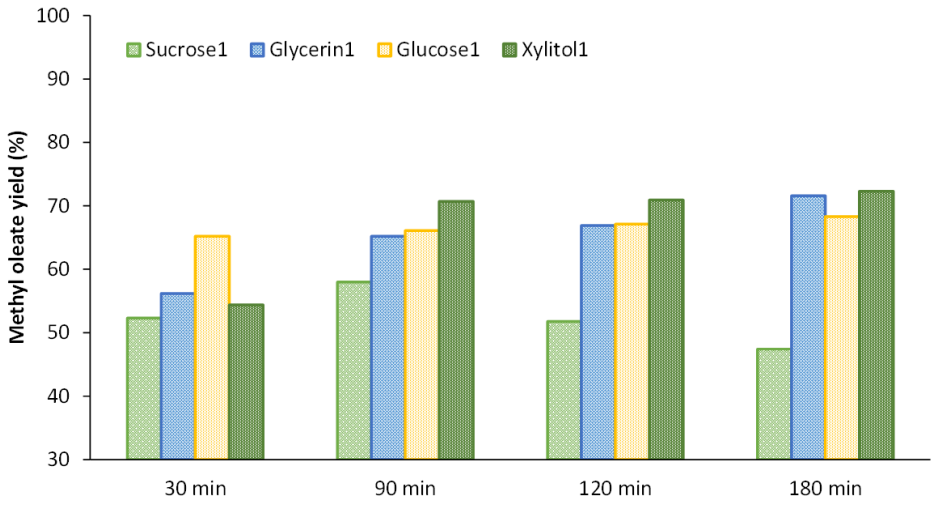

Figure 32 - Methyl oleate yield over time for (1:1) catalysts obtained from FTIR analysis.

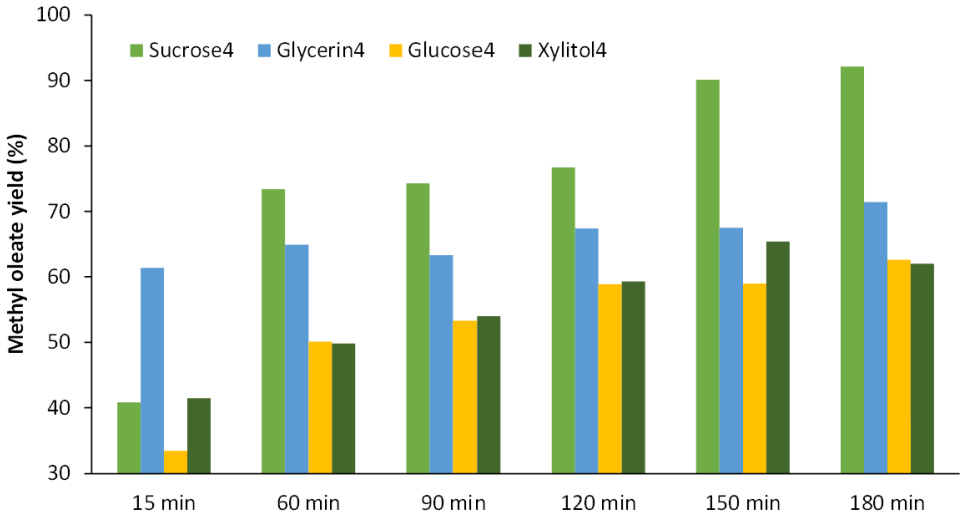

Figure 33 – Methyl oleate yield over time for (1:4) catalysts obtained from FTIR analysis.

From figure 32, the FAME yield for sucrose1 appeared to be somewhat stable until it reached a maximum of 59.1% at minute 90 and then rapidly declined to 51.2% conversion. While on figure 33, FTIR analysis indicated that the highest FAME % yield, 71.5%, was obtained at minute 150 and stated decreasing afterwards. This might be due to an earlier than expected equilibrium shift in the reaction, meaning that for these catalysts, even more excess methanol might be needed. Although both catalysts, xylitol4 and sucrose1, contained a high amount of sulphur in their composition in their fresh state, as confirmed by EDS analyses, it is possible that there was a rapid catalyst deactivation compared to the other types of catalysts.

Another similar case, in figure 33, and also presented in figure 34 for the FTIR spectra of methyl oleate obtained in the presence of sucrose4 over a period of 180 minutes. There is a relevant ester conversion in the first 15 minutes already and then the conversion happens progressively. The conversion reaches its peak at minute 135, reaching a yield of 92.1% and it remains at the same percentage of yield for the remainder of the time.

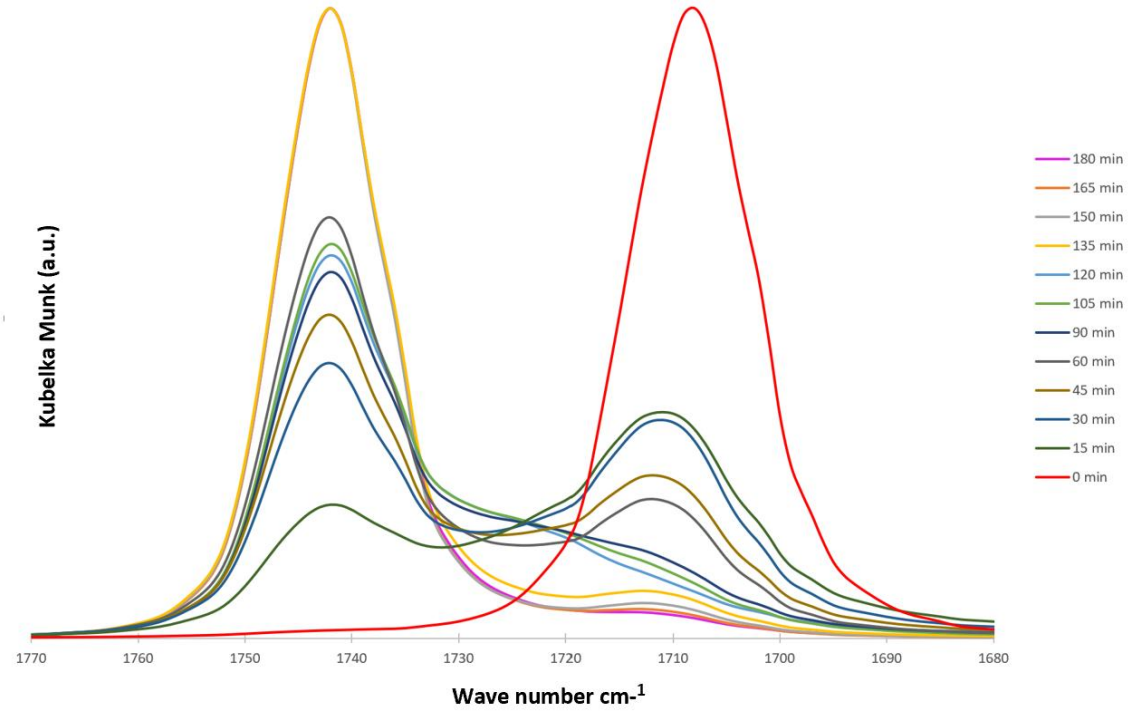

Figure 34 - FTIR spectra (1680 – 1770 cm^{-1}) of obtained methyl oleate from esterification over time in the presence of sucrose4.

Furthermore, all catalysts have shown a significantly high and rapid conversion in the first 30 minutes of the esterification process. Figure 35 shows the FAME yield for all the catalysts at minutes 30 and 180 of reaction. This fact could indicate that the catalysts facilitated the reaction by providing a pathway with lower activation energy. During the initial stage of the reactions, all catalysts proved to be highly active, resulting in faster reaction kinetics, leading to a rapid conversion of oleic acid to FAME.

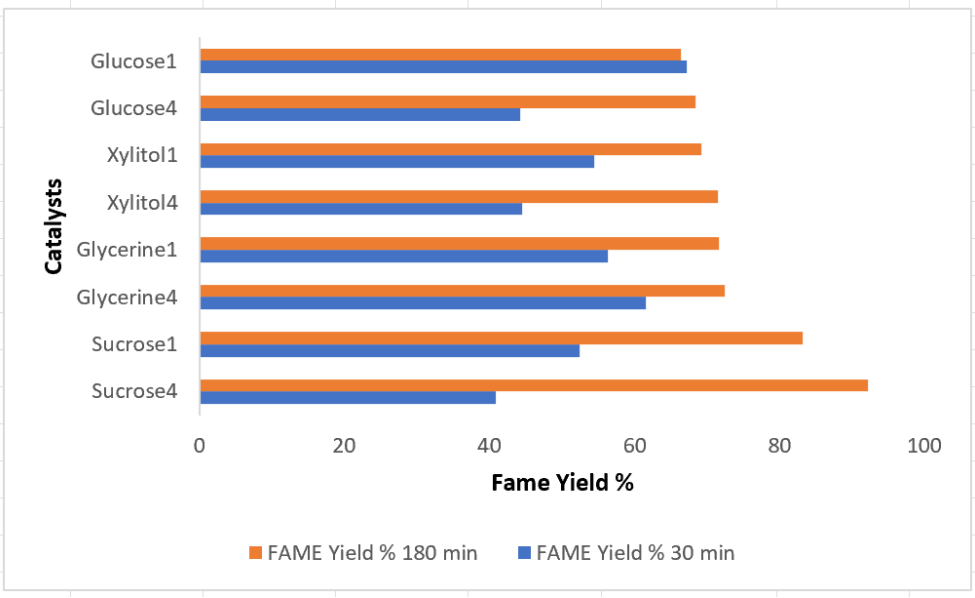

Figure 35 – FAME Yield % of all catalysts between minutes 30 and 180.

As for the rate of conversion, from figure 35, some catalysts including glucose1 and glycerine4, for example, seem to have a very low or even negative rate of reaction. However, it is difficult to calculate such rate since there was not a linear rate of reaction between the initial and final times. Therefore, the rate could have varied over time and a more detailed analysis would be required to account for that (Heynderickx et al. 2020).

4.2.4 Esterification Reaction

Subsequently, the catalysts were evaluated in the esterification of oleic acid with methanol to produce biodiesel at 67°C in the presence of 5 wt% of catalyst in 180 minutes. The catalyst was also successfully employed for the esterification of FFA present in oleic acid (Devi et al. 2014). As discussed in the previous section, the esterification reaction was conducted successfully with all reaction products yielding more than 50% of FAME.

The catalysts acted as an acidic catalyst, promoting the esterification reaction between oleic acid and methanol. The sulfonic acid groups on the catalyst surface protonated the carboxylic acid group (-COOH) of oleic acid, making it more reactive towards nucleophilic attack by methanol. This led to the formation of FAME and water as a by – product (Devi et al. 2014). Figure 36 presents the FTIR spectra of the methyl oleate obtained through the esterification reaction of oleic acid in the presence of the sugar derived carbon sulfonated catalysts.

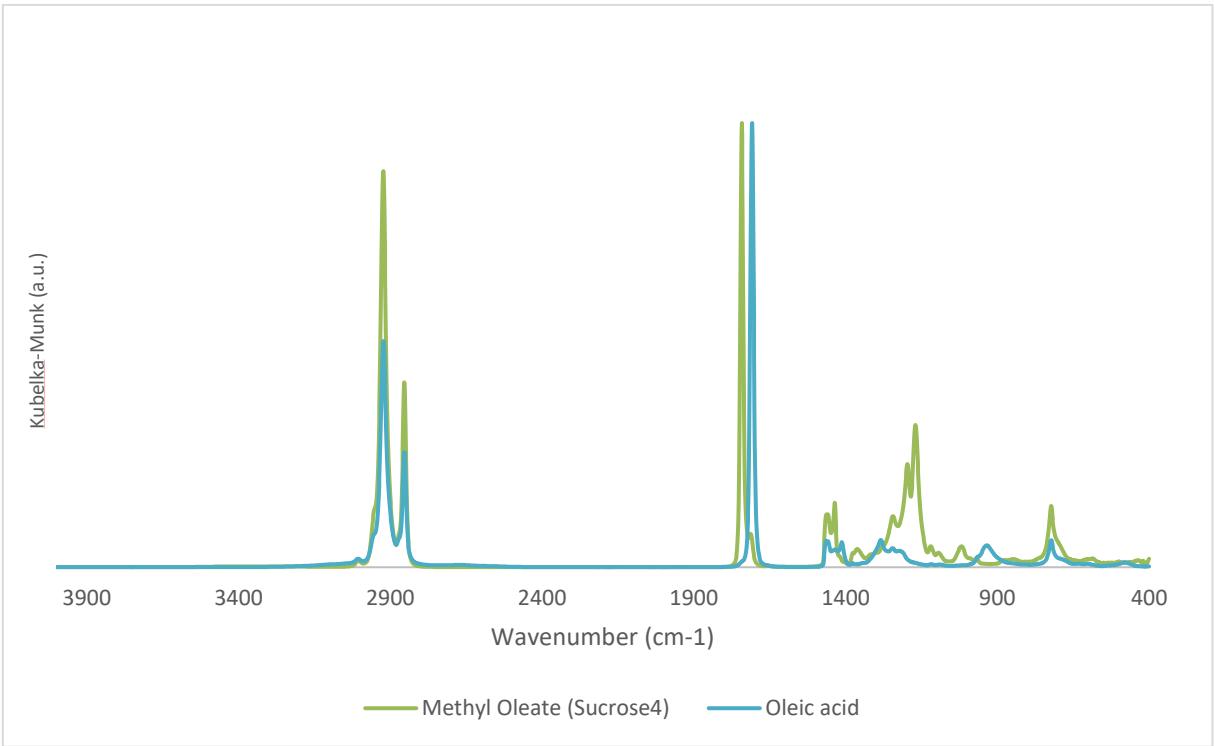

Figure 36 – FTIR spectra of the obtained methyl oleate obtained from esterification reaction.

The obtained FTIR spectrum of methyl oleate was analysed characteristic functional groups and absorbance peaks were identified. The methyl oleate presents an ester functional group (C=O), which exhibits a strong absorption band in the range of 1740 - 1730 cm^{-1}, as seen in figure 37. In fact, that is one of the most important characteristics to look for when analysing the effectiveness of the reaction (Rosset and Perez-Lopez, 2019).

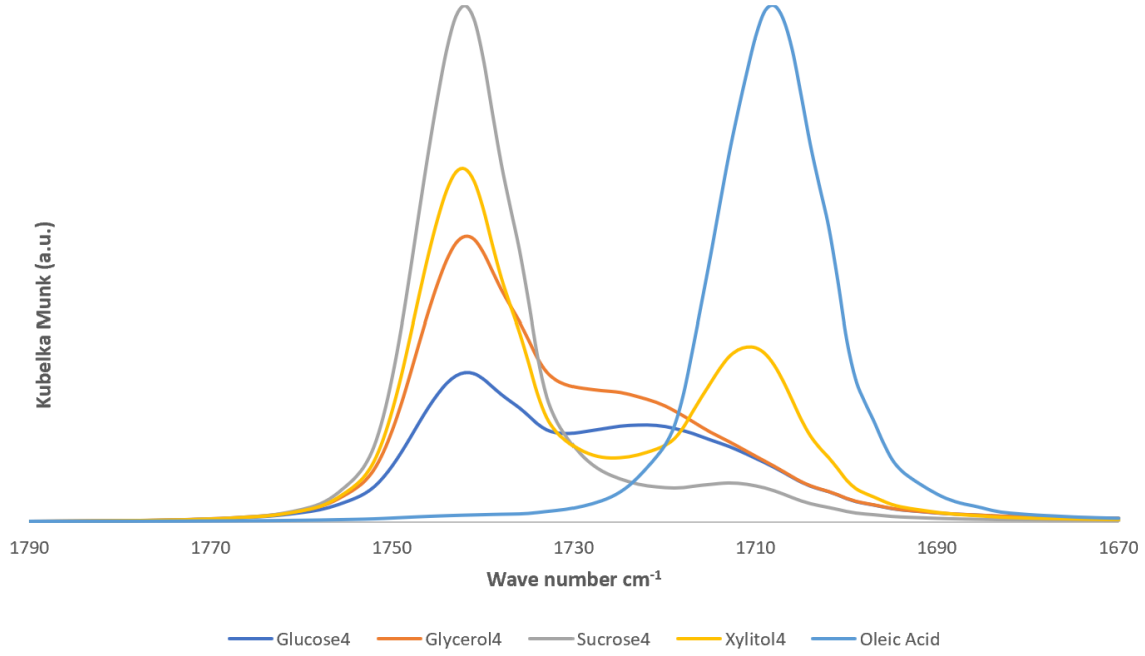

Figure 37 – FTIR spectra (1670 – 1790 cm^{-1}) of obtained methyl oleate from esterification in the presence of sugar derived catalysts with 1:4 concentration.

Oleic acid presents a symmetric peak in the range of 1799 – 1729 cm^{-1} and as conversion occurs, the absorbance in this range decreases while it increases in the 1740 - 1730 cm^{-1}, indicating the presence of esters. At the optimal time of reaction for xylitol4, in figure 37, there is a significant amount of material to be converted, confirming the instability of the reaction discussed in the previous section (Rosset and Perez-Lopez, 2019). Conversely, there a “complete” shift/conversion of esterification product obtained in the presence of sucrose4, which indicates total conversion, as also discussed in the previous section.

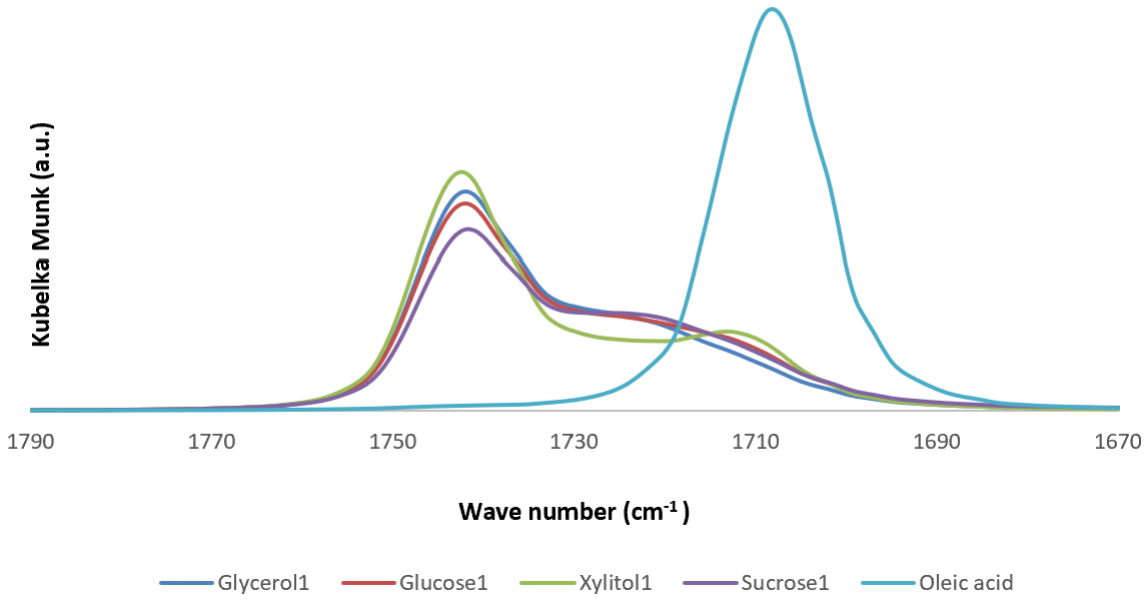

Figure 38 – FTIR spectra (1670 – 1790 cm^{-1}) of obtained methyl oleate from esterification in the presence of sugar derived catalysts with 1:1 concentration.

Figure 38 presents the FTIR spectra of the obtained methyl oleate from esterification reaction in the presence of the sugar catalysts derived catalysts with 1:1 concentration. It is possible to observe that xylitol1 also displays the say pattern behaviour, confirming the aforementioned inferences (Mahamuni and Adewuyi, 2009). Additionally, the peaks ranging from 1750 – 1730 cm^{-1} are much lower compared with the peak ranging from 1690 – 1720 cm^{-1}, confirming the FAME yield presented for these samples. From that, it could be inferred that there is a much higher presence of esters in samples reacted with catalysts with a higher percentage of sulfuric acid.

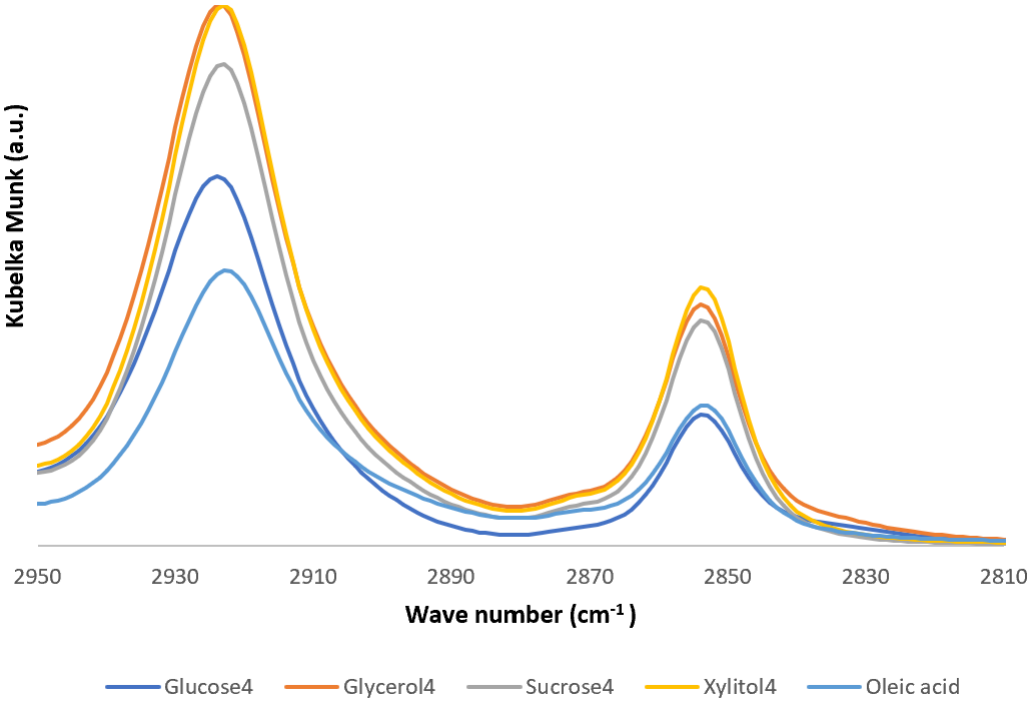

Figure 39 - FTIR spectra (2810 – 2950 cm^{-1}) of obtained methyl oleate from esterification in the presence of sugar derived catalysts with 1:4 concentration.

The presence of C-H bonds in the methyl group and the aliphatic chain of the oleate moiety resulted in absorption bands in the range of 2950-2850 cm^{-1}. These bands indicate the stretching vibrations of these C-H bonds. Figure 39 presents the FTIR spectra for the methyl oleate obtained in the presence of catalysts with higher concentration of sulfuric acid (1:4) in their preparation. The peak in this region is more accentuated and narrow compared to that of catalysts with lower sulfuric acid concentrations (1:1), which is lower and much wider (figure 40). This confirms that there is higher formation of -C-H bonds during the esterification of 1:4 catalysts (Rosset and Perez-Lopez, 2019). Glycerol4 presents the highest yield of carbon bonds among all the other catalysts.

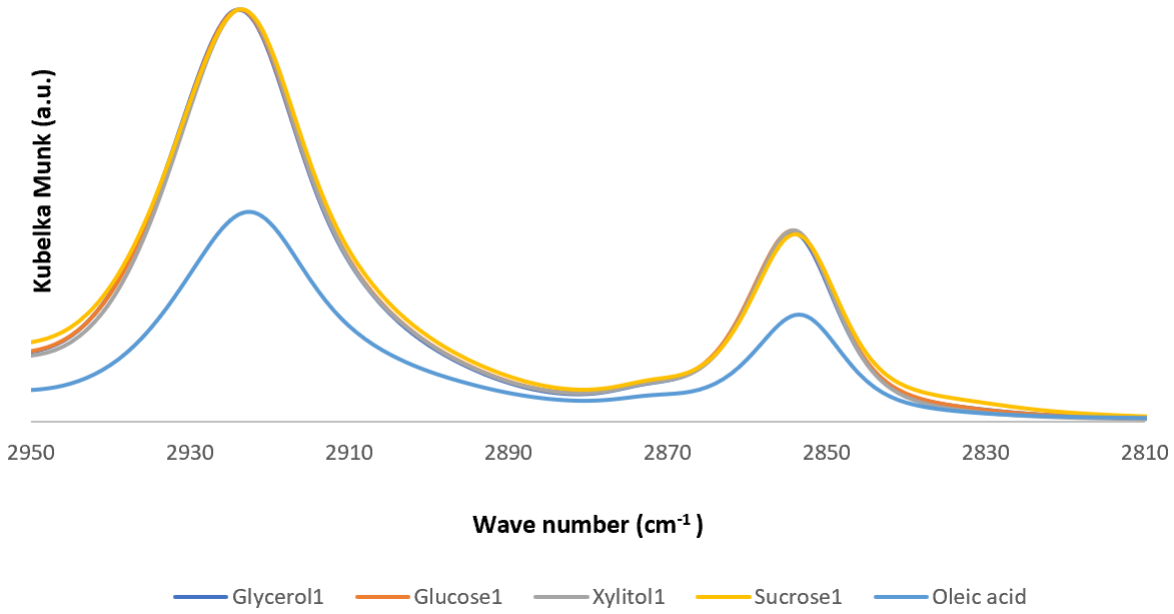

Figure 40 - FTIR spectra (2810 – 2950 cm^{-1}) of obtained methyl oleate from esterification in the presence of sugar derived catalysts with 1:1 concentration.

Moreover, the methyl oleate also contains a carbon-carbon double bond (C=C) in the oleate portion. This resulted in a characteristic absorption band in the range of 1640-1620 cm^{-1}, corresponding to the stretching vibration of the C=C bond.

Another important point to take into account is the influence of water in the reaction medium. Water is often generated as a by product during esterification reactions. The presence of water can adversely affect the reaction equilibrium by shifting it towards the reverse direction. Water can react with FAME to form free fatty acids and methanol through hydrolysis. Additionally, water can also hinder the reactant's accessibility to the catalyst and decrease reaction rates, further reducing FAME yield (Rosset and Perez-Lopez, 2019). To confirm that, experimental esterification reactions were conducted with oleic acid with 10% and 20% of water in the presence of sucrose4. Since this catalyst promoted the highest FAME yield, it was selected for this part of the experiment. Figure 41 displays the FTIR spectra of the methyl oleate for the experiments involving water.

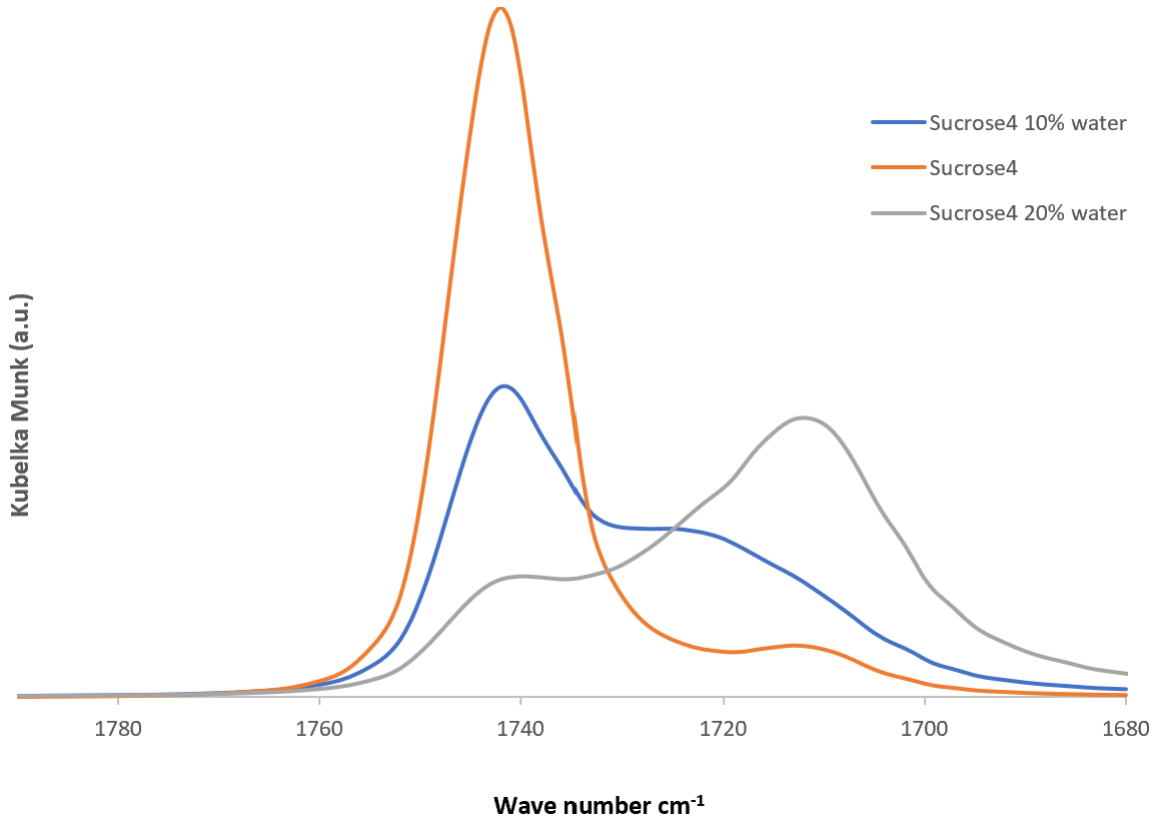

Figure 41 - FTIR spectra (1680 – 1780 cm^{-1}) of obtained methyl oleate from esterification in the presence of water with 10% and 20% concentrations with sucrose4.

The higher the water concentration in the reaction, the lower the FAME yield. In fact, there is no conversion for the reaction involving 20% of water since the peak for ester in the FTIR spectra is extremely low. Since the esterification is reversible and water is produced as a by product of the reaction, the presence of water in the reactant and water as a by product could have shifted the equilibrium of the reaction towards the reactants, oleic acid and methanol, rather than the formation of the desired product, FAME. Also, water could have participated in side reactions during the esterification process, hydrolysing the formed ester back into the carboxylic acid and methanol, reversing the esterification reaction. This side reaction can compete with the desired esterification and reduce the FAME yield. The presence of water has also led to sucrose4 deactivation or leaching of the active species, reducing the catalytic efficiency and potentially affecting the reaction rate and FAME yield, as also seen in figure 42.

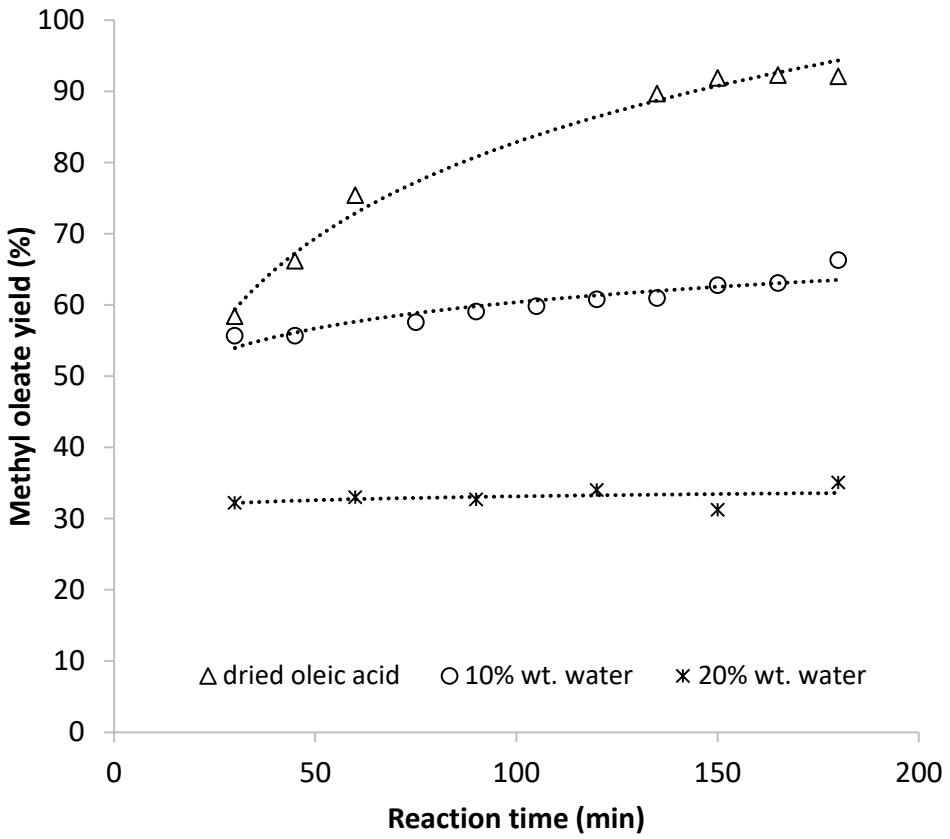

Figure 42 – Effect of water on FAME conversion reaction.

For oleic acid 80%, the reaction starts to occur at as soon as 30 minutes, however, simultaneously, all the active sites are occupied by water molecules shifting the reaction equilibrium towards reactants and, therefore, inhibiting the reaction, figure 42. Therefore, to enhance the conversion and yield of FAME, it is crucial for the raw material, specially those with high water concentrations, to undergo pre-treatment to remove the water from the reaction mixture. Therefore, it will help drive the reaction towards completion and increase the FAME yield. Also, controlling the water content for the other experiments in the reaction mixture was crucial for optimizing the esterification reactions.

.

Chapter 5

Conclusions and Future Work

5.1 Conclusions

The fundamental proposal of this work to synthesize an efficient and economical heterogeneous acidic catalyst derived from sugars – sucrose, xylitol, glycerol, and glucose - for biodiesel production from oleic acid oil and methanol was properly achieved. The methodology applied, based on the partial carbonization and sulfonation of the sugars with sulfuric acid was capable to produce a series of acidic catalysts with different phase composition. These catalysts performed, accordingly and differently for biodiesel production via esterification.

The data collected via Raman, XRD, FTIR, TGA, and SEM-EDS were capable of highlighting the differences among the obtained catalysts and indicate the reasons why for the differences in FAME conversion performance. Specifically, the most prominent heterogeneous catalysts developed were glycerol4 and sucrose4, both following an equal methodology, and holding very equivalent thermal stability and crystalline structures. Beyond that, these catalysts achieved even higher conversion levels for FAME when compared to traditional homogeneous catalysts.

Several characteristics related to these catalysts differentiate them from others, such as the elevated presence of sulfonic and carboxylic groups as well as high graphitization, all well-known characteristics of efficient biodiesel catalysts. These structures remain after esterification process, proving that they could be reused further in other reactions. This characteristic favours the material to be a good catalyst since it can present different active sites of acidic origin.

After this discussion, it is very interesting to note is the fact that sugar derived carbon sulfonated catalysts can positively impact the energy matrix for the enhancement of biodiesel production. Specially for glycerol derived catalysts, which contribute to the circular economy and valorisation of this biodiesel by product. Alternatives are all around claiming sometimes support, courage and dedication of governments and people to turn carbon neutral fuels it into reality. Definitely, there is still space for oil and gas, even with their known side effects, which can be extenuated at some level. Yet, there is also much space for sugar valorisation, biomass and biofuels, wind and solar energies, and any other creative idea that could cooperate to the main objective of caring for the globe and harnessing a brighter and clean future for the coming generations.

5.2 Future Work

Although the catalysts obtained in this study were proved to be very efficient, some of them, specially the ones obtained from lower concentrations of sulfuric acid presented a considerably low FAME yield. Kitano et al. (2009) explained that hydrophilic groups can prevent the access of hydrophobic molecules into the bulk, so that the reactions generally occur on the surface of the catalyst, decreasing the catalytic activity. Therefore, the development of surface area for those catalysts with low FAME yield can work around this problem, maintaining the hydrophobicity of the catalyst surface.

The increase in the surface area of the catalysts can be made through the Milled Ball mechanism. The milling process involves the use of rotating balls to apply mechanical forces to break down the catalysts into smaller pieces. After the milling process, the particles can be subjected to a balling mechanism, which involves tumbling the milled particles in a container. The rolling action will help to further break down the particles and create irregular shapes, resulting in increased surface area.

After that, the BET (Brunauer-Emmett-Teller) surface area analysis can be used to determine the specific surface area of the Milled Balled catalysts. The BET method measures the adsorption of gas molecules onto the surface of the catalyst and utilizes the resulting isotherm data to calculate the surface area. Subsequently, by comparing the specific surface area values of the milled and balled catalyst samples with the original ones, it will be possible to determine the extent of surface area increase achieved through the milled ball mechanism. Then, to access the effectiveness of the milling and balling process in enhancing the catalysts' surface area a repetition of the esterification reactions with the new and old catalysts would be needed.

Furthermore, an increase in the sulfonic groups can also contribute to higher catalytic performance. The activation process at 350°C with an oxygen muffler promotes the oxidation and development of pores within the catalysts can also lead to increased surface area and improved adsorption capacity. The duration of the activation process will vary depending on the desired level of activation and the properties of the catalysts, keeping in mind that longer activation times generally lead to greater pore development and surface area enhancement.

Also, the increase in carbonization temperatures may favour the functionalization of the catalysts with the sulfonic groups. Therefore, an analysis of catalysts carbonized at different temperatures might be useful. This increase in the carbonization temperature may also culminate in a more effective introduction of the group $-SO_3H$ and formation of -COOH after the sulfonation process.

Even though acidic catalysts are more suitable for esterification reactions, it would be interesting to evaluate the activity of the catalysts in transesterification reactions with proper conditions. Su and Guo (2014) explained that the partially carbon sulfonated catalysts have shown high catalytic performance for transesterification of triolein proceeding at 130 °C and 700 kPa, and its activity outperformed conventional solid acids such as silica-supported Nafion (Nafion SAC-13), Amberlyst-15, and Nafion NR50. The high pressure and temperature would, therefore, yield great results for the transesterification reaction.

Another proposed process is the investigation of the reusability and deactivation of the catalysts. This study would take place by reusing the catalysts in the esterification reaction as many times until there is a significant drop in conversion rate of the esterification product. According to the literature, partially sulfonated catalysts can be used up to 10 times without decrease in activity.

Finally, in future studies, Gas chromatography (GC) should be used to analyse the fatty acid composition of the methyl oleate, including the measurement of monoacylglycerols (MAGs), diacylglycerols (DAGs), and triacylglycerols (TAGs). Analyzing the MAGs, DAGs, and TAGs in obtained methyl oleate will be crucial for quality control, stability assessment, regulatory compliance, process optimization, and predicting its performance in various applications.

Appendix A

Supporting Figures and Tables

A.1 Supporting Figures

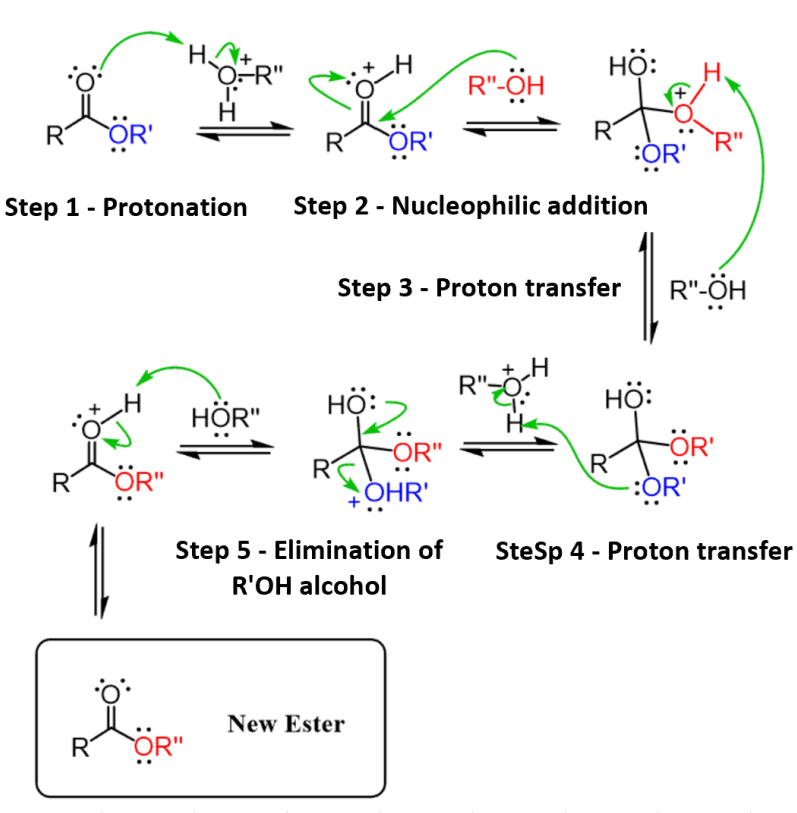

Figure A 1 - Representation of the transesterification mechanism. Adapted from: Organic Chemistry LCC (2022).

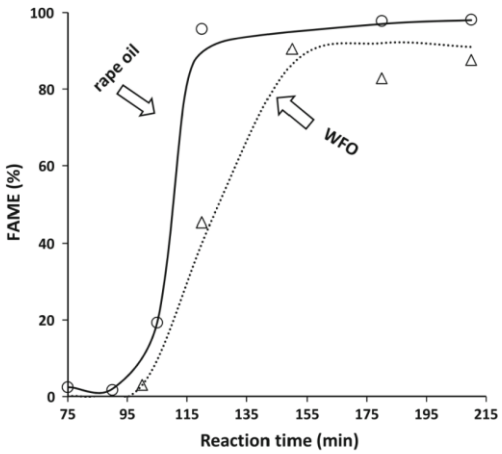

Figure A 2 - Sigmoidal curve of the transesterification reactions of rapeseed oil and waste fried oil. (Puna et al., 2013).

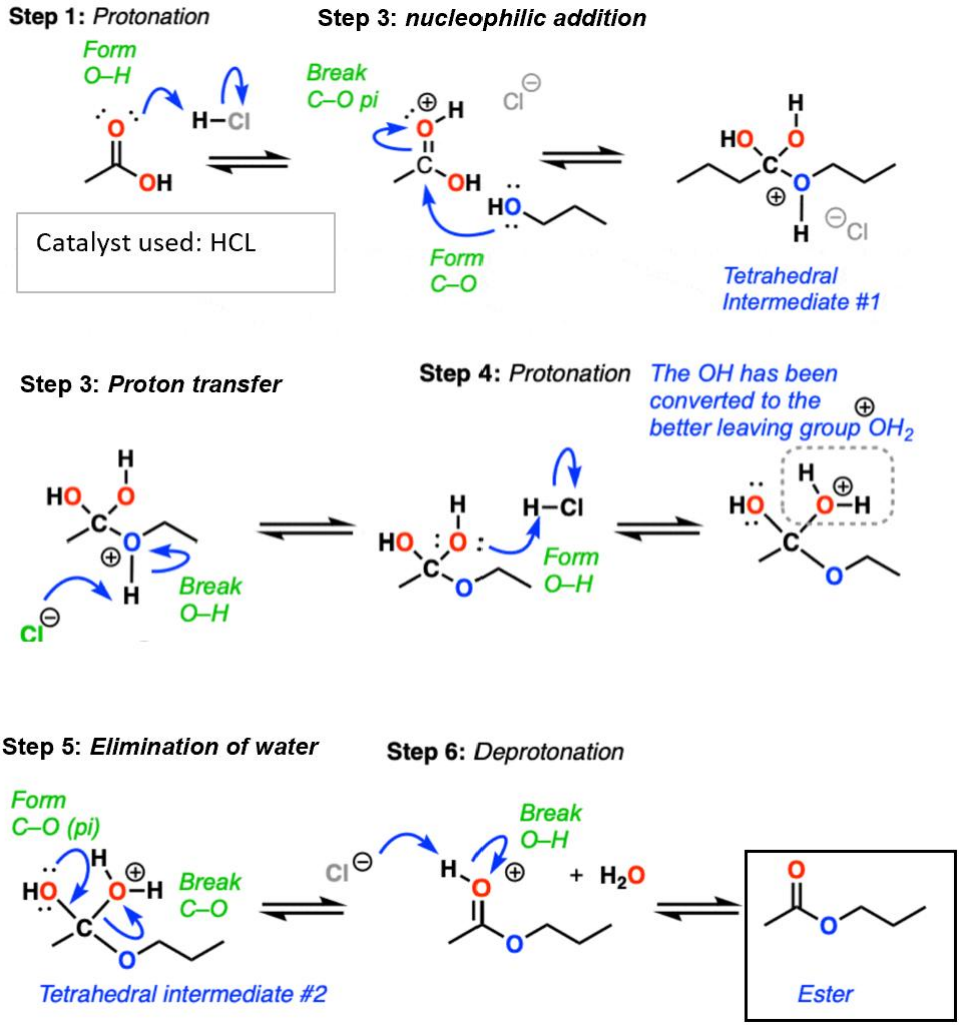

Figure A 3 – Representation of the Fischer-Spier esterification mechanism. Adapted from: Organic Chemistry LCC (2022).

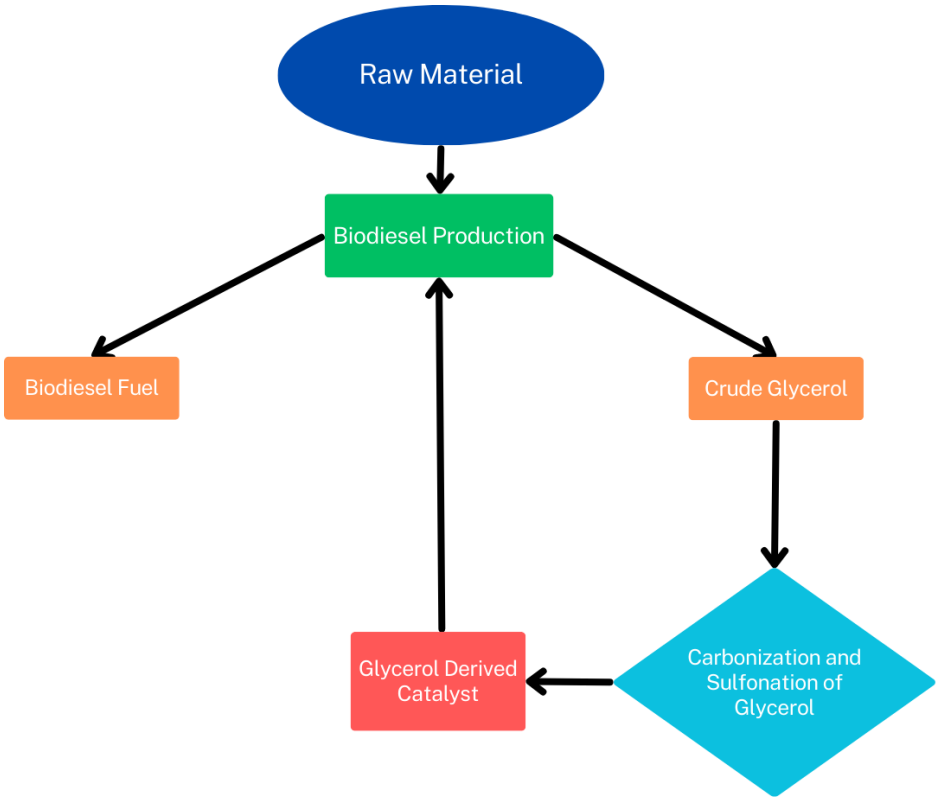

Figure A 4 – Crude glycerol valorisation schematic.

A.2 Supporting Tables

Table A 1 - Biodiesel technical Standards ASTM D6751 and EN 14214

Property	Unit	ASTM D6751		EN 14214	
		Limits	Test Method	Limits	Test Method
Flash point, min	°C	93	D93	101	EN ISO 2719
Water & sediment, max	% vol	0.05	D2709	-	-
Water, max	mg/kg	-	-	500	EN ISO 12937
Total contamination, max	mg/kg	-	-	24	EN 12662
Distillation temperature (% vol recovered)	°C	90%: 360 (max)	D1160	-	-
Kinematic viscosity	mm^2/s	1.9-6.0 mm^2/s	D445	3.5-5.0	EN ISO 3104
Density	kg/m^3	-	-	860-900	EN ISO 3675 EN ISO 12185
Ester content	%	-	-	96.5 (min)	EN 14103
Sulfated Ash, max	% (m/m)	0.02	D874	0.02	ISO 3987
Sulfur, max	ppm | mg/kg	Two grades: S15 0.0015 S500 0.05	D5453	10.0 mg/kg	EN ISO 20846 EN ISO 20884 EN ISO 13032
Copper strip corrosion, max	-	No. 3	D130	class 1	EN ISO 2160
Cetane number, min	-	47	D613	51	EN ISO 5165
Cloud point	°C	Report	D2500	Location & season dependent	EN 23015
Carbon residue on 10% distillation residue, max	% (m/m)	0.05	D4530	-	-
Acid number, max	mg KOH/g	0.50	D664	0.5	EN 14104
Oxidation stability	hrs	3 (min)	EN 14112	8 (min)	EN 14112
Iodine value, max	-	-	-	120[1] g Iod/100g	EN 14111 EN 16300
Linolenic acid methyl ester, max	% (m/m)	-	-	12	EN 14103
Polyunstatured methyl esters, max	% (m/m)			1	EN 15779
Alcohol control	% (m/m)	0.2 methanol (max) 130°C flash point (min)	EN14110 D93	0.20 methanol (max)	EN 14110
Monoglycerides, diglycerides & triglycerides, max	% (m/m)	MG 0.40	D6584	MG 0.70 DG 0.20 TG 0.20	EN 14105
Group I metals (Na + K), max	mg/kg	5	EN 14538	5	EN 14108 EN 14109 EN 14538
Group II metals (Ca + Mg), max	mg/kg	5	EN 14538	5	EN 14538
Free glycerin, max	% (m/m)	0.02	D6584	0.02	EN 14105 EN 14106
Total glycerin, max	%(m/m)	0.24	D6584	0.25	EN 14105
Phosphorous, max	% (m/m) | mg/kg	0.001	D4951	4	EN 14107 EN 16294

Sources: ACEA (2009); ASTM (2002).

Table A 2 - Properties of fossil diesel, biodiesel (from edible and nonedible sources), and its blends.

Property	Unit	Fossil Diesel	Non-edible oil BD (Rapeseed)	Edible oil BD (Sunflower)	BD + Diesel Blends 5%	BD + Diesel Blends 10%	BD + Diesel Blends 15%
Cetane Number	-	47.8	54.4	47.8	60.5	61.8	62.6
Flash Point	°C	80	> 110	173	-	-	-
Cloud Point	°C	-12.2	-2.2	1	-16.6	-12.4	-9.7
Pour Point	°C	-28.9	-9.4	-6	-	-	-
Viscosity at 40 °C	-	3.2	6.2	4.87	2.7	2.8	2.9
Conductivity at 100°C	W/Mk	0.11	0.2	-	-	-	-
Surface Tension at 100°C	Mn / m^2	22.5	25.4	-	-	-	-
Lower Heating Value	kJ/kg	45,300	40,600	-	-	-	-
Density	kg/m^3	852	874	841	831	833	837
Sulphur Content	%wt	0.32	0.031	0.4	-	-	-
Carbon	%wt	87.26	77.2	79.5	-	-	-
Hydrogen	%wt	13.44	12.6	10.3	-	-	-
Oxygen	%wt	0	10.9	8.9	-	-	-
Reference	-	[A]	[A]	[B] [C]	[D]	[D]	[D]

Sources: [A] Zhou et al., 2003 [B] Dey et al., 2020 [C] Tutunea et al., 2018 [D] Rodriguez-Fernandez et al., 2019.

Table A 3 – Classification of major fatty acids. Adapted from: Khan Academy (2014)

Common name	Lipid No.	IUPAC's Official Name
Saturated fatty acids		
Proprionic	C3:0	Propanoic
Butyric	C4:0	Butanoic
Caprylic	C8:0	Octanoic
Capric	C10:0	Decanoic
Lauric	C12:0	Dodecanoic
Myristic	C14:0	Tetradecanoic
Palmitic	C16:0	Hexadecanoic
Stearic	C18:0	Octadecanoic
Behenic	C22:0	Docosanoic
Lignoceric	C24:0	Tetracosanoic
Cerotic	C26:0	Hexacosanoic
Monounsaturated fatty acids		
Palmitoleic	C16:1 n-7	9 – hexadecaenoic (cis)
Oleic	C18:1 n-9 (cis)	9 – octadecaenoic (cis)
Elaidic	C18:1 n-9 (trans)	9 – octadecaenoic (trans)
Polyunsaturated fatty acids		
Linoleic	C18:2 n-6 (all cis)	9, 12 – octadecadienoic
Alpha-linolenic	C18:3 n-3 (all cis)	6, 9, 15 – octadecatrienoic (cis)
Gamma-linolenic	C18:3 n-6	6, 9, 12 – octadecatrienoic (cis)
Arachidonic	C20:4 n-6 (all cis)	5, 8, 11, 14 – eicosatetraenoic (cis)
Timnodonic	C20:5 n-3 (all cis)	5, 8, 11, 14, 17 – eicosapentaenoic (cis)
Cervonic	C22:6 n-3 (all cis)	4, 7, 10, 13, 16, 19 – docosahexaenoic (cis)

Note:

The nomenclature "Lipid Number" indicates the quantity of carbons (number followed by C) and the quantity of double bonds (after the ":" punctuation).

The nomenclature "n-x" indicates the location of the double bond in the carbon chain (carbon-carbon) considering as referential the last carbon of the chain.

Table A 4 - Fatty Acid Composition of major raw materials for biodiesel production in Europe

Fatty Acid	Lipid No.	Soybean	Palm	Palm Kernel	Sunflower	Rapeseed	Beef Tallow	Poutry Fat	WCO
Capric	C10:0	-	-	3.5	-	-	-	-	-
Lauric	C12:0	0.1	0.1	47.8	-	-	-	0.2	-
Myristic	C14:0	0.1	1.1	16.3	< 0.2	0.05	2.8	1.2	0.1
Palmitic	C16:0	11.86	44	8.5	5.5	4.8	26.8	0.4	8.8
Palmitoleic	C16:1	0.1	-	-	< 0.3	0.06	2.1	22.3	4.7
Stearic	C18:0	4.7	4.5	2.4	3.8	0.1	34.8	7.2	4.2
Oleic	C18:1	21.6	39.2	15.4	32.8	62.7	30.2	6.1	45.1
Linoleic	C18:2	52.6	10.1	2.4	60.1	22.4	0.7	41.4	39.7
Alpha - Linoleic	C18:3	7.6	0.4	-	< 0.3	7.5	0.9	-	0.2
Lignoceric	C24:0	0.07	-	-	< 0.5	-	-	-	0.3
Reference		[B]	[A]	[A]	[C]	[D]	[E]	[F]	[G]

Note:

WCO composition varies depending on the sample used, values are averaged.

[A] Mancini et al., 2015 [B] Feng et al., 2015 [C] Rosa et al., 2009 [D] Cristea et al., 2018 [E] Selvam & Vadivel, 2012 [F] Grimmes 1996 [G] Bautista et al., 2009

Table A 5 – Examples of catalysts used for biodiesel production.

Catalyst	Type of Catalyst	Feedstock	Reaction Conditions				Yield	Ref.
			Temp. (°C)	Time (min)	Alcohol: Oil Ratio	Catalysts Content (%wt)		
Homogeneous Catalyst								
KOH	alkaline	WCO	65	60	6:01	1	96	[A]
NaOH	alkaline	WCO	50	70	6:01	1	89.8	[B]
$NaOCH_3$	alkaline	WCO	65	60	6:01	0.75	96.6	[C]
H_2SO_4	acidic	Chicken tallow	65	180	30:01:00	2.5	93.2	[D]
$C_2HF_3O_2$	acidic	Soybean oil	65	180	20:01	2	98.4	[E]
Heterogeneous Catalysts								
Earth Metal Oxides								
CaO	alkaline	Sunflower oil	65	180	13:01	8	94	[F]
Transition Metal Oxides								
Na_2MoO_4	alkaline	Soybean oil	120	180	54:01:00	0.5	95.6	[I]
Zeolites								
CaO@NaY zeolite	alkaline	Soybean oil	65	180	9:01	3	95	[J]
Aluminium-Supported								
K@KOH @Al_2O_3	alkaline	Rapeseed oil	60	60	9:01	4	96	[K]
Hydrotalcites								
Mg–Al HT	alkaline	Jatropha oil	160	240	30:01:00	5	93.4	[L]
Biomass-Based								
Chicken eggshell	alkaline	Karanja oil	65	150	8:01	2.5	95	[M]
Coconut husk	alkaline	JCO	45	60	12:01	7	99.8	[O]
Ion Exchange Resins								
Amberlyst-26	acidic	Canola oil	45	90	6:01	3	67	[P]
Sulfated								
$Ti(SO_4)O$	acidic	WCO	75	180	9:01	1.5	97.1	[R]
Sufonated Carbon-Based								
Sulfonated sugar	acidic	Oleic acid	80	240	10:01	7.4	NR	[S]
Glycerol	acidic	Palmitic acid	65	240	9.7:1	10	99	[T]
Biochar	acidic	Oleic acid	315	180	30:01:00	5	92	[U]
Bamboo-SO_3H	acidic	Oleic acid	90	360	7:01	2	98.4	[V]
Enzymes								
Lipase@[bmim][PF6]	acidic	Food compost	50	840	6:01	40	72	[W]
Bifunctional								
γ-Al_2O_3–CeO2	-	WCO	110	270	30:01:00	7	81.1	[Y]

References: [A] Refaat et al. (2007); [B] Meng, Chen, & Wang (2008); [C] Chen et al. (2012); [D] Bhatti et al. (2008); [E] Miao, Li, & Yao (2009); [F] Granados et al. (2007); [G] Mootabadi et al. (2010); [H] Silva et al. (2008); [I] Nakagaki et al. (2008); [J] Wu et al. (2013); [K] Ma et al. (2008); [L] Helwani et al. (2013); [M] Sharma, Singh, & Korstad (2010); [N] Shankar and Jambulingam (2017); [O] Vadery et al. (2014); [P] Ilgen, Akin, & Boz (2009); [Q] Jalinejad et al. (2019); [R] Gardy et al. (2016); [S] Toda et al. (2005); [T] Devi et al. (2009); [U] Dehkhoda and Elis (2013); [V] Zhou, Niu, and & Li (2016); [W] Taher et al. (2019); [X] Muanruksa and Kaewkannetra (2020); [Y] Ramli and Farooq (2015); [Z] Jeon et al. (2019)

Appendix B

Additional Experimental Results

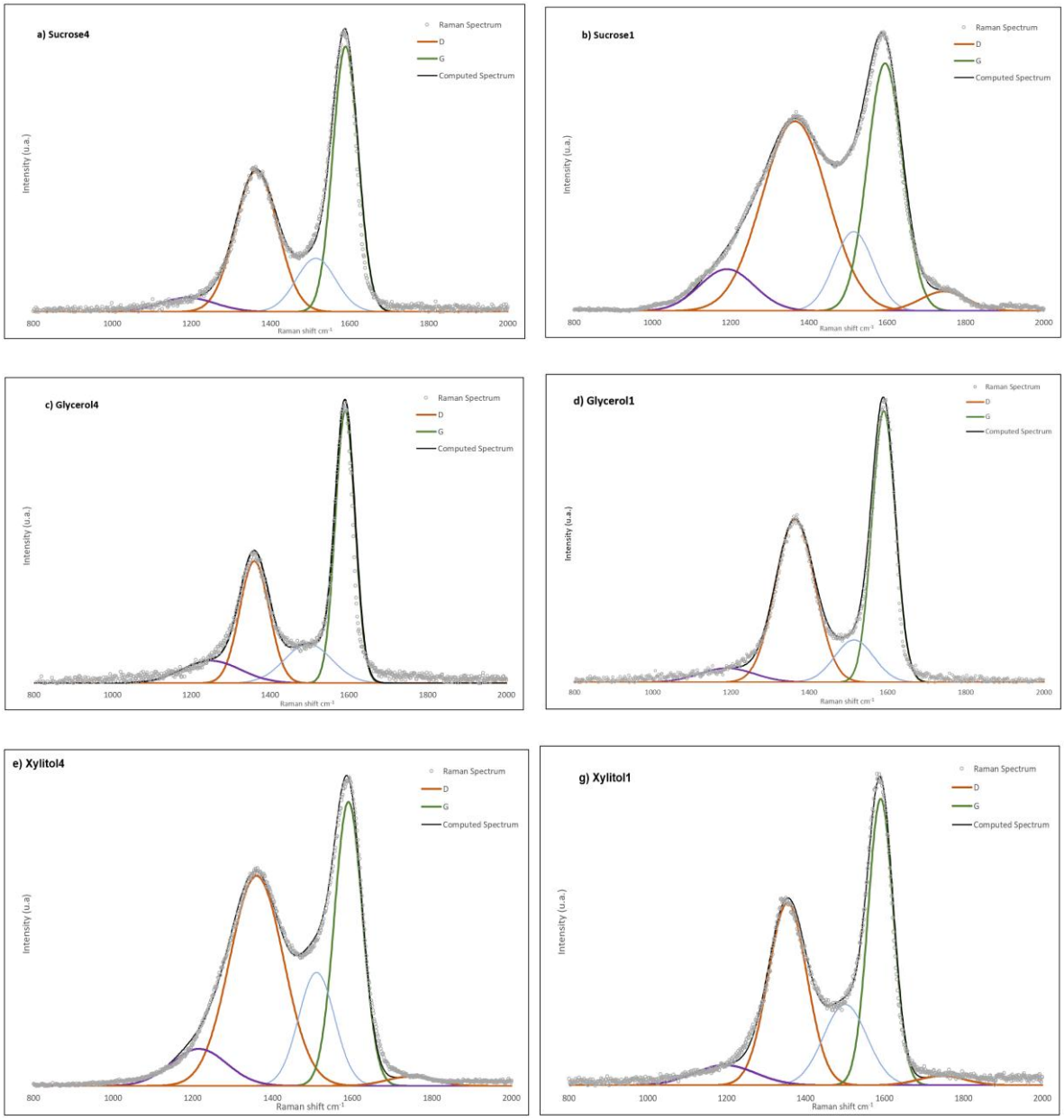

Figure B 1 – Deconvoluted Raman spectrum for all catalysts.

References

Aatola, H., Larmi, M., Sarjovaara, T., & Mikkonen, S. (2008). Hydrotreated Vegetable Oil (HVO) as a Renewable Diesel Fuel: Trade-off between NOx, Particulate Emission, and Fuel Consumption of a Heavy-Duty Engine. SAE Int. J. Engines, 1(1), 1251–1262. https://doi.org/10.4271/2008-01-2500

Abdullah, S. H. Y. S., Hanapi, N. H. M., Azid, A., Umar, R., Juahir, H., Khatoon, H., & Endut, A. (2017). A review of biomass-derived heterogeneous catalyst for a sustainable biodiesel production. Renewable and Sustainable Energy Reviews, 70(September 2015), 1040–1051. https://doi.org/10.1016/j.rser.2016.12.008

ACEA, 2009. Worldwide Fuel Charter Committee. “Biodiesel Guidelines”, European Automobile Manufacturers Association, Brussels, Belgium, March 2009.

Ahvad, A., & Marchetti, J. (2016). Innovation in solid heterogeneous catalysis for the generation of economically viable and ecofriendly biodiesel: A review. Catalysis Reviews, 58, 157-208.

Ahvad, A., & Marchetti, J. (2016). Innovation in solid heterogeneous catalysis for the generation of economically viable and ecofriendly biodiesel: A review. Catalysis Reviews, 58, 157-208.

Aliske, M. A., Zagonel, G. F., Costa, B. J., Veiga, W., & Saul, C. K. (2007). Measurement of biodiesel concentration in a diesel oil mixture. Fuel, 86(10–11), 1461–1464. doi: 10.1016/j.fuel.2006.11.008

Alsaiari, R. A., Musa, E. M., & Rizk, M. A. (2023). Biodiesel production from date seed oil using hydroxyapatite-derived catalyst from waste camel bone. Heliyon, 9(5). doi:10.1016/j.heliyon.2023.e15606.

Altarazi, Y. S. M., Abu Talib, A. R., Yu, J., Gires, E., Abdul Ghafir, M. F., Lucas, J., & Yusaf, T. (2022). Effects of biofuel on engines performance and emission characteristics: A Review. Energy, 238, 121910. doi:10.1016/j.energy.2021.121910.

Alves, C. T., Peters, M. A., & Onwudili, J. A. (2022). Application of thermogravimetric analysis method for the characterisation of products from triglycerides during biodiesel production. Journal of Analytical and Applied Pyrolysis, 168, 105766. doi:10.1016/j.jaap.2022.105766

Aranda, D. A. G., & Machado, G. D. (2016). Biodiesel Production by Hydroesterification: Simulation Studies BT - Green Fuels Technology: Biofuels (C. R. Soccol, S. K. Brar, C. Faulds & L. P. Ramos, Eds.). doi:10.1007/978-3-319-30205-8_13.

Aransiola, E. F., Ikhu-Omoregbe, D. I. O., Madzimbamuto, T. F., Ojumu, T. V., & Oyekola, O. O. (2013). A review of current technology for biodiesel production: State of the art. Biomass and Bioenergy, 61, 276–297. doi:10.1016/j.biombioe.2013.11.014.

Aransiola, E., Ojumu, T., Oyekola, O., Madzimbamuto, T., & Ikhu-Omoregbe, D. (2014). A review of current technology for biodiesel production: state of the art. Biomass and bioenergy, 61, 276- 297.

Ashcroft, W., Mermin, D. (1976). Solid state physics. New York: Holt, Rinehart and Winston. ISBN 0030839939. OCLC 934604.

ASTM, 2002. “Standard Specification for Biodiesel Fuel (B100) Blend Stock for Distillate Fuels”,

American Society for Testing and Materials, D6751-02.

Atadashi, I. M., Aroua, M. K., & Aziz, A. A. (2011). Biodiesel separation and purification: A Review. Renewable Energy, 36(2), 437–443.

Atadashi, I. M., Aroua, M. K., Abdul Aziz, A. R., & Sulaiman, N. M. N. (2013). The effects of catalysts in biodiesel production: A Review. Journal of Industrial and Engineering Chemistry, 19(1), 14–26.

Avhad, M. R., & Marchetti, J. M. (2015). A review on recent advancement in catalytic materials for biodiesel production. Renewable and Sustainable Energy Reviews, 50, 696–718.

Bautista, L. F., Vicente, G., Rodríguez, R., & Pacheco, M. (2009). Optimisation of fame production from waste cooking oil for biodiesel use. Biomass and Bioenergy, 33(5), 862–872.

BHATTI, H., HANIF, M., QASIM, M., & ATAURREHMAN. (2008). Biodiesel production from waste tallow. Fuel, 87(13–14), 2961–2966. doi:10.1016/j.fuel.2008.04.016.

BIOENERGY AND BIOFUELS. (2013). Food and Agriculture Organization. Biofuels and the sustainability challenge: a global assessment of sustainability issues, trends and policies for biofuels and related feedstocks. Italy. ISBN : 9789251074145.

Booramurthy, V. K., Kasimani, R., Pandian, S., & Ragunathan, B. (2020). Nano-sulfated zirconia catalyzed biodiesel production from Tannery Waste Sheep fat. Environmental Science and Pollution Research, 27(17), 20598–20605. doi:10.1007/s11356-020-07984-1.

Borges, M. E., Díaz, L., Gavín, J., & Brito, A. (2011). Estimation of the content of fatty acid methyl esters (FAME) in biodiesel samples from dynamic viscosity measurements. *Fuel Processing Technology*, *92*(3), 597–599. doi:10.1016/j.fuproc.2010.11.016.

Canakci, M. (2007). The potential of restaurant waste lipids as biodiesel feedstocks. Bioresource Technology, 98(1), 183-190. Chakraborty, R. G. (2014). Conversion of slaughterhouse and poultry farm animal fats and wastes to biodiesel: Parametric sensitivity and fuel quality assessment. Renewable and Sustainable Energy Reviews, 29, 120-134.

Catarino, M., Ramos, M., Dias, A. P., Santos, M. T., Puna, J. F., & Gomes, J. F. (2017). Calcium rich food wastes-based catalysts for biodiesel production. Waste and Biomass Valorization, 8(5), 1699–1707.

Chakraborty, R. G. (2014). Conversion of slaughterhouse and poultry farm animal fats and wastes to biodiesel: Parametric sensitivity and fuel quality assessment. Renewable and Sustainable Energy Reviews, 29, 120-134.

Chand, P., Reddy, C., Verkade, J., Wang, T. and Grewell, D. (2008) Novel characterization method of biodiesel produced from soybean oil using thermogravimetric analysis. In 2008 Providence, Rhode Island, June 29–July 2, 2008, page 1. American Society of Agricultural and Biological Engineers.

Chand, P., Reddy, C., Verkade, J., Wang, T., and Grewell, D. (2009) Thermogravimetric quantification of biodiesel produced via alkali catalyzed transesterification of soybean oil. Energy & Fuels, 23(2): 989–992.

Changmai, B., Vanlalveni, C., Ingle, A. P., Bhagat, R., & Rokhum, S. L. (2020). Widely used catalysts in biodiesel production: A Review. RSC Advances, 10(68), 41625–41679.

Che M. and Vedrine, J. (2012) Characterization of solid materials and heterogeneous catalysts: From structure to surface reactivity. John Wiley & Sons.

Chen, K.-S., Lin, Y.-C., Hsu, K.-H., & Wang, H.-K. (2012). Improving biodiesel yields from waste cooking oil by using sodium methoxide and a microwave heating system. Energy, 38(1), 151–156. doi:10.1016/j.energy.2011.12.020.

Chouhan, A. P. S., & Sarma, A. K. (2011). Modern heterogeneous catalysts for biodiesel production: A comprehensive review. Renewable and Sustainable Energy Reviews, 15(9), 4378– 4399.

Ciriminna, R., Pina, C. D., Rossi, M., & Pagiliaro, M. (2014). Understanding the Glycerol Market. Eur. J. Lipid Sci. Technol, 116, 1432-1439. doi:10.1002/ejlt.201400229.

Clohessy, J., & Kwapinski, W. (2020a). Carbon-based catalysts for biodiesel production—a review. Applied Sciences, 10(3), 918. doi:10.3390/app10030918.

Corrêa, A. P. da L., da Silva, P. M., Gonçalves, M. A., Bastos, R. R., da Rocha Filho, G. N., & da Conceição, L. R. (2023). Study of the activity and stability of sulfonated carbon catalyst from Agroindustrial Waste in biodiesel production: Influence of pyrolysis temperature on functionalization. Arabian Journal of Chemistry, 16(8), 104964.

Cristea, G. C., Cazamir, D., Dima, D., Georgescu, C., & Deleanu, L. (2018). Influence of tio2 as nano additive in rapeseed oil. IOP Conference Series: Materials Science and Engineering, 444, 022011.

Cruz, M., Almeida, M. F., Alvim-Ferraz, M. da C., & Dias, J. M. (2019). Monitoring Enzymatic Hydroesterification of Low-Cost Feedstocks by Fourier Transform Infrared Spectroscopy. Catalysts, 9(5), 535.

Dehkhoda, A. M., & Ellis, N. (2013). Biochar-based catalyst for simultaneous reactions of esterification and transesterification. Catalysis Today, 207, 86–92.

Demirbaş, A. (2008). Comparison of transesterification methods for production of biodiesel from vegetable oils and fats. Energy Conversion and Management, 49(1), 125–130.

DEMIRBAS, A. (2010). Biorefineries for biomass upgrading facilities. Springer.

Demirbas, A., Bafail, A., Ahmad, W., & Sheikh, M. (2016). Biodiesel production from non-edible plant oils. Energy Exploration and Exploitation, 34(2), 290–318.

Deng, X., Fang, Z., & Liu, Y.-hu. (2010). Ultrasonic transesterification of Jatropha curcas L. Oil to biodiesel by a two-step process. Energy Conversion and Management, 51(12), 2802–2807..

Deshmane, V. G., Gogate, P. R., & Pandit, A. B. (2008). Ultrasound-assisted synthesis of biodiesel from palm fatty acid distillate. Industrial & Engineering Chemistry Research, 48(17), 7923–7927.

Devi, B., Gangadhar, K., Prasad, P., Jagannadh, B., & Prasad, R. (2009). A Glycerol-based Carbon Catalyst for the Preparation of Biodiesel. ChemSusChem, 2, 617-620. doi:10.1002/cssc.200900097.

Dey, P., & Ray, S. (2020). Comparative analysis of waste vegetable oil versus transesterified waste vegetable oil in diesel blend as alternative fuels for compression ignition engine. Clean Technologies and Environmental Policy, 22(7), 1517–1530.

Dharma, S., Masjuki, H. H., Ong, H. C., Sebayang, A. H., Silitonga, A. S., Kusumo, F., & Mahlia, T. M. I. (2016). Optimization of biodiesel production process for mixed jatropha curcas–ceiba pentandra biodiesel using response surface methodology. Energy Conversion and Management, 115, 178–190.

Di Serio, M., Tesser, R., Dimiccoli, M., Cammarota, F., Nastasi, M., & Santacesaria, E. (2005). Synthesis of biodiesel via homogeneous Lewis's acid catalyst. Journal of Molecular Catalysis A: Chemical, 239(1–2), 111–115.

do Nascimento, L. A., Angélica, R. S., da Costa, C. E. F., Zamian, J. R., & da Rocha Filho, G. N. (2011). Comparative study between catalysts for esterification prepared from kaolins. Applied Clay Science, 51(3), 267–273.

Duffy, P. (1853). On the Constitution of Stearic Acid. The quarterly journal of the chemical society of

Džimbeg-Malčić , V., Barbarić-Mikočević, Ž., & Itrić, K. (2011). Kubelka-Munk theory in describing optical properties of paper (I) [Kubelka-Munk teorija u opisivanju optičkih svojstava papira (I)]. Tehnicki Vjesnik. ISSN 1330-3651

Edington J. (1976) Practical electron microscopy in materials science (N. V. Philips' Gloeilampenfabrieken, Eindhoven) ISBN 1-878907-35-2, Appendix 2.

Endalew, A. K., Kiros, Y., & Zanzi, R. (2011). Inorganic heterogeneous catalysts for biodiesel production from vegetable oils. Biomass and Bioenergy, 35(9), 3787–3809.

Endalew, A. K., Kiros, Y., & Zanzi, R. (2011a). Heterogeneous catalysis for biodiesel production from Jatropha curcas oil (JCO). Energy, 36(5), 2693–2700.

Endalew, A. K., Kiros, Y., & Zanzi, R. (2011b). Inorganic heterogeneous catalysts for biodiesel production from vegetable oils. Biomass and Bioenergy, 35(9), 3787–3809.

EIA. (2019a). Biofuels Explained. Retrieved from www.eia.gov/energyexplained/biofuels/.

EU. Directive (2003) 2003/30/EC of the European Parliament and of the Council of 8 May 2003 on the promotion of the use of biofuels or other renewable fuels for transport. , 4 Official Journal of the European Union.

Faix. O. (1992). Fourier Transform Infrared Spectroscopy. 233-241. doi: 10.1007/978-3-642-74065-7_16.

Feng, Y., Ding, Y., Liu, J., Tian, Y., Yang, Y., Guan, S., & Zhang, C. (2015). Effects of dietary omega-3/omega-6 fatty acid ratios on reproduction in the young breeder rooster. BMC Veterinary Research, 11(1). doi:10.1186/s12917-015-0394-9.

Ferrari, A., Robertson, J., 2000. Interpretation of Raman spectra of disordered and amorphous carbon. Phys. Rev. B Condens. Matter 61, 14095e14107. Doi:10.1103/PhysRevB.61.14095.

Fischer, E., & Speier, A. (1895). Darstellung der Ester. Berichte Der Deutschen Chemischen Gesellschaft, 28(3), 3252–3258.

Fonseca, J. M., Spessato, L., Cazetta, A. L., Silva, C. d., & Almeida, V. d. (2022). Sulfonated carbon: synthesis, properties, and production of biodiesel. Chemical Engineering and Processing - Process Intensification, 170.

Fonseca, J. M., Spessato, L., Cazetta, A. L., Silva, C. d., & Almeida, V. d. (2022). Sulfonated carbon: synthesis, properties, and production of biodiesel. Chemical Engineering and Processing - Process Intensification, 170.

Galadima, A., & Muraza, O. (2014). Biodiesel production from algae by using heterogeneous catalysts: A critical review. Energy, 78, 72–83. https://doi.org/10.1016/j.energy.2014.06.018.

Gardy, J., Hassanpour, A., Lai, X., & Ahmed, M. H. (2016a). Synthesis of ti(so 4)O solid acid nano-catalyst and its application for biodiesel production from used cooking oil. Applied Catalysis A: General, 527, 81–95.

Georgogianni, K. G., Katsoulidis, A. K., Pomonis, P. J., Manos, G., & Kontominas, M. G. (2009). Transesterification of rapeseed oil for the production of biodiesel using homogeneous and heterogeneous catalysis. Fuel Processing Technology, 90(7-8), 1016–1022.

Giurlani, W., Berretti, E., Innocenti, M., & Lavacchi, A. (2020). Measuring the thickness of metal coatings: A review of the methods. Coatings, 10(12), 1211.

Gonçalves, M., Rodrigues, R., Galhardo, T.S., Carvalho, W.A., (2016). Highly selective acetalization of glycerol with acetone to solketal over acidic carbon-based catalysts from biodiesel waste. Fuel 181, 46-54.

Gouadec, G., & Colomban, P. (2007). Raman spectroscopy of nanomaterials: How spectra relate to disorder, particle size and mechanical properties. Progress in Crystal Growth and Characterization of Materials, 53(1), 1–56.

Granados, D. A., Velásquez, H. I., & Chejne, F. (2014). Energetic and exergetic evaluation of residual biomass in a torrefaction process. Energy, 74, 181–189.

Granados, M. L., Poves, M. D. Z., Alonso, D. M., Mariscal, R., Galisteo, F. C., Moreno-Tost, R., Santamaría, J., & Fierro, J. L. G. (2007). Biodiesel from sunflower oil by using activated calcium oxide. Applied Catalysis B: Environmental, 73(3–4), 317–326.

GRIMES, J. L., MAURICE, D. V., LIGHTSEY, S. F., & GAYLORD, T. G. (1996). Dietary prilled fat and layer chicken performance and egg composition . Poultry Science, 75(2), 250–253.

Guldhe, A., Singh, P., Ansari, F. A., Singh, B., & Bux, F. (2017). Biodiesel synthesis from microalgal lipids using tungstated zirconia as a heterogeneous acid catalyst and its comparison with homogeneous acid and enzyme catalysts. Fuel, 187, 180–188. doi: 10.1016/j.fuel.2016.09.053.

Gupta, V., & Pal Singh, K. (2023). The impact of heterogeneous catalyst on biodiesel production; a review. Materials Today: Proceedings, 78, 364–371. Doi: 10.1016/j.matpr.2022.10.175.

Gurdus, L. (2020). Crude prices plunge to the lowest level in history — what Cramer and others are watching. Retrieved from CNBC.

Hargreaves, J. (2005) Powder x-ray diffraction and heterogeneous catalysis. Crystallography Reviews, 11(1):21–34.

Helwani, Z., Aziz, N., Bakar, M. Z. A., Mukhtar, H., Kim, J., & Othman, M. R. (2013). Conversion of jatropha curcas oil into biodiesel using re-crystallized hydrotalcite. Energy Conversion and Management, 73, 128–134.

Helwani, Z., Othman, M. R., Aziz, N., Fernando, W. J. N., & Kim, J. (2009a). Technologies for production of biodiesel focusing on green catalytic techniques: A review. Fuel Processing Technology, 90(12), 1502–1514.

Helwani, Z., Othman, M. R., Aziz, N., Kim, J., & Fernando, W. J. N. (2009b). Solid heterogeneous catalysts for transesterification of triglycerides with methanol: A review. Applied Catalysis A: General, 363(1–2), 1–10.

Heynderickx, P. M., Chaemchuen, S., & Verpoort, F. (2020). Kinetic modeling of heterogeneous esterification reaction using initial reaction rate analysis: Data extraction and evaluation of mass transfer criteria. Data in Brief, 31, 106027.

Ibrahim, S. F., Asikin-Mijan, N., Ibrahim, M. L., Abdulkareem-Alsultan, G., Izham, S. M., & Taufiq-Yap, Y. H. (2020). Sulfonated functionalization of carbon derived corncob residue via hydrothermal synthesis route for esterification of palm fatty acid distillate. Energy Conversion and Management, 210, 112698. Doi:10.1016/j.enconman.2020.112698.

IEA (2021), Key World Energy Statistics 2021, IEA, Paris https://www.iea.org/reports/key-world-energy-statistics-2021, License: CC BY 4.0.

IEA (2022), Biofuels, IEA, Paris https://www.iea.org/reports/biofuels, License: CC BY 4.0.

IEA, Global share of total energy supply by source, 2019, IEA, Paris https://www.iea.org/data-and-statistics/charts/global-share-of-total-energy-supply-by-source-2019, IEA. Licence: CC BY 4.0.

ILGEN, O., AKIN, A. N., & BOZ, N. (2009). Investigation of biodiesel production from canola oil using amberlyst-26 as a catalyst. Turkish Journal of Chemistry. Doi:10.3906/kim-0809-30.

Ivanoiu, A., Schmidt, A., Peter, P., & Rusnac, L.-M. (2011). Comparative study on biodiesel synthesis from different vegetables oils. Chem Bull, 56.

Jalilnejad Falizi, N., Güngören Madenoğlu, T., Yüksel, M., & Kabay, N. (2019). Biodiesel production using gel-type cation exchange resin at different ionic forms. International Journal of Energy Research, 43(6), 2188–2199. Doi:10.1002/er.4434.

Jamil, F., Murphin Kumar, P. S., Al-Haj, L., Tay Zar Myint, M., & Al-Muhtaseb, A. H. (2021). Heterogeneous carbon-based catalyst modified by alkaline earth metal oxides for biodiesel production: Parametric and Kinetic Study. Energy Conversion and Management: X, 10, 100047. Doi:10.1016/j.ecmx.2020.100047.

Jeon, Y., Chi, W. S., Hwang, J., Kim, D. H., Kim, J. H., & Shul, Y.-G. (2019). Core-shell nanostructured heteropoly acid-functionalized metal-organic frameworks: Bifunctional heterogeneous catalyst for Efficient Biodiesel production. Applied Catalysis B: Environmental, 242, 51–59.

Jiménez Espadafor, F., Torres García, M., Becerra Villanueva, J., & Moreno Gutiérrez, J. (2009). The viability of pure vegetable oil as an alternative fuel for large ships. Transportation Research Part D: Transport and Environment, 14(7), 461–469.

Joo, H., & Kumar, A. (2019). World Biodiesel Policies and Production (1st ed.). https://doi.org/https://doi.org/10.1201/9780429282881.

Karnjanakom, S., Maneechakr, P., Samart, C., Guan, G., (2018). Ultrasound-assisted acetylation of glycerol for triacetin production over green catalyst: a liquid biofuel candidate. Energy Convers. Manag. 173, 262-270.

Kastner, J.R., Miller, J., Geller, D.P., Locklin, J., Keith, L.H., Johnson, T., 2012. Catalytic esterification of fatty acids using solid acid catalysts generated from biochar and activated carbon. Catal. Today 190, 122-132.

Khan Academy. (2014). Lipids (article) | Macromolecules. Khan Academy. Retrieved from www.khanacademy.org/science/biology/macromolecules/lipids/a/lipids.

Khayoon, M.S., Triwahyono, S., Hameed, B.H., Jalil, A.A., (2014). Improved production of fuel oxygenates via glycerol acetylation with acetic acid. Chem. Eng. J. 243, 473e484.

Kimpe, K., Jacobs, P. A., & Waelkens, M. (2001). Analysis of oil used in late roman oil lamps with different mass spectrometric techniques revealed the presence of predominantly olive oil together with traces of animal fat. Journal of Chromatography A, 937(1–2), 87–95.

Kirkbride, K. P. (2000). Analytical techniques | spectroscopic techniques. *Encyclopedia of Forensic Sciences*, 179–191.

Knothe, Gerhard (2005). The History of Vegetable Oil-Based Diesel Fuels. In Knothe, Krahl, and Van Gerpen (Eds.), The Biodiesel Handbook. Champaign, IL: AOCS Press.

Koberg, M., & Gedanken, A. (2013). Using microwave radiation and SRO as a catalyst for the complete conversion of oils, cooked oils, and microalgae to biodiesel. New and Future Developments in Catalysis, 209–227.

Kutney, G. (2016, June 1). Where did biofuels technologies come from? Biofuels Digest. www.biofuelsdigest.com/bdigest/2016/06/01/where-did-biofuels-technologies-come-from/.

Le Pevelen, D. D. (2010). Small molecule X-ray crystallography, theory and workflow. Encyclopedia of Spectroscopy and Spectrometry, 2559–2576. Doi:10.1016/b978-0-12-374413-5.00359-6.

Lee, A. F., Bennett, J. A., Manayil, J. C., & Wilson, K. (2014). Heterogeneous catalysis for sustainable biodiesel production via esterification and transesterification. Chemical Society Reviews, 43(22), 7887–7916.

Lee, H. V., Juan, J. C., & Taufiq-Yap, Y. H. (2015). Preparation and application of binary acid-base CaO-La2O3 catalyst for biodiesel production. Renewable Energy, 74, 124–132.

Leofanti, G. Tozzola, Padovan, M., Petrini, G. Bordiga, S. and Zecchina, A. (1997) Catalyst characteri zation: characterization techniques. Catalysis today, 34(3):307–327.

Leung, D., Wu, X., & Leung, M. (2010). A review on biodiesel production using catalyzed. Applied Energy, 87, 1083-1095.

Leung, D., Wu, X., & Leung, M. (2010). A review on biodiesel production using catalyzed. Applied Energy, 87, 1083-1095.

Li, Z., Ding, S., Chen, C., Qu, S., Du, L., Lu, J., & Ding, J. (2019). Recyclable Li/Nay Zeolite as a heterogeneous alkaline catalyst for biodiesel production: Process optimization and kinetics study. Energy Conversion and Management, 192, 335–345. https://doi.org/10.1016/j.enconman.2019.04.053 London, London, 5, p. 303.

Lim, W.-R., Park, J.-H., & Lee, C.-H. (2023). Characterizing crystalline phase transitions in zeolitization of coal fly ash using focused ion beam-scanning electron microscopy. Surfaces and Interfaces, 36, 102536. Doi: 10.1016/j.surfin.2022.102536.

Liu, X.Y., Huang, M., Ma, H.L., Zhang, Z.Q., Gao, J.M., Zhu, Y.L., Han, X.J., Guo, X.Y., (2010). Preparation of a carbon-based solid acid catalyst by sulfonating activated carbon in a chemical reduction process. Molecules 15, 7188-7196.

Loridant, S. (2021). Raman spectroscopy as a powerful tool to characterize Ceria-based catalysts. Catalysis Today, 373, 98–111.

Ma, F., & Hanna, M. (1999). Biodiesel production: a review. Bioresource technology. doi:70(1):1–15.

Ma, H., Li, S., Wang, B., Wang, R., & Tian, S. (2008). Transesterification of rapeseed oil for synthesizing biodiesel by K/KOH/γ-al2o3 as heterogeneous base catalyst. Journal of the American Oil Chemists' Society, 85(3), 263–270.

Mahamuni, M., Adewuyi, G., (2009). Fourier transform infrared spectroscopy (FTIR) method to monitor soy biodiesel and soybean oil in transesterification reactions, petrodiesel - biodiesel blends, and blend adulteration with soy oil, Energy Fuels, 76, 3773–3782.

Makhlouf, A. S. H., & Aliofkhazraei, M. (Eds.). (2016). Handbook of Materials Failure Analysis with Case Studies from the Oil and Gas Industry (1st ed.). doi: 10.1016/C2014-0-01712-1.

Maleki, B., Ashraf Talesh, S. S., & Mansouri, M. (2022). Comparison of catalysts types performance in the generation of sustainable biodiesel via transesterification of various oil sources: A review study. Materials Today Sustainability, 18, 100157.

Manara, P., Zabaniotou, A., 2016. Co-valorization of crude glycerol waste streams with conventional and/or renewable fuels for power generation and industrial symbiosis perspectives. Waste. Biomass. Valor. 7, 135-150.

Mancini, A., Imperlini, E., Nigro, E., Montagnese, C., Daniele, A., Orrù, S., & Buono, P. (2015). Biological and nutritional properties of palm oil and palmitic acid: Effects on health. Molecules, 20(9), 17339–17361.

Mardhiah, H. H., Ong, H. C., Masjuki, H. H., Lim, S., & Lee, H. V. (2017). A review on latest developments and future prospects of heterogeneous catalyst in biodiesel production from non-

edible oils. Renewable and Sustainable Energy Reviews, 67, 1225–1236.

Mardhiah, H. H., Ong, H. C., Masjuki, H. H., Lim, S., & Lee, H. V. (2017). A review on latest developments and future prospects of heterogeneous catalyst in biodiesel production from nonedible oils. Renewable and Sustainable Energy Reviews, 67, 1225–1236.

Martin, M., Wetterlund, E., Hackl, R., Holmgren, K. M., & Peck, P. (2017). Assessing the aggregated environmental benefits from by-product and utility synergies in the Swedish biofuel industry. Biofuels, 11(6), 683–698.

Mello, V. M., Oliveira, F. C., Fraga, W. G., do Nascimento, C. J., & Suarez, P. A. (2008). Determination of the content of fatty acid methyl esters (FAME) in biodiesel samples obtained by esterification using 1H-NMR spectroscopy. Magnetic Resonance in Chemistry, 46(11), 1051–1054.

Meng, X., Chen, G., & Wang, Y. (2008). Biodiesel production from waste cooking oil via alkali catalyst and its engine test. Fuel Processing Technology, 89(9), 851–857.

Miao, X., Li, R., & Yao, H. (2009). Effective acid-catalyzed transesterification for biodiesel production. Energy Conversion and Management, 50(10), 2680–2684.

Mootabadi, H., Salamatinia, B., Bhatia, S., & Abdullah, A. Z. (2010). Ultrasonic-assisted biodiesel production process from palm oil using alkaline earth metal oxides as the heterogeneous catalysts. Fuel, 89(8), 1818–1825.

Mootabadi, H., Salamatinia, B., Bhatia, S., & Abdullah, A. Z. (2010a). Ultrasonic-assisted biodiesel production process from palm oil using alkaline earth metal oxides as the heterogeneous catalysts. Fuel, 89(8), 1818–1825.

Moser, B. R. (2016). Fuel property enhancement of biodiesel fuels from common and alternative feedstocks via complementary blending. Renewable Energy, 85, 819–825.

Muanruksa, P., & Kaewkannetra, P. (2020). Combination of fatty acids extraction and enzymatic esterification for biodiesel production using sludge palm oil as a low-cost substrate. Renewable Energy, 146, 901–906.

Mulyatun, M., Prameswari, J., Istadi, I., & Widayat, W. (2022). Production of non-food feedstock-based biodiesel using acid-base bifunctional heterogeneous catalysts: A Review. Fuel, 314, 122-149.

Nakagaki, S., Bail, A., Santos, V. C., Souza, V. H., Vrubel, H., Nunes, F. S., & Ramos, L. P. (2008). Use of anhydrous sodium molybdate as an efficient heterogeneous catalyst for soybean oil methanolysis. Applied Catalysis A: General, 351(2), 267–274.

Nakajima, K., & Hara, M. (2012). Amorphous Carbon with SO3H Groups as a Solid Brønsted Acid Catalyst. ACS Catalysis, 2(7), 1296-1304.

Narasimharao. K, L. A. (2007). Catalysts in Production of Biodiesel: a Review. Journal of Biobased Materials and Bioenergy, 1(1), 19-30.

Nata, I. F., Putra, M. D., Irawan, C., & Lee, C.-K. (2017). Catalytic performance of sulfonated carbon-based solid acid catalyst on esterification of waste cooking oil for biodiesel production. Journal of Environmental Chemical Engineering, 5(3), 2171–2175.

Ngaosuwan, K., Goodwin, J.G., Prasertdham, P., (2016). A green sulfonated carbon-based catalyst derived from coffee residue for esterification. Renew. Energy 86, 262-269. Doi:10.1016/j.renene.2015.08.010.

O'Donnell, S., Demshemino, I., Yahaya, M., Nwandike, I., and Okoro, L. (2013) A review on the spectroscopic analyses of biodiesel. European International Journal of Science and Technology, 2(7):137–146.

Organic Chemistry LCC (2022, October 15). Fischer esterification. Chemistry Steps. Retrieved from www.chemistrysteps.com/fischer-esterification/.

Pahl, Greg (2005). Biodiesel: Growing a New Energy Economy. White River Junction. Economy today, 23 (2): 123-130.

Perego, G. (1998) Characterization of heterogeneous catalysts by x-ray diffraction techniques. Catalysis today, 41(1):251–259.

Piker, A., Perkas, N., Tabah, B., & Gedanken, A. (2016). A green and low-cost room temperature biodiesel production method fron waste cooking oil using egg shells as catalyst. 182, 34-41.

Prabhavathi Devi, B. L. A., Gangadhar, K. N., Sai Prasad, P. S., Jagannadh, B., & Prasad, R. B. N. (2009). A glycerol-based carbon catalyst for the preparation of biodiesel. ChemSusChem, 2(7), 617–620.

Pradana, Y. S., Fauzi, A., Pratama, S. H., & Sudibyo, H. (2018). Simulation of biodiesel production using hydro-esterification process from wet microalgae. MATEC Web of Conferences, 154. Doi:10.1051/matecconf/201815401007.

Prankl, H., Körbitz, W., Mittelbach, M., & Wörgetter, M. (2004). Review on biodiesel standardization world-wide. IEA Bioenergy Task, 39(May), 38–46.

Predojevic, Z. J. (2008). The production of biodiesel from waste frying oils: A comparison of different purification steps. Fuel, 87, 3522-3528.

Predojevic, Z. J. (2008). The production of biodiesel from waste frying oils: A comparison of different purification steps. Fuel, 87, 3522-3528.

Prestigiacomo, C., Biondo, M., Galia, A., Monflier, E., Ponchel, A., Prevost, D., Scialdone, O., Tilloy, S., & Bleta, R. (2022). Interesterification of triglycerides with methyl acetate for biodiesel production using a cyclodextrin-derived Sno@γ-Al2O3 composite as heterogeneous catalyst. Fuel, 321, 124-126.

Puna, J. F., Correia, M. N., Dias, A. S., Gomes, J., & Bordado, J. (2013). Biodiesel production from waste frying oils over lime catalysts. doi:10.1007/s11144-013-0557-2.

Rades, S., Hodoroaba, V.-D., Salge, T., Wirth, T., Lobera, M. P., Labrador, R. H., Natte, K., Behnke, T., Gross, T., & Unger, W. E. (2014). High-resolution imaging with SEM/T-SEM, EDX and Sam as a combined methodical approach for morphological and elemental analyses of single engineered nanoparticles. RSC Adv., 4(91), 49577–49587.

Ramos, M., Soares Dias, A., Puna, J. F., Gomes, J., & Bordado, J. C. (2019). Biodiesel Production Processes and Sustainable Raw Materials. Energies, 12.

Refaat, A. A., Attia, N. K., Sibak, H. A., El Sheltawy, S. T., & ElDiwani, G. I. (2007). Production optimization and quality assessment of biodiesel from waste vegetable oil. International Journal of Environmental Science & Technology, 5(1), 75–82.

Rodríguez-Fernández, J., Hernández, J. J., Calle-Asensio, A., Ramos, Á., & Barba, J. (2019). Selection of blends of diesel fuel and advanced biofuels based on their physical and thermochemical properties. Energies, 12(11), 1–13.

Ruhul, A. M., Kalam, M. A., Masjuki, H. H., Fattah, I. M. R., Reham, S. S., & Rashed, M. M. (2015). State of the art of biodiesel production processes: A review of the heterogeneous catalyst. RSC Advances, 5(122), 101023–101044.

Saifuddin, N. M., Hussein, R., & Ong, M. Y. (2018). Sustainability of biodiesel production in Malaysia by production of bio-oil from crude glycerol using microwave pyrolysis: A review. 11(2), 135-157.

Sarkar, A., Das, P., Laskar, I. B., Vadivel, S., Puzari, A., & Paul, B. (2023). Parkia speciosa: A basic heterogeneous catalyst for production of soybean oil-based biodiesel. Fuel, 348, 128-137. doi:10.1016/j.fuel.2023.128537.

Selvam, D. J. P., & Vadivel, K. (2012). Performance and emission analysis of DI diesel engine fuelled with methyl esters of beef tallow and diesel blends. Procedia Engineering, 38, 342–358.

Sendzikiene, E., Makareviciene, V., Janulis, P., & Kitrys, S. (2004). Kinetics of free fatty acids esterification with methanol in the production of biodiesel fuel. European Journal of Lipid Science and Technology, 106(12), 831–836.

Shankar, V., & Jambulingam, R. (2017). Waste crab shell derived Cao impregnated na-ZSM-5 as a solid base catalyst for the transesterification of neem oil into biodiesel. Sustainable Environment Research, 27(6), 273–278.

Sharma, Y. C., Singh, B., & Korstad, J. (2010). Application of an efficient nonconventional heterogeneous catalyst for biodiesel synthesis from pongamia pinnata oil. Energy and Fuels, 24(5), 3223–3231. doi:10.1021/ef901514a.

Sharma, Y. C., Singh, B., & Korstad, J. (2010). Application of an efficient nonconventional heterogeneous catalyst for biodiesel synthesis from Pongamia Pinnata Oil. Energy & Fuels, 24(5), 3223–3231.

Sharma, Y., Singh, B., & Upadhyay, S. (2008). Advancements in development and characterization of biodiesel: a review. Fuel, 87(12), 2355-2373.

Sharma, Yogesh C., Singh, B., & Korstad, J. (2011a). Advancements in solid acid catalysts for ecofriendly and economically viable synthesis of biodiesel. Biofuels, Bioproducts and Biorefining, 5(1), 69–92. doi:10.1002/bbb.253.

Sharma, Yogesh C., Singh, B., & Korstad, J. (2011b). Latest developments on application of heterogenous basic catalysts for an efficient and eco friendly synthesis of biodiesel: A review. Fuel, 90(4), 1309–1324. doi:10.1016/j.fuel.2010.10.015.

Scholz, D., Kro¨cher, O., Vogel, F., (2018). Deactivation and regeneration of sulfonated carbon catalysts in hydrothermal reaction environments. Chem. Sus. Chem. 11, 2189–2201. Doi:10.1002/cssc.201800678.

Siatis, N. G., Kimbaris, A. C., Pappas, C. S., Tarantilis, P. A., & Polissiou, M. G. (2006). Improvement of biodiesel production based on the application of ultrasound: Monitoring of the procedure by FTIR spectroscopy. JAOCS, Journal of the American Oil Chemists' Society, 83(1), 53–57. Doi:10.1007/s11746-006-1175-1

Silva, R. B., Lima Neto, A. F., Soares dos Santos, L. S., de Oliveira Lima, J. R., Chaves, M. H., dos Santos, J. R., de Lima, G. M., de Moura, E. M., & de Moura, C. V. (2008). Catalysts of cu(ii) and co(ii) ions adsorbed in chitosan used in transesterification of soy bean and babassu oils – a new route for biodiesel syntheses. Bioresource Technology, 99(15), 6793–6798.

Singh, M., & Vander Wal, R. L. (2022). Carbon composites—graphene-oxide-catalyzed sugar graphitization. C, 8(1), 15. Doi:10.3390/c8010015.

Soares Dias, A. P., Bernardo, J., Felizardo, P., & Neiva Correia, M. J. (2012). Biodiesel production over thermal activated cerium modified Mg-Al hydrotalcites. Energy, 41(1), 344–353. doi:10.1016/j.energy.2012.03.005.

Spataru, D., Soares Dias, A. P., & Vieira Ferreira, L. F. (2021). Acetylation of biodiesel glycerin using glycerin and glucose derived catalysts. Journal of Cleaner Production, 297, 126686. doi:10.1016/j.jclepro.2021.126686.

Stumborg, M., Wong, A., & Hogan, E. (1996). Hydroprocessed vegetable oils for diesel fuel

improvement. Bioresource Technology, 56(1), 13–18. Doi:10.1016/0960- 8524(95)00181-6.

Su, F., & Guo, Y. (2014). Advancements in solid acid catalysts for biodiesel production. 2934-2957. doi:10.1039/C3GC42333F.

Sugunuma, S., Nakajima, K., Kitano, M., Yamaguchi, D., Kato, H., Hayashi, S., & Hara, M. (2008). Hydrolysis of Cellulose by Amorphous Carbon Bearing SO3H, COOH, and OH Groups. Journal of the American Chemical Society, 130(38), 12787-12793. doi:10.1021/ja803983h.

Taher, H., Nashef, E., Anvar, N., & Al-Zuhair, S. (2017). Enzymatic production of biodiesel from waste oil in Ionic Liquid Medium. Biofuels, 10(4), 463–472. doi:10.1080/17597269.2017.1316145.

Tamborini, L. H., Militello, M. P., Balach, J., Moyano, J. M., Barbero, C. A., & Acevedo, D. F. (2019). Application of sulfonated nanoporous carbons as acid catalysts for Fischer esterification reactions. Arabian Journal of Chemistry, 12(8), 3172–3182. doi:10.1016/j.arabjc.2015.08.018.

Thanh, L. T., Okitsu, K., Sadanaga, Y., Takenaka, N., Maeda, Y., & Bandow, H. (2010). Ultrasound-assisted production of biodiesel fuel from vegetable oils in a small scale circulation process. Bioresource Technology, 101(2), 639–645.

Toda, M., Takagaki, A., Okamura, M., Kondo, J. N., Hayashi, S., Domen, K., & Hara, M. (2005). Biodiesel made with Sugar Catalyst. Nature, 438(7065), 178–178.

Toikka, M., Kuzmenko, P., Samarov, A., & Trofimova, M. (2022). Phase behavior of the oleic acid – methanol – methyl oleate – water mixture as a promising model system for BIODIESEL PRODUCTION: Brief Data Review and new results at 303.15 K and atmospheric pressure. Fuel, 319, 123-130. doi:10.1016/j.fuel.2022.123730.

Tutunea, D., Dumitru, I., Racila, L., Otat, O., Matei, L., & Geonea, I. (2018). Characterization of sunflower oil biodiesel as alternative for Diesel Fuel. Proceedings of the 4th International Congress of Automotive and Transport Engineering (AMMA 2018), 172–180.

Vadery, V., Narayanan, B. N., Ramakrishnan, R. M., Cherikkallinmel, S. K., Sugunan, S., Narayanan, D. P., & Sasidharan, S. (2014). Room temperature production of jatropha biodiesel over coconut husk ash. Energy, 70, 588–594. Doi:10.1016/j.energy.2014.04.045.

Van Gerpen, Jon H., Charles L. Peterson, and Carroll Goering (2007). Biodiesel: An Alternative Fuel for Compression Ignition Engines.St. Joseph, MI: ASABE.VT: Chelsea Green Publishing Company.

Vargas, E. M., Ospina, J. L., Tarelho, L. A. C., & Nunes, M. I. (2020). Fame production from residual materials: Optimization of the process by box–behnken model. *Energy Reports*, *6*, 347–352.

Vega-Lizama, T., Díaz-Ballote, L., Hernández-Mézquita, E., May-Crespo, F., Castro-Borges, P., Castillo-Atoche, A., González-García, G., & Maldonado, L. (2015). Thermogravimetric analysis as a rapid and simple method to determine the degradation degree of Soy Biodiesel. Fuel, 156, 158–162.

Wen, F., Min, F., Zhang, Y.-J., & Yang, C. (2018, October 11). Crude oil price shocks, monetary policy, and China's economy. doi:10.1002/ijfe.1692.

Wu, H., Zhang, J., Wei, Q., Zheng, J., & Zhang, J. (2013). Transesterification of soybean oil to biodiesel using zeolite supported Cao as strong base catalysts. Fuel Processing Technology, 109, 13–18. doi:10.1016/j.fuproc.2012.09.032.

Xie, W., & Yang, D. (2012). Transesterification of soybean oil over WO3 supported on Alpo4 as a solid acid catalyst. Bioresource Technology, 119, 60–65. doi:10.1016/j.biortech.2012.05.110.

Xu, J., Liu, J., Ling, P., Zhang, X., Xu, K., He, L., Wang, Y., Su, S., Hu, S., Xiang, J., (2020). Raman spectroscopy of biochar from the pyrolysis of three typical chinese biomasses: a novel method for rapidly evaluating the biochar property. Energy 202,. Doi:10.1016/j.energy.2020.117644

117644.

Xu, J., Liu, J., Zhang, X., Ling, P., Xu, K., He, L., Su, S., Wang, Y., Hu, S., Xiang, J., 2020b. Chemical imaging of coal in micro-scale with Raman mapping technology. Fuel 264. Doi:10.1016/j.fuel.2019.116826 116826.

Xu, C., Nasrollahzadeh, M., Selva, M., Issaabadi, Z., Luque, R., 2019. Waste-to-wealth: biowaste valorization into valuable bio(nano)materials. Chem. Soc. Rev. 48, 4791–4822. Doi:10.1039/C8CS00543E.

Xu, J., Tang, H., Su, S., Liu, J., Xu, K., Qian, K., Wang, Y., Zhou, Y., Hu, S., Zhang, A., 2018. A study of the relationships between coal structures and combustion characteristics: the insights from microraman spectroscopy based on 32 kinds of chinese coals. Appl. Energy 212, 46–56. Influence of pyrolysis temperature on functionalization 17.

Yuan, Y., Jiang, W., & Li, J. (2019). Preparation of solid acid catalyst SO42−/TiO2/γ-al2o3 for esterification: A study on catalytic reaction mechanism and kinetics. Chinese Journal of Chemical Engineering, 27(11), 2696–2704. doi:10.1016/j.cjche.2018.11.021.

Zaera, F. (2014). New advances in the use of infrared absorption spectroscopy for the characterization of heterogeneous catalytic reactions. Chemical Society Reviews, 43(22), 7624-7663.

Zhang, K., Zhang, Y., Wang, S., 2013. Enhancing thermoelectric properties of organic composites through hierarchical nanostructures. Sci. Rep. 3, 1-7. Doi:10.1038/srep03448.

Zhang, Q., Zhang, Y., Deng, T., Wei, f., Jin j., and Ma, P. (2020) Sustainable production of biodiesel over heterogeneous acid catalysts, Elsevier B.V., 407–432.

Zhang, B., Gao, M., Geng, J., Cheng, Y., Wang, X., Wu, C., Wang, Q., Liu, S., Cheung, S.M., (2021). Catalytic performance and deactivation mechanism of a one-step sulfonated carbon-based solid-acid catalyst in an esterification reaction. Renew. Energy 164, 824–832.

Zhao, B., O'Connor, D., Zhang, J., Peng, T., Shen, Z., Tsang, D.C.W., Hou, D., 2018. Effect of pyrolysis temperature, heating rate, and residence time on rapeseed stem derived biochar. J. Clean. Prod.174, 977–987.

Zhou, P. L., Fet, A. M., Michelsen, O., & Fet, K. (2003). A feasibility study of the use of biodiesel in recreational boats in the United Kingdom. Proceedings of the Institution of Mechanical Engineers, Part M: Journal of Engineering for the Maritime Environment, 217(3), 149–158.

Zhou, Y., Niu, S., & Li, J. (2016). Activity of the carbon-based heterogeneous acid catalyst derived from bamboo in esterification of oleic acid with ethanol. Energy Conversion and Management, 114, 188–196. doi:10.1016/j.enconman.2016.02.027.

Zong, M.-H., & Smith, T. (2007). Preparation of a sugar catalyst and its use for highly efficient production of biodiesel. Green Chemistry (7).